USGS
science for a changing world

Geochemical Assessment of Metals and Dioxin in Sediment from the San Carlos Reservoir and the Gila, San Carlos, and San Francisco Rivers, Arizona

Scientific Investigations Report 2005-5086

U.S. Department of the Interior
U.S. Geological Survey

Geochemical Assessment of Metals and Dioxin in Sediment from the San Carlos Reservoir and the Gila, San Carlos, and San Francisco Rivers, Arizona

By Stanley E. Church, LaDonna M. Choate, Marci E. Marot, David L. Fey, Monique Adams, Paul H. Briggs, and Zoe Ann Brown

Prepared in cooperation with the Bureau of Indian Affairs

Scientific Investigations Report 2005-5086

U.S. Department of the Interior
U.S. Geological Survey

U.S. Department of the Interior
Gale A. Norton, Secretary

U.S. Geological Survey
P. Patrick Leahy, Acting Director

U.S. Geological Survey, Reston, Virginia: 2005

This publication is available online at URL:
http://pubs.usgs.gov/sir/2005/5086/
and as Scientific Investigations Report 2005-5086 in printed form

For information on other USGS products and ordering information:
World Wide Web: http://www.usgs.gov/pubprod/
Telephone: 1-888-ASK-USGS

For more information on the USGS—the Federal source for science about the Earth, its natural and living resources, natural hazards, and the environment:
World Wide Web: http://www.usgs.gov/
Telephone: 1-888-ASK-USGS

Suggested citation:
Church, S.E., Choate, L.M., Marot, M.E., Fey, D.L., Adams, Monique, Briggs, P.H., and Brown, Z.A., 2005, Geochemical assessment of metals and dioxin in sediment from the San Carlos Reservoir and the Gila, San Carlos, and San Francisco Rivers, Arizona: U.S. Geological Survey Scientific Investigations Report 2005-5086, 61 p.

Contents

Figures

Tables

Appendix Figures (on CD-ROM—see note below)

[For the online version of this report, Appendix figures (in PDF format) and tables (in Excel format) are available for download at the URL shown on the backstitle page. Reference in the text to Appendix material on CD-ROM likewise refer to these downloadable files]

Appendix Tables (on CD-ROM—see note below)

[For the online version of this report, Appendix figures (in PDF format) and tables (in Excel format) are available for download at the URL shown on the backstitle page. Reference in the text to Appendix material on CD-ROM likewise refer to these downloadable files]

Geochemical Assessment of Metals and Dioxin in Sediment from the San Carlos Reservoir and the Gila, San Carlos, and San Francisco Rivers, Arizona

By Stanley E. Church, LaDonna M. Choate, Marci E. Marot, David L. Fey, Monique Adams, Paul H. Briggs, and Zoe Ann Brown

Abstract

In October 2004, we sampled stream-bed sediment, terrace sediment, and sediment from the San Carlos Reservoir to determine the spatial and chronological variation of six potentially toxic metals—Cu, Pb, Zn, Cd, As, and Hg. Water levels in the San Carlos Reservoir were at a 20-year low at an elevation of 2,409 ft (734.3 m). Four cores were taken from the reservoir: one from the San Carlos River arm, one from the Gila River arm, and two from the San Carlos Reservoir just west of the Pinal County line. Radioisotope chronometry (^{7}Be, ^{137}Cs, and ^{210}Pb) conducted on sediment from the reservoir cores provides a good chronological record back to 1959. Chronology prior to that, during the 1950s, is based on our interpretation of the ^{137}Cs anomaly in reservoir cores. During and prior to the 1950s, the reservoir was dry and sediment-accumulation rates were irregular; age control based on radioisotope data was not possible. We recovered sediment at the base of one 4-m-long core that may date back to the late 1930s. The sedimentological record contains two discrete events, one about 1978–83 and one about 1957, where the Cu concentration in reservoir sediment exceeded recommended sediment quality guidelines and should have had an effect on sensitive aquatic and benthic organisms. Concentrations of Zn determined in sediment deposited during the 1957(?) event also exceeded recommended sediment quality guidelines. Concentration data for Cu from the four cores clearly indicate that the source of this material was upstream on the Gila River.

Lead isotope data, coupled with the geochemical data from a 2M HCl–1 percent H_2O_2 leach of selected sediment samples, show two discrete populations of data. One represents the dominant sediment load derived from the Safford Valley, and a second reflects sediment derived from the San Francisco River. The Cu concentration spikes in the reservoir cores have chemical and Pb isotope signatures that indicate that deposits in a porphyry copper deposit from the Morenci district is the likely source of these Cu-rich sedimentary deposits. Copper concentrations and Pb isotope data in premining terrace-sediment deposits indicate that the Cu peaks could not have resulted from erosion of premining sediment from terrace deposits downstream on the Gila River. The chemical and Pb isotope data also indicate that agricultural practices in the Safford Valley have resulted in an increased sediment load to the Gila River since large-scale farming began, prior to the time when the San Carlos Reservoir was built.

Analyses of dioxin, which is an impurity in one of the herbicides used in the late 1960s and early 1970s, were completed in sediment from one of the cores in the reservoir to determine whether any of these pesticide residues have accumulated in the reservoir sediment. Dioxin concentration is expressed in terms of its toxicity (toxic equivalent concentration or TEQ). Concentrations of dioxin in the sediment ranged from 0.68 to 1.37 pg/g and are less than any of the benchmark concentrations recommended as threshold values for adverse effects of dioxin in sediment (> 2.5–10 pg/g).

Introduction

Mining activity, particularly open-pit mining, is a massive operation, resulting in the excavation, moving, and crushing of very large volumes of rock to remove the metals that are required to supply the global economy. Phelps Dodge Morenci, Inc., operates the Morenci open-pit Cu mine located on the San Francisco River near Clifton, Ariz. Open-pit mining did not begin in the Morenci district until 1937 when stripping of surficial material began (Moolick and Durek, 1966). Since then, a very large tonnage of rock has been removed and processed at this site. The Morenci open-pit mine is one of the largest in North America (http://lead.geosys.t.u-tokyo.ac.jp/mogi/US/Morenc1.html). Processing of this ore from the open pit began at the site in 1942. The total past production and proven reserves at the Morenci deposit exceeds 6.7 billion metric tons of ore at a grade of 0.42 percent Cu (Enders, 2000). Phelps Dodge Morenci, Inc., processed more than 300 million metric tons of ore and produced more than 450,000 metric tons of Cu in 2003.

The Morenci porphyry Cu district is located within the headwaters of the San Francisco River, a tributary of the Gila River, 190 river km (120 mi) upstream of the San Carlos Reservoir. The deposit was exposed in Chase Creek, which cut through the area of the open-pit mine and is a tributary of the San Francisco River. Phelps Dodge Morenci, Inc., has taken numerous steps over the past 2 decades to eliminate or reduce release of contaminants to the San Francisco River from the Morenci open-pit site. The San Carlos Reservoir is located about 100 km (60 mi) east of Phoenix, Ariz., on the Gila River. The reservoir was constructed in 1929 and began filling in October 1930. The reservoir is used for irrigation and recreational purposes and contains a substantial freshwater fish resource. This reservoir acts as the major sediment catchment basin on the lower Gila River and thus retains an integrated sedimentological record of upstream activity. The reservoir sediment contains a record of environmental changes that have affected aquatic resources over the life of the open-pit mining operation at Morenci.

Purpose and Scope

Phelps Dodge Morenci, Inc., is actively mining for Cu at the Morenci deposit near Clifton, Ariz. Our understanding of the environmental effects of metal mining on aquatic life has increased substantially since the mine began open-pit operation. We were asked by the Bureau of Indian Affairs, on behalf of the San Carlos Apache Indian Tribe, to assess the possible impact that mining activities upstream may have had on the aquatic resources in the reservoir because several of the metals associated with porphyry Cu mineral production are known to be potentially toxic to aquatic life. Sampling of the San Carlos Reservoir—and the Gila, San Carlos, and San Francisco Rivers—was undertaken October 20–29, 2004, to evaluate the source of metal anomalies in the reservoir sediment.

Herbicides were used extensively during the 1960s and 1970s to eradicate tamarisk on the Gila River flood plain upstream of the San Carlos Reservoir. Dioxin is an impurity formed during the manufacture of some of these herbicides. Analyses of dioxin in sediment were preformed to determine whether the dioxin concentrations exceeded the toxicity thresholds for aquatic life in sediment from the San Carlos Reservoir.

Acknowledgments

We thank the San Carlos Apache Indian Tribe for access to tribal lands and Clark Richins for arranging logistical support during our sampling period (Oct. 20–29, 2004). Without the use of all-terrain vehicles and a backhoe, operated by Melvin Kindelay, sampling of the sediment in the San Carlos River and Gila River arms of the reservoir would not have been possible. We thank John Krause of the Bureau of Indian Affairs for arranging funding for this study. We acknowledge assistance from Charles W. Holmes for his insight on the interpretation of the geochronological data and Christopher Schmitt for his insight in evaluation of the data from the National Contaminants Database. Finally, we thank Steve Smith and Laurie Balistrieri for their reviews this manuscript.

Previous Work

The San Carlos Reservoir is an irrigation reservoir formed behind Coolidge Dam, which was built in 1928–29 (fig. 1). The Gila River watershed upstream of the dam covers an area of about 33,000 km^2. The headwaters extend east into New Mexico. Elevations range from more than 2,000 m in the headwaters to 744 m at the dam. The study area is a part of the border lands of the Sonoran Desert in Arizona. Temperatures range from –12°C to 46°C, and the study area receives an average of 214 mm of rain per year (75 to 445 mm/yr; Sellers, 1960; Culler and others, 1982), mostly during the winter months.

Burkham (1970) analyzed historical annual discharge records of the Gila River from 1868 to 1967 and demonstrated that rainfall varied substantially on cycles of 30 to 60 years. Peak rainfall occurred between 1875–90 and 1905–25, with long periods of low rainfall from 1890–1905 and 1925–68. Native vegetation in the area includes mesquite, ironwood, palo verde, catclaw, acacia, and several varieties of cactus in the lower valleys, and native grasses, scrub oak, juniper, and pinõn pine in the higher elevations (Kamilli and Richard, 1998). Saltcedar or tamarisk has extensively replaced seepwillow and cottonwood along the banks and on the flood plain of the Gila River since 1944 (Turner, 1974).

The Gila River reach immediately upstream from the San Carlos Reservoir was studied extensively by the U.S. Geological Survey (USGS) in 1963–72 to evaluate the effects of evapotranspiration by tamarisk (*Tamarix pentandra* Pall.) on the water resources in the reservoir and the effectiveness of various tamarisk eradication practices on the Gila River flood plain (Culler and others, 1970). Detailed summaries of sediment accumulation, water budget, and effect of phreatophyte vegetation on the storage capacity are summarized in detail in U.S. Geological Survey Professional Paper 655 (Culler and others, 1970). Various chapters in this Professional Paper discuss the geomorphic, sedimentation, and discharge history of the Gila River and its effect on storage capacity and water use in the San Carlos Reservoir. Growth of tamarisk, also known as saltcedar, became so prevalent on the Gila River flood plain that vegetation impaired flow in the Gila River upstream of the reservoir during periods of heavy rainfall, threatening the upstream population and filling the reservoir with debris. The phreatophyte project evaluated the use of several herbicides as well as mechanical clearing of the flood plain as mechanisms for removal of these invasive species and restoring the ground water to earlier levels. Burkham (1972) showed that the changes in flow regime and the stabilization of the river banks by tamarisk subsequent to the development of the San

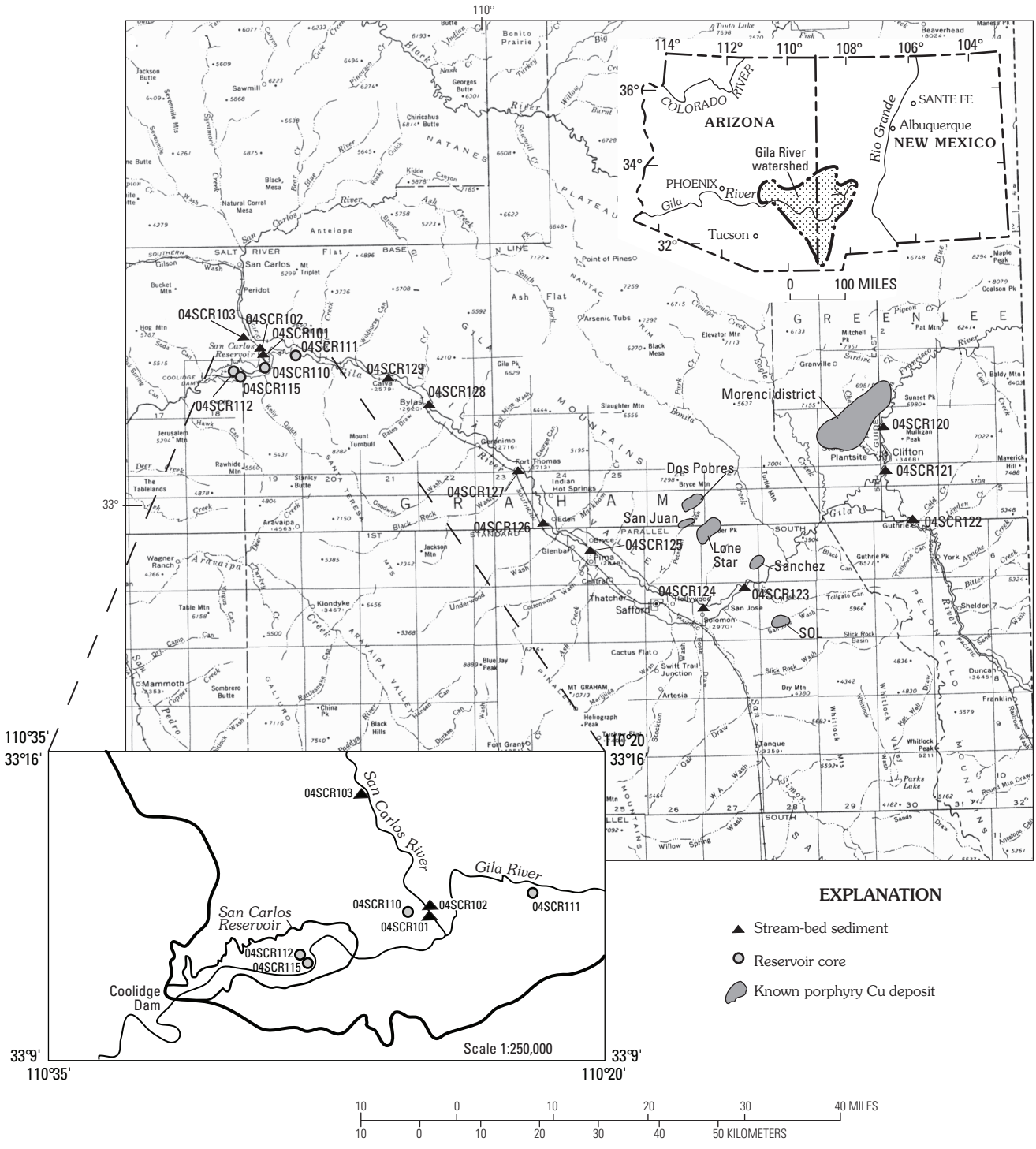

Figure 1. Regional mineral deposit and sample locality map (scale 1:1,000,000). Samples collected during this study are shown plotted on the Gila, San Carlos, and San Francisco Rivers and in the San Carlos Reservoir (outline shown on inset map of San Carlos Reservoir at elevation of 2,430 ft; water-level elevation at time of sampling was 2,409 ft; scale of inset map is 1:250,000). Locations of porphyry Cu deposits from Keith and others (1983). Base map from U.S. Geological Survey (1974), scale: 1:1,000,000, NAD27 datum, Lambert conformal conic projection based on standard parallels 33° and 45°.

Carlos Reservoir has substantially changed the flow characteristics of the Gila River and has drastically affected the width of the active flood plain, causing it to incise. Furthermore, tamarisk has replaced native species of riparian vegetation and resulted in changes in the ground-water flow regime. Cullers and others (1982) demonstrated that evaporative loss by removal of phreatophytes, mostly tamarisk, from the flood plain immediately upstream of the San Carlos Reservoir would result in recovery of ground water lost by evapotranspiration by about 50 percent, or from 43–56 in/yr to 25 in/year. However, some of these losses would not be realized if the flood plain were planted in native forage grasses.

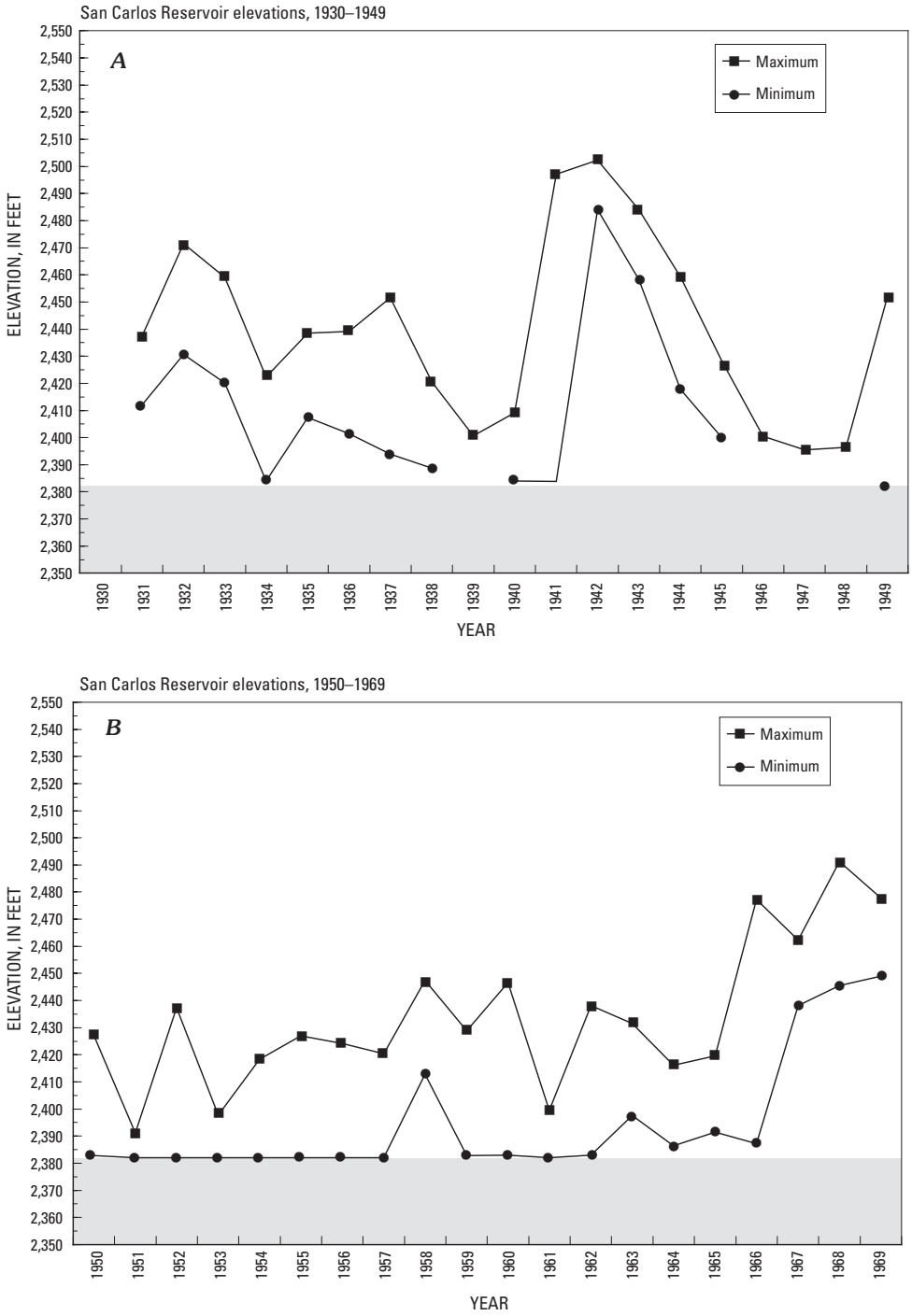

Figure 2 (above and facing page). Annual minimum and maximum water levels in the San Carlos Reservoir, Coolidge Dam (1929–2003; USGS gauging station 09469000). Data compiled from annual water resource data reports for Arizona listed in table 1.

Schmitt and Brumbaugh (1990) reported monitoring data on environmental contaminants in biological samples from the San Carlos Reservoir beginning in 1971. Studies of sediment quality and metal and organochlorine concentrations in lizard, avian, and fish filets were conducted in 1990 (Baker and King, 1994). According to Baker and King (1994), elevated pesticide concentrations previously had been documented in starlings (*sturnus vulgaris*) near Pima, Ariz., in the Safford Valley. One fish tissue sample from the site at Ft. Thomas (site no. 7 on the Gila River; Baker and King, 1994) was analyzed for dioxin. No dioxin was detected in this sample at a detection limit of 0.01 µg/g. We reoccupied many of the same sample sites during this study to look at possible changes in trace element concentrations in stream-bed sediment with time.

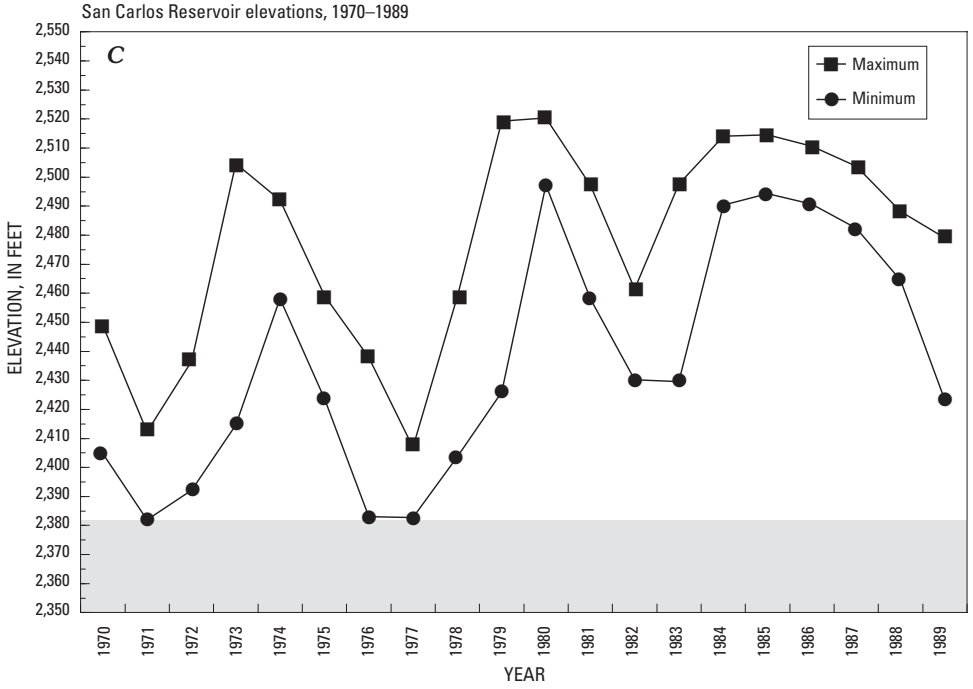

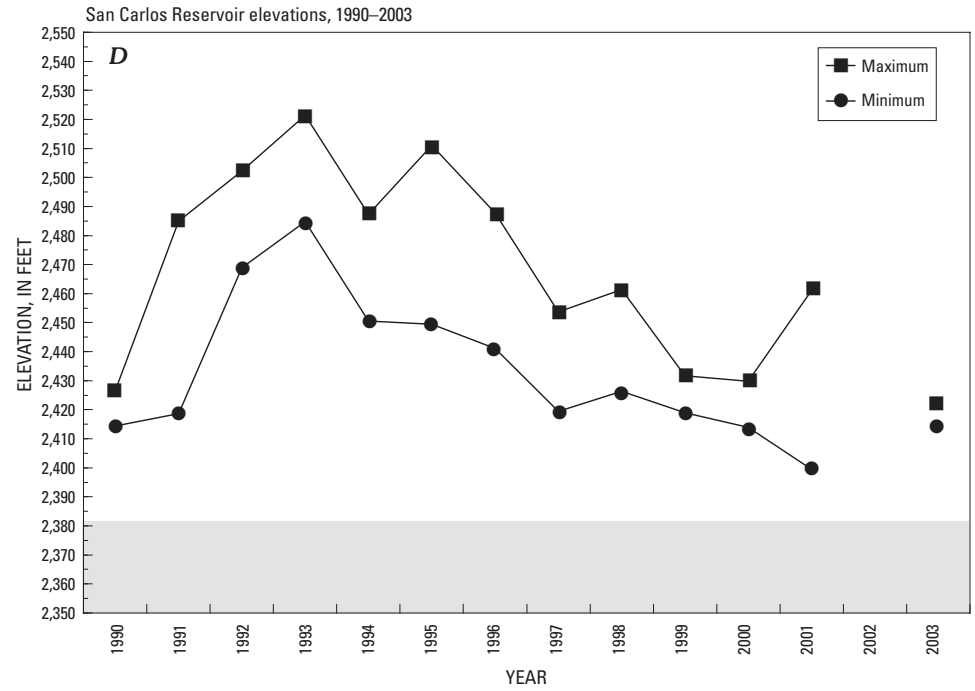

Hydrologic Setting

Water levels in the San Carlos Reservoir vary greatly throughout the year depending upon the demand for water by downstream users, but generally reach an elevation of 2,450 ft (749 m) in an average year. Data from the National Water Information System (NWIS—http://waterdata.usgs.gov/nwis/inventory) and from historical records provided by the USGS gauge stations on the Gila and San Carlos Rivers and Coolidge

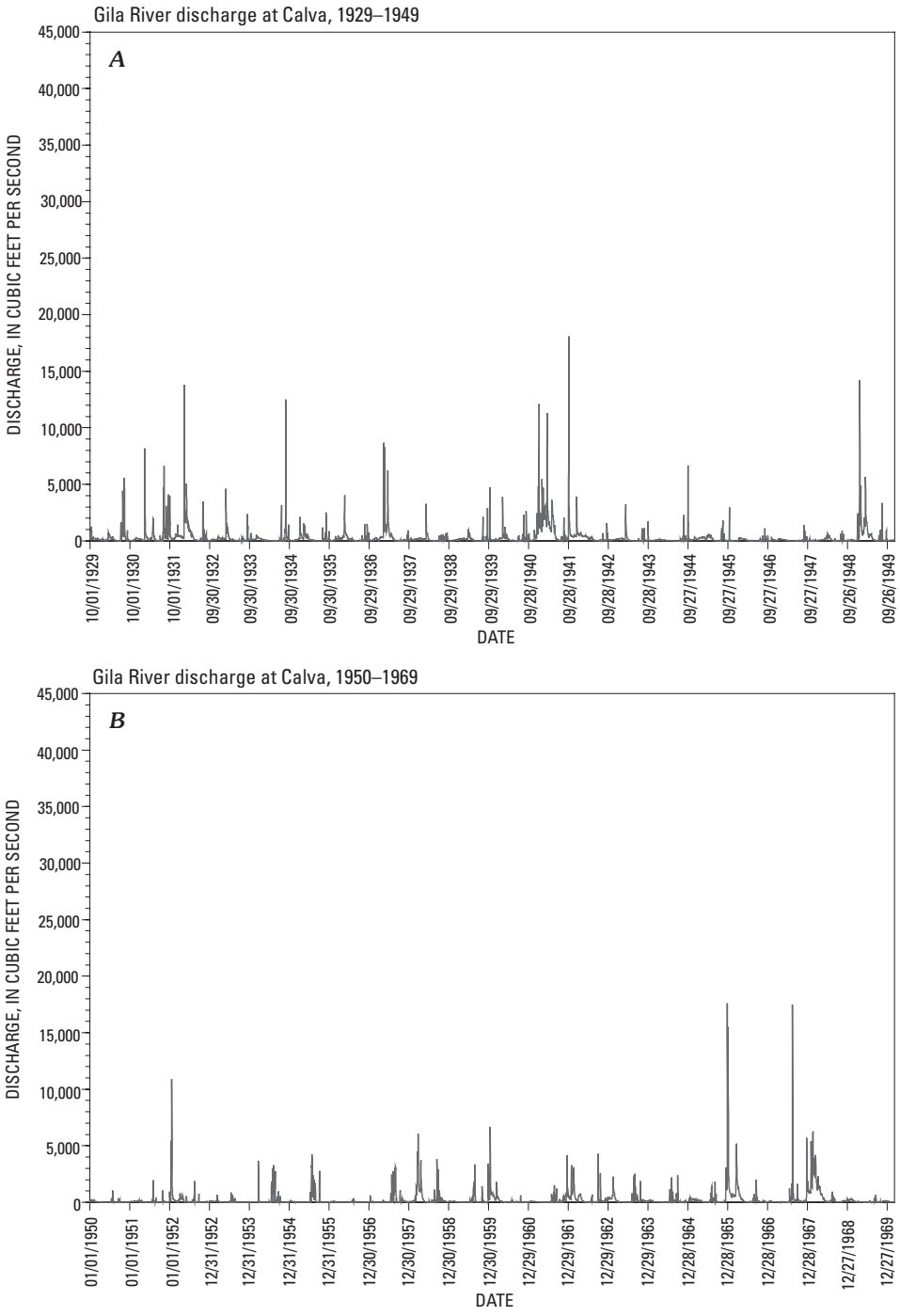

Figure 3 (above and facing page). Annual discharge records for Gila River at Calva (1929–2003; USGS gauging station 09466500). Dates on *x*-axis expressed as month, day, year for maximum discharge.

Dam have been used to construct the hydrologic history of the Gila and San Carlos Rivers and their impact on water supply and storage in the San Carlos Reservoir over the time period following completion of the reservoir (figs. 2–4 and table 1). The reservoir has gone dry during many years when precipitation has been low. Minimum and maximum reservoir elevations measured at stream gauge 09469000 at Coolidge Dam are plotted by year over the life of the reservoir in figure 2. Estimates of annual discharge for the Gila River from 1868–1968 (Burkham, 1970, pl. 2) show distinct periods of low flow

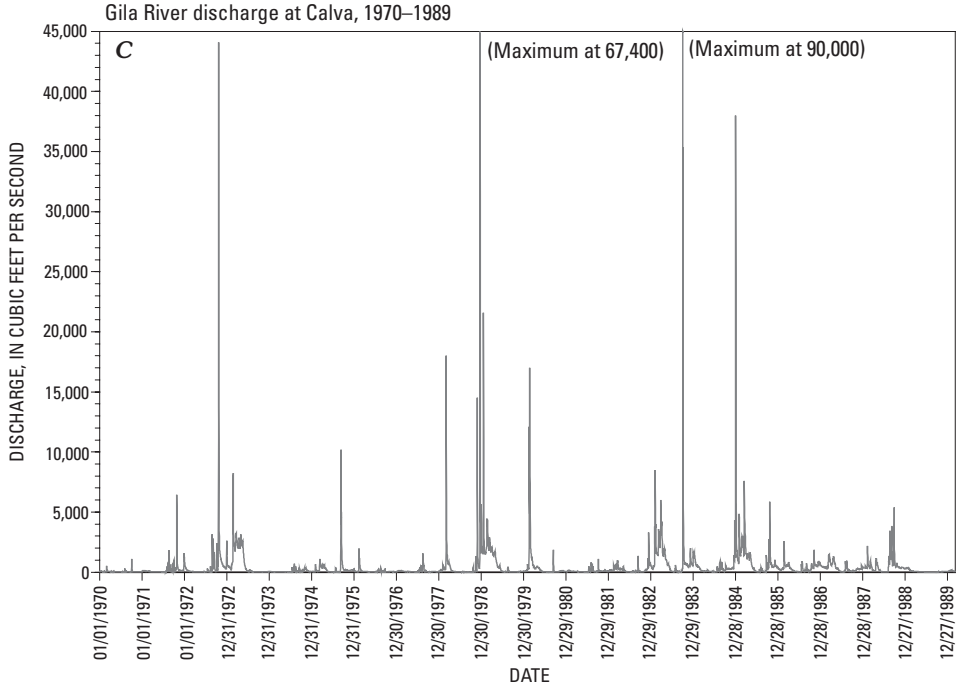

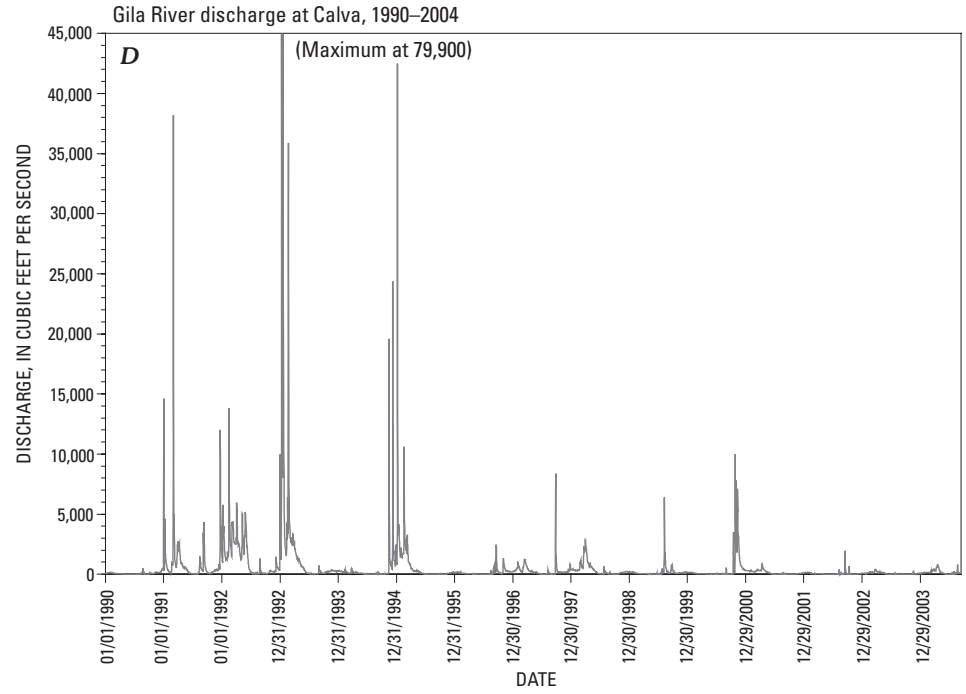

followed by major floods that occurred in 1874, 1891, 1905, 1906, 1915, 1916, 1941, and 1965–67. The inflow channel of the Gila River became blocked by flood debris at various sites, within 4.1 miles (6.6 km) upstream from the reservoir, from 1962–65. A channel was excavated parallel to this section of the plugged natural channel in the summer of 1965 and

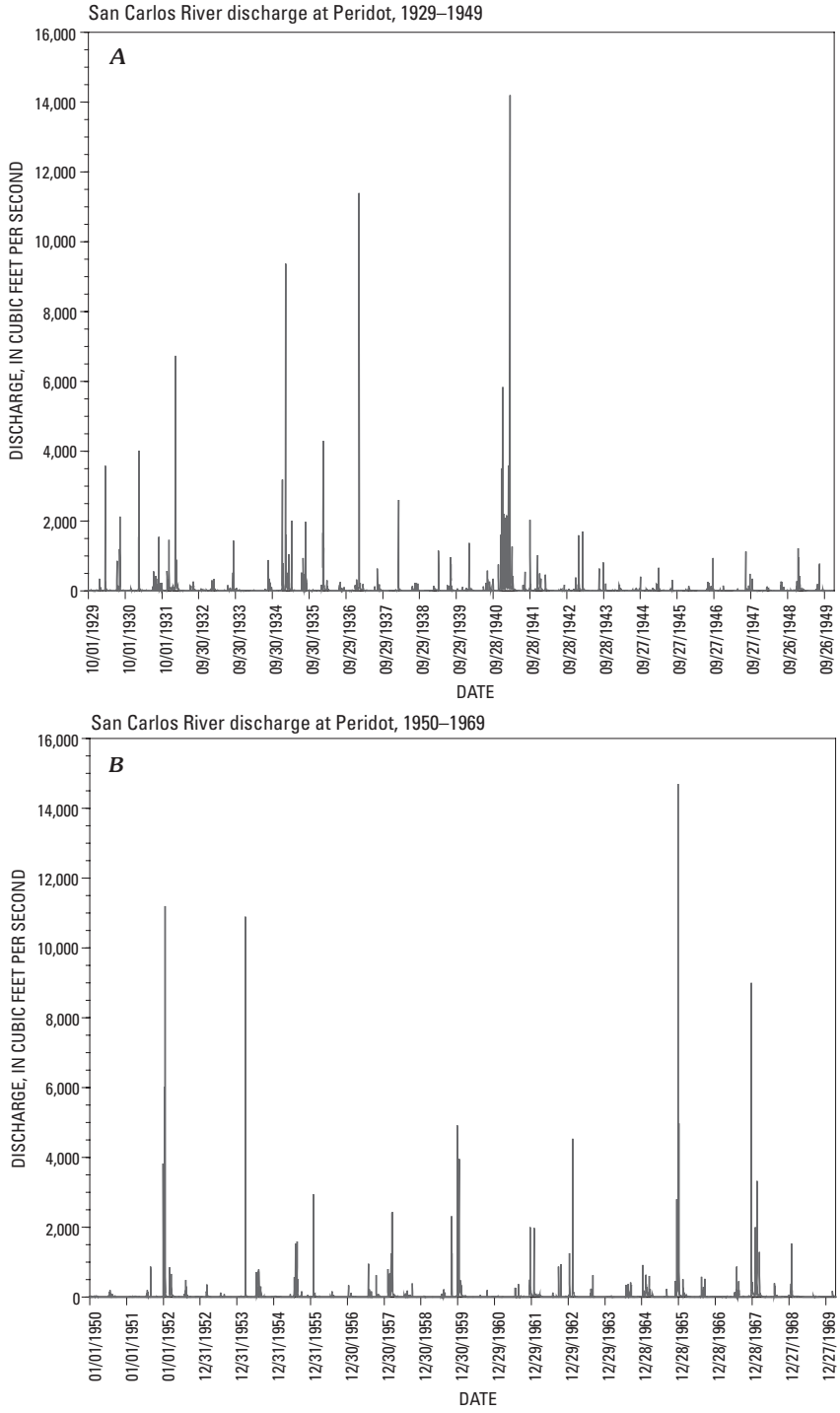

Figure 4 (above and facing page). Annual discharge records for San Carlos River at Peridot (1929–2003; USGS gauging station 09468500). Dates on *x*-axis expressed as month, day, year for maximum discharge.

has been maintained since 1966 (Kipple, 1977). Subsequent discharge records for the Gila River at Calva show that major floods occurred in 1972, 1978, 1983, 1984, 1991, 1992, and 1994 on the Gila River (> 35,000 cfs, fig. 3; gauge 09466500) and in 1936, 1940, 1952, 1953, 1965, 1977, 1978, 1991, 1992, and 1994 on the San Carlos River (> 10,000 cfs, fig. 4, gauge

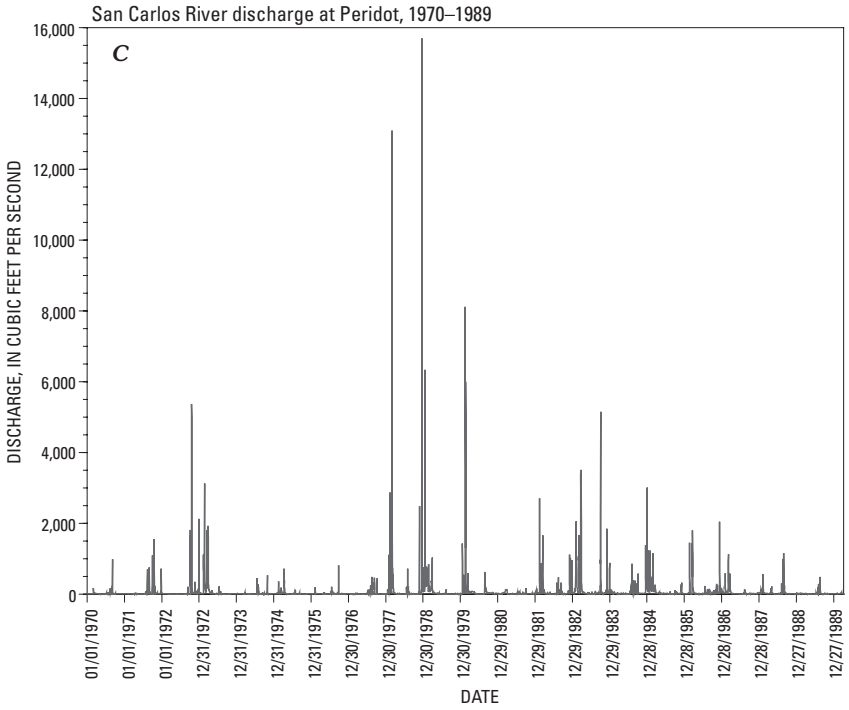

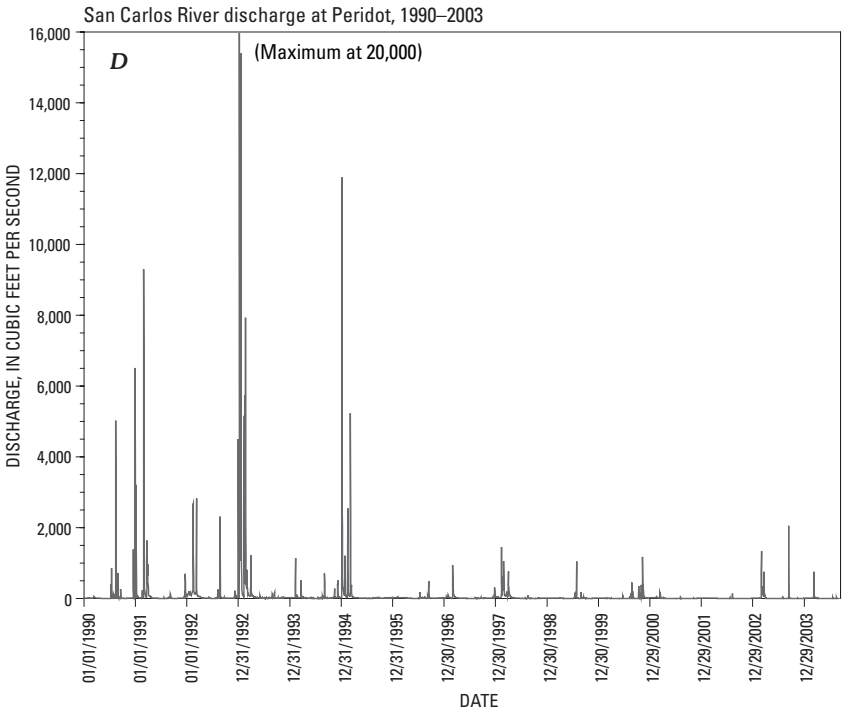

Table 1. Sources of data for San Carlos Reservoir depths by year.

Year(s)	Reference
1931	U.S. Geological Survey Water Supply Paper 719
1932	U.S. Geological Survey Water Supply Paper 734
1933	U.S. Geological Survey Water Supply Paper 749
1934	U.S. Geological Survey Water Supply Paper 764
1935	U.S. Geological Survey Water Supply Paper 789
1936	U.S. Geological Survey Water Supply Paper 809
1937	U.S. Geological Survey Water Supply Paper 829
1938	U.S. Geological Survey Water Supply Paper 859
1939	U.S. Geological Survey Water Supply Paper 879
1940	U.S. Geological Survey Water Supply Paper 899
1941	U.S. Geological Survey Water Supply Paper 929
1942	U.S. Geological Survey Water Supply Paper 959
1943	U.S. Geological Survey Water Supply Paper 979
1944	U.S. Geological Survey Water Supply Paper 1009
1945	U.S. Geological Survey Water Supply Paper 1039
1946	U.S. Geological Survey Water Supply Paper 1059
1947	U.S. Geological Survey Water Supply Paper 1089
1948	U.S. Geological Survey Water Supply Paper 1119
1949	U.S. Geological Survey Water Supply Paper 1149
1950	U.S. Geological Survey Water Supply Paper 1179
1951	U.S. Geological Survey Water Supply Paper 1213
1952	U.S. Geological Survey Water Supply Paper 1243
1953	U.S. Geological Survey Water Supply Paper 1283
1954	U.S. Geological Survey Water Supply Paper 1343
1955	U.S. Geological Survey Water Supply Paper 1393
1956	U.S. Geological Survey Water Supply Paper 1443
1957	U.S. Geological Survey Water Supply Paper 1513
1958	U.S. Geological Survey Water Supply Paper 1563
1959	U.S. Geological Survey Water Supply Paper 1633
1960	U.S. Geological Survey Water Supply Paper 1713

09468500). Flow on the San Carlos River also exceeded 17,000 cfs during the 1965 and the 1967 flood events.

According to Burkham (1972), major floods in the period from 1903–17 produced major changes in the Gila River flood plain, ripping out many of the cottonwoods and willows that stabilized the banks of the rivers and greatly widening the flood plain from a few hundred feet to more than 1,000–2,000 ft. These changes are shown by a series of three historical photographs in figure 5. Figure 5*A*, taken near Geronimo in 1909, and figure 5*B* taken near Calva in 1932 show a wide flood plain with an anastomosing river bed that occupies a broad flood plain. The Gila River has incised the flood plain and, beginning with its introduction in the 1920s, tamarisk or saltcedar has replaced the native flood-plain vegetation immediately upstream from the San Carlos Reservoir (fig. 5*B*). The 1964 photograph take near Calva (fig. 5*C*) shows how the tamarisk has taken over the flood plain, causing the Gila River to incise about 8 to 10 ft. The upper fine silt from the terrace-deposit samples (samples 04SCR129Ta to 04SCR129Tg) at Calva is interpreted to represent this major flood-plain reconstruction period. The thickness of this terrace deposit at the Bylas site (04SCR128, fig. 1) was more than 5 ft.

Geologic Setting

The Gila River upstream of the San Carlos Reservoir drains the southwestern border of the Colorado Plateau province in the headwaters of the San Francisco River into the Safford Valley, which is a graben in the Basin and Range province. Erosion in the headwaters of the San Francisco River has exposed deformed Precambrian schist and gneiss upon which were deposited both Paleozoic and Mesozoic marine sandstone, shale, and limestone. These rocks were intruded by granitic plutons ranging in age from about 70 to 55 Ma (Kamilli and Richard, 1998), some of which formed the porphyry Cu deposits at Morenci currently being exploited in the Clifton, Ariz., area (Lindgren, 1905). Following Basin-and-Range faulting in the early Tertiary, volcanic rocks from middle Miocene to Oligocene age (32–11 Ma; Richard and others, 2000; Kamilli and Richard, 1998) covered much of the Paleozoic and Mesozoic rocks exposed along the northern portion of the Gila River watershed. Tertiary volcanic rocks covered the Morenci deposit. Subsequent erosion in the late Tertiary, mostly from 13 to 4 Ma, resulted

Table 1. Sources of data for San Carlos Reservoir depths by year—*Continued*.

Year(s)	Reference
1961–1964	Surface Water Records for Arizona
1965–1974	Water-Resources Data for Arizona, Part 1: Surface-Water Records
1975	Water Resources Data for Arizona, U.S. Geological Survey Water-Data Report AZ-75-1
1976	Water Resources Data for Arizona, U.S. Geological Survey Water-Data Report AZ-76-1
1977	Water Resources Data for Arizona, U.S. Geological Survey Water-Data Report AZ-77-1
1978	Water Resources Data for Arizona, U.S. Geological Survey Water-Data Report AZ-78-1
1979	Water Resources Data for Arizona, U.S. Geological Survey Water-Data Report AZ-79-1
1980	Water Resources Data for Arizona, U.S. Geological Survey Water-Data Report AZ-80-1
1981	Water Resources Data for Arizona, U.S. Geological Survey Water-Data Report AZ-81-1
1982	Water Resources Data for Arizona, U.S. Geological Survey Water-Data Report AZ-82-1
1983	Water Resources Data for Arizona, U.S. Geological Survey Water-Data Report AZ-83-1
1984	Water Resources Data for Arizona, U.S. Geological Survey Water-Data Report AZ-84-1
1985	Water Resources Data for Arizona, U.S. Geological Survey Water-Data Report AZ-85-1
1986	Water Resources Data for Arizona, U.S. Geological Survey Water-Data Report AZ-86-1
1987	Water Resources Data for Arizona, U.S. Geological Survey Water-Data Report AZ-87-1
1988	Water Resources Data for Arizona, U.S. Geological Survey Water-Data Report AZ-88-1
1989	Water Resources Data for Arizona, U.S. Geological Survey Water-Data Report AZ-89-1
1990	Water Resources Data for Arizona, U.S. Geological Survey Water-Data Report AZ-90-1
1991	Water Resources Data for Arizona, U.S. Geological Survey Water-Data Report AZ-91-1
1992	Water Resources Data for Arizona, U.S. Geological Survey Water-Data Report AZ-92-1
1993	Water Resources Data for Arizona, U.S. Geological Survey Water-Data Report AZ-93-1
1994	Water Resources Data for Arizona, U.S. Geological Survey Water-Data Report AZ-94-1
1995	Water Resources Data for Arizona, U.S. Geological Survey Water-Data Report AZ-95-1
1996	Water Resources Data for Arizona, U.S. Geological Survey Water-Data Report AZ-96-1
1997	Water Resources Data for Arizona, U.S. Geological Survey Water-Data Report AZ-97-1
1998	Water Resources Data for Arizona, U.S. Geological Survey Water-Data Report AZ-98-1
1999	Water Resources Data for Arizona, U.S. Geological Survey Water-Data Report AZ-99-1
2000	Water Resources Data for Arizona, U.S. Geological Survey Water-Data Report AZ-00-1
2001	Water Resources Data for Arizona, U.S. Geological Survey Water-Data Report AZ-01-1
2002–2004	NWIS station number 09469000, San Carlos Reservoir at Coolidge Dam, Ariz.

in the formation of the supergene Cu ore body being mined today (Enders, 2000). According to Enders (2000), the ten areas mined at Morenci are all supergene ore deposits; that is, deposits are of secondary Cu minerals produced by weathering of primary chalcopyrite ore. The supergene enrichment process removed Cu mineralization from rocks exposed at the surface by weathering, and transported and redeposited the metal tens to hundreds of meters below the surface, below the paleo ground-water table. This process resulted in an increase in the grade and uniformity of the Cu deposit. The average grade of the supergene ore is 0.47 percent Cu (4,700 ppm) and 0.01 percent Mo (100 ppm) over a thickness of several hundred meters. By comparison, the leached caprock overlying the deposit contains only 700 ppm Cu and 80 ppm Mo (Enders, 2000). The Morenci deposit was dissected by Chase Creek and its tributaries, which deeply incised the leached caprock zone and eroded into the supergene enrichment zone prior to mining. Erosion from this drainage would have raised the premining Cu concentration in sediment supplied to the San Francisco River.

The Gila River basin also contains at least one additional discovered, but unmined, porphyry Cu deposit (Kamilli and Roberts, 1998). The Dos Pobres porphyry Cu deposit (fig, 1) contains 5.8 billion lb of Cu reserves (Keith and others, 1983). They also reported Cu production from the San Juan deposit (1903–78; 2,400 metric tons of Cu and 33 metric tons of base metal production) and the Lone Star deposit (1904–66; 110 metric tons of Cu and 4.5 metric tons of Pb), all of which are located on the south flank of the Gila Mountains, downstream from the Morenci porphyry Cu deposit. Subsequent erosion has filled the Safford Valley with thick deposits of Quaternary gravel (Houser and others, 1985), which exceeds 6,400 ft (> 1,950 m) in thickness near the town of Safford (Kamilli and Richard, 1998). Much of the sediment load carried by the Gila River to the San Carlos Reservoir is derived from erosion of this poorly consolidated alluvial-valley fill.

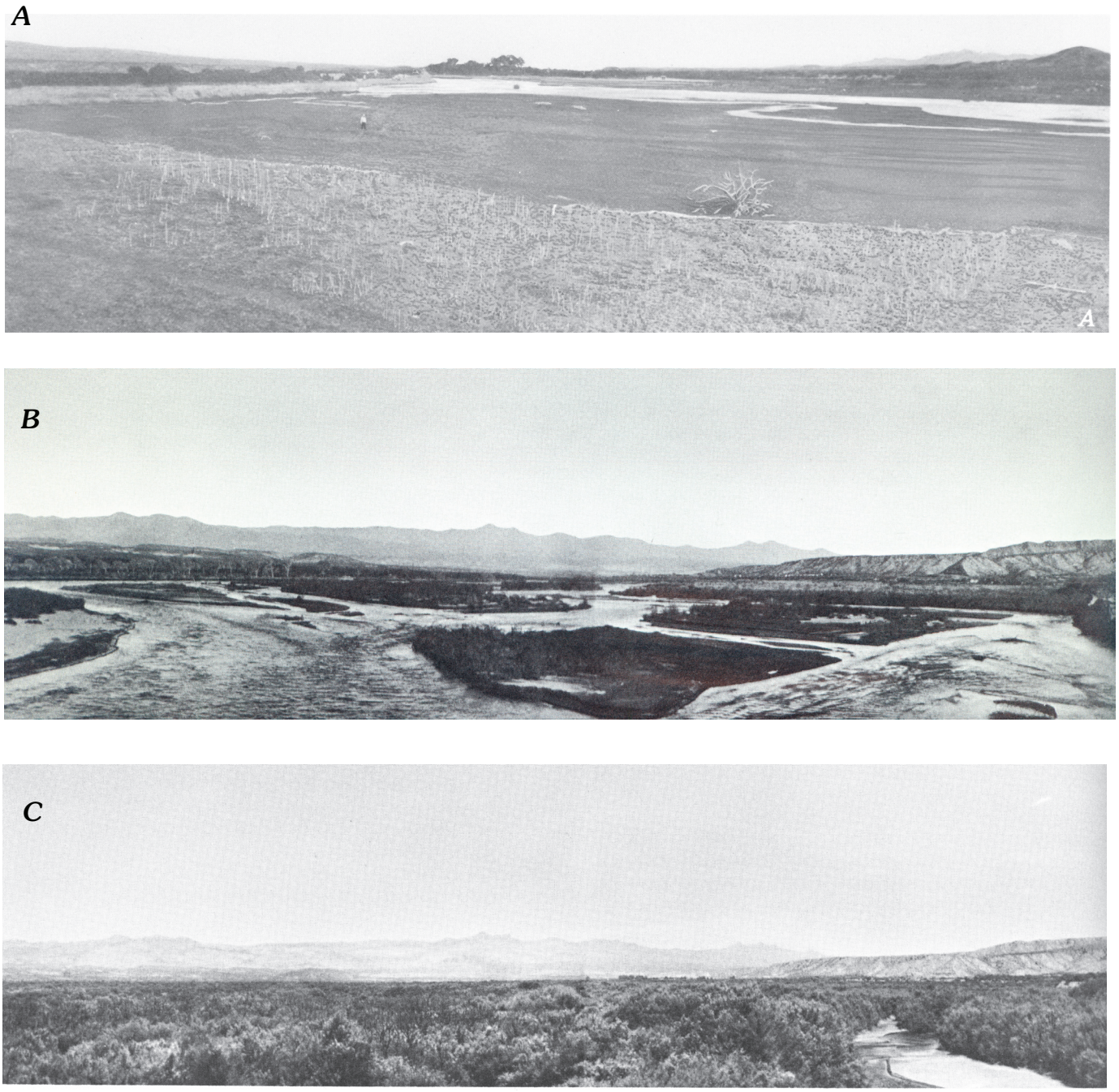

Figure 5. Historical photographs of the Gila River flood plain showing changes in riparian habitat and character of the flood plain. *A*, near Geronimo, 1909 (Burkham, 1972); *B*, near Calva, 1932 (Culler and others, 1970); *C*, near Calva, 1964 (Culler and others, 1970).

Sampling Methods

All samples were collected from Oct. 20–Oct. 29, 2004. There was one small rain storm during the period when the reservoir core samples were collected on October 28, but the amount of precipitation was small and inconsequential. Sample locations were determined using two different Garmin GPS units. In general, the GPS readings gave a small location error of ± 20 to 30 ft (6 to 9 m). All locality coordinates are reported with reference to the commonly used North American Datum of 1927 (NAD27).

Reservoir-Sediment Samples

Samples were taken at three localities in the reservoir using a 7.6-cm-diameter aluminum irrigation pipe and a gasoline-powered vibrator to penetrate the reservoir sediment.

Table 2. Locations, depth of penetration, and depth to ground-water table in cores from San Carlos Reservoir.

Core no.	Latitude (decimal degrees)	Longitude (decimal degrees)	Depth of penetration (cm)	Length* of core (cm)	Number of core segments	Depth to ground-water table (cm)
04SCR110	33.20500	–110.41491	203	142	4	174
04SCR111	33.21602	–110.36141	279	170	4	229
04SCR112	33.19218	–110.47103	365	305	1	--
04SCR115	33.18978	–110.46752	525	440	1	--

*Depths of core were not corrected for compaction; recovery of all cores was 100 percent except for core 04SCR115, in which the bottom 25 cm was lost.

Samples were taken from a small pontoon boat (figs. 6*A*, 6*B*). Maximum penetration was limited by the length of pipe used (20 ft; 6.1 m). The cores were cut into 5-ft (150 cm) sections in the field, sealed, and stored upright for transport to Denver, Colo. Two additional cores were driven by hand in the dry reservoir bed in the San Carlos River and the Gila River arms of the reservoir to document the metal concentrations being supplied from these two river drainage basins (fig. 1). These cores were extracted in short segments using a backhoe. Penetration was limited by high resistance, presumably caused by the high clay content of the sediment (fig. 7). Sample localities and depths of penetration are shown in table 2. Core 04SCR112 was collected on October 27; core 04SCR115 was collected on October 29. Stormy weather on October 28 resulted in the loss of core 04SCR113 and we had poor recovery of core 04SCR114; therefore, no samples from cores 04SCR113 or core 04SCR114 were analyzed. Because of the poor recovery in cores 04SCR113 and 04SCR114, we installed a brass core catcher at the base of the aluminum core tube used to collect core 04SCR115 to increase the probability that we would recover sediment at our final core site.

Analyses of the aluminum irrigation pipe and the brass core catcher material were performed to determine the composition of possible contaminants used during the sample collection. The aluminum irrigation pipe contained 0.6 percent Fe, 1.1 percent Mg, minor Ca, Na, Mn, and P, and 340 ppm Cr, 1,400 ppm Cu, 38 ppm Mo, 110 ppm Ni, 100 ppm V, and 1,000 ppm Zn. Microscopic examination of the samples from core 04SCR110 indicated no contamination by particles of the aluminum pipe occurred during the sawing process following cleaning of the exterior of the core. We saw no chemical evidence that any of the reservoir-sediment samples were contaminated by fragments of the aluminum core pipe. The brass core catcher used in core 04SCR115 broke free during insertion of the core. The brass contained about 62 percent Cu and 38 percent Zn with minor to trace amounts of Fe, Al, P, Ag, As, Ni, Sn, and Pb. We intentionally excluded sediment from along the walls of the core as well as along the trace of the brass core catcher from the geochemical sample prepared for analysis. We saw no chemical evidence that any of the samples in core 04SCR115 were contaminated by fragments of the core catcher, and, furthermore, we did not see any fragments of core-catcher material in the core samples.

Stream-Bed- and Terrace-Sediment Samples

In addition to the coring of sediment in the reservoir, stream-bed-sediment samples were taken where there was public access in the Gila, San Carlos, and San Francisco Rivers at irregularly spaced intervals to map the changes in metal concentrations in sediment from the Clifton, Ariz., area downstream to the reservoir. Sediment was collected at each locality using a long-handled, plastic (PVC, polyvinyl chloride) scoop from 5 to 10 sites along an interval of about 30 m of stream reach. Stream-bed sediment was sieved in the field using a stainless-steel < 2-mm screen until about 5 kilograms of fine sediment was accumulated in a plastic gold pan. This material was transferred to large plastic containers and sealed for transport to Denver, Colo., for further processing. Sample localities, plot distances, and the pH and conductivity of the river water are shown in table 3.

In addition to the stream-bed-sediment sampling, we also evaluated terrace deposits at three sites to determine the premining geochemical baseline. Samples were taken either by driving a 7.6-cm-diameter plastic pipe (PVC) into the terrace sediment (fig. 8*A*) when it consisted of unconsolidated silt or sand or by channel sampling the stratigraphic interval and sieving the sample in the field. Photographs of these three sites are in figure 8; localities are also shown in table 3.

Sample Processing

Stream-bed-sediment samples were air-dried in the laboratory prior to sample processing. Stream-bed-sediment and terrace-sediment samples were disaggregated, sieved to < 2 mm, split using a Jones splitter, and a representative sample sieved to < 80 mesh using stainless steel sieves. The resulting sample was then ground to <150 µm prior to chemical analysis. Samples are archived by the U.S. Geological Survey in Denver, Colo.

The reservoir cores were frozen upon arrival at our laboratories in Denver, Colo. The aluminum irrigation pipe was subsequently sawn longitudinally with a skill saw using a carbide blade, cutting the wall of the irrigation pipe and putting a shallow groove in the frozen reservoir sediment. The outside of the cores was rinsed with deionized water to remove

Figure 6. *A*, photograph of pontoon boat used for core sampling. Vibrator used to take vibracores shown on front of boat. *B*, photograph showing recovery of core 04SCR112, Stan Church (left) and Marci Marot (right) are removing the vibracore head from the core pipe.

Figure 7. Photograph showing core recovery at site 04SCR110 (Melvin Kindelay, backhoe operator). Dry reservoir bed is overgrown with cocklebur.

all traces of carbide, aluminum, and sediment dislodged during the pipe-cutting process. The cores were wrapped in plastic and refrozen. The frozen cores were subsequently split longitudinally using a new, cleaned hand saw, and the sawn surfaces were then scraped with a stainless-steel spatula to remove all loose material. Half of the core was wrapped in aluminum foil and frozen for subsequent organic analyses, and the other half of the core was placed in a locked laboratory to dry. About 2 weeks later, the cores were sampled for analysis. Descriptions of the samples and the sampled intervals are in tables A1–A4 in the Appendix (on CD-ROM). Photographs of the two cores showing the sampled intervals are in figures A1–A4 in the appendix (on CD-ROM). During sampling of the core, each interval (generally 5 cm) was gently crushed in the aluminum core pipe or disaggregated in a large ceramic mortar and pestle, and a chip sample was taken through the interval for chemical analysis. The geochemical samples were all taken from interior sites within the core to minimize possible cross-contamination by smearing along the core walls or along the sawn surfaces, or contamination by either the aluminum irrigation pipe or the brass core catcher (04SCR115). About 5–7 g of material was hand-ground in an agate mortar and pestle and submitted for chemical analysis; the balance of the material was submitted for geochronological analysis (tables A5–A8). Loss on ignition at 550°C was conducted on all core samples to obtain the final water-free sample weight. All geochemical data from the reservoir core samples are reported on a water-free basis (tables A9–A12 on CD-ROM).

Dioxin analyses were preformed by Severn Trent Laboratories, Inc. Chip samples of about 100 g each were taken from the frozen core over each analyzed interval using a cleaned steel chisel. The remainder of the core was preserved frozen for future organic analyses, if needed.

Analytical Methods

Radioisotope Methods

^{210}Pb activity was measured by alpha spectroscopy. The ^{210}Pb ($t_{1/2}$ = 22.3 years) alpha method is based on determining the activity of ^{210}Po, which is assumed to be in secular equilibrium with its parent ^{210}Pb. The analytical method exploits the ability of polonium to self-plate onto silver planchets, which facilitates the alpha counting (Flynn, 1968). Briefly, 5 g of sediment was hand-ground in a mortar and pestle and fired in a muffle furnace at 550°C for 6 hr to determine loss on ignition. The fired material was transferred to a glass beaker, ^{210}Po was acid-leached from the sediment, and a known activity of the tracer ^{209}Po was added to the solution prior to autoplating the polonium isotopes onto silver planchets. The planchets were counted in low-level alpha spectrometers coupled to a pulse-height analyzer. Randomly selected subsets of samples were analyzed in triplicate. Data from these replicate samples have a relative standard deviation of less than 5 percent. Excess ^{210}Pb activity was calculated by subtracting the ^{226}Ra activity from the total ^{210}Pb activity.

Gamma spectroscopy was used to determine the ^{7}Be ($t_{1/2}$ = 53 days), ^{137}Cs ($t_{1/2}$ = 30.2 years), and ^{226}Ra ($t_{1/2}$ = 1,600 years) activities in each sample (Cutshall and others, 1983). A 50-g aliquot of dried and ground sample was sealed in a plastic

Table 3. Stream-bed- and terrace-sediment sample localities with pH and conductivity measurements of river water.

[DD, decimal degrees. Collection dates in year 2004]

Sample number	Date collected	Latitude (DD)	Longitude (DD)	River	Locality	Distance from Coolidge Dam#	pH	Specific conductance (µS/cm)
04SCR101	20 Oct	33.20513	–110.41211	San Carlos	Upstream of river confluence	16	--	--
04SCR102	20 Oct	33.20694	–110.41085	San Carlos	Upstream of previous sample	17	--	--
04SCR103*	22 Oct	33.24959	–110.43752	San Carlos	Upstream of previous sample	24	--	--
04SCR120	25 Oct	33.07338	–109.29781	San Francisco	North of Clifton	198	7.52	838
04SCR121	25 Oct	33.03825	–109.29911	San Francisco	Downstream from Morenci in Clifton	191	7.17	1,530
04SCR122	25 Oct	32.94659	–109.25416	Gila	West of RR tracks at Guthrie	195	8.77	660
04SCR123	25 Oct	32.86139	–109.54319	Gila	Upstream of bridge north of Buena Vista	141	8.49	1,200
04SCR124*	25 Oct	32.82759	–109.63284	Gila	Upstream of bridge north of Solomon	129	8.53	1,220
04SCR125	25 Oct	32.91413	–109.82560	Gila	Upstream of bridge north of Pima	105	8.54	1,190
04SCR126	26 Oct	32.96039	–109.91381	Gila	Upstream of bridge west of Eden	92	8.42	1,300
04SCR127	26 Oct	33.04965	–109.96620	Gila	Upstream of bridge north of Ft. Thomas	77	8.20	2,560
04SCR128	26 Oct	33.12546	–110.10539	Gila	Bylas	58	8.42	2,950
04SCR129*	26 Oct	33.18757	–110.18305	Gila	Calva gauge	41	8.41	3,540

* Terrace samples also collected at these three localities.
\# Distance expressed in river kilometers upstream from gauge on Coolidge Dam.

counting jar. Sealed samples were stored for at least 20 days to allow ^{222}Ra and ^{214}Pb activity to come into equilibrium with their parent isotope (^{226}Ra). Samples were counted in a high-purity germanium detector for low-energy gamma rays (2,000 mm^2 active area) and data collected using an 8,191-channel multichannel analyzer. Samples were typically counted for 24 hours (depending on sample size) or until counting errors were less than 10 percent. The gamma system was calibrated using a National Institute of Standards and Technology (NIST) traceable multiline radioisotope standard in a soil matrix with the same counting geometry as the samples. Specific activity of ^{226}Ra was determined from counts associated with the photopeaks of ^{214}Pb (295 and 351 kev) and ^{214}Bi (609 kev). Activities calculated from the three peaks were combined to yield a weighted mean reported value and standard deviation. ^{7}Be and ^{137}Cs activities were determined by counting the 477-kev and 661.6-kev gamma-ray peaks, respectively. All activities were decay corrected to the date of sample collection. The reported errors are the statistical counting errors at the 95-percent confidence interval. Total analytical errors are about ±6.5 percent based on replicate sample analyses. Analytical data are reported in tables A5–A8 in the Appendix (on CD-ROM).

ICP-AES Analytical Method

All samples from the cores were digested using a four-acid digestion (HCl, HNO_3, $HClO_4$ and HF; Briggs, 2002). The resulting solutions were analyzed for 40 elements by ICP-AES (inductively coupled plasma–atomic emission spectroscopy) in the USGS laboratory in Denver, Colo. To monitor quality of the analyses, laboratory duplicates were analyzed to assess precision, and three standard reference materials (SRM-2709, SO-2, and SRG-1) were analyzed with each sample set to assess analytical accuracy. Precision and accuracy of the analyses of the standard reference materials (SRMs) are discussed below.

In addition, a subset of samples was leached in high-purity, 2M HCl–1 percent H_2O_2 (Church and others, 1997) to remove loosely bound or sorbed metals. These samples were subsequently analyzed by ICP-AES to determine metal concentrations. Leachate solutions were further processed and analyzed to determine their Pb isotope compositions.

ICP-MS Analytical Method

The same four-acid sample digestion procedure (Briggs, 2002) was used to prepare samples for the determination of trace metal concentrations by ICP-MS (inductively coupled plasma–mass spectrometry; Briggs and Meier, 2002). Immediately prior to analyses, the sample solutions were diluted by a factor of 10 using 2-percent distilled HNO_3. As the sample was injected, three internal standards (^{6}Li, Rh, and Ir) were mixed in line with the sample solution before analysis to monitor the stability of the ICP-MS during the analysis in the

Figure 8 (facing column and above). Photographs of terrace sample sites. *A*, site 04SCR103 on the San Carlos River. Stan Church is holding 7.6-cm-diameter PVC pipe that was driven into unconsolidated terrace deposit to preserve stratigraphy; *B*, site 04SCR124 on the Gila River near Solomon—6-ft (180 cm) tape shown for scale; *C*, site 04SCR129 on the Gila River near Calva—6-ft (180 cm) tape shown for scale. Upper 1-m section (white PVC pipe) is silt section that we interpret as that deposited during the 1905-1917 flood-plain reconstruction period (Burkham, 1972).

USGS laboratory in Denver, Colo. To monitor the quality of the analyses, laboratory duplicates were analyzed to assess precision, and four standard reference materials (MAG-1, SGR-1, SRM-2709, and SO-2) were analyzed with each sample set to assess the accuracy.

ICP-MS Pb Isotope Analytical Method

Leachate solutions from the 2M HCl–1 percent H_2O_2 digestion were evaporated to dryness in a laminar-flow hood. The residue was dissolved in a minimal volume of high-purity 9M HBr and again evaporated to dryness to change the acid medium. The residue was dissolved in 5 mL of 0.5M HBr, centrifuged, and loaded onto a 1-mL (free column volume, FCV) AG 1X8 ion exchange column to separate the Pb from other ions. After washing the column with dilute HBr followed by dilute HCl, Pb was eluted in 8M HCl and an aliquot was diluted to a concentration of approximately 25 µg/L Pb with 2 percent HNO_3. This solution was spiked to produce a 10 µg/L solution of Tl. The solution was aspirated through a desolvation chamber and into an argon plasma. Lead isotope analyses were performed on a Nu Plasma, high-resolution, double focusing, multicollector ICP-MS. A 25-µg/L solution of Pb gave about 3 volts of ^{208}Pb signal. Forty-five isotope ratio measurements were collected over a period of about 7 minutes, and each observed ratio was normalized to a ^{205}Tl/^{203}Tl value of 2.3871. Seven replicate analyses of SRM-981 were run over the course of the Pb isotope analyses to monitor precision and accuracy. The isotope ratios determined for SRM-981 were within 1 part in 10,000 of the NIST-certified values.

Hg Analytical Method

Analyses for total Hg were determined using continuous-flow cold-vapor atomic absorption spectrometry (Brown and others, 2002). Limits of determination using a 1 g sample were 2 ng/g. Analyses of blind duplicate samples are in good agreement, and data from of SRM materials compare well with accepted published values.

Analytical Method 8290 for Dioxins/Furans

The frozen half of core 04SCR112 was subsampled in 30-cm increments and sent to Severn Trent Laboratories, Inc. (STL), for dioxins/furans analysis, Dioxins are an impurity produced in the manufacturing of the herbicide 2,4,5-trichlorophenoxyacetic acid (2,4,5-T). Seventeen polychlorinated dibenzo-p-dioxins/polychlorinated dibenzo-furans (PCDD/PCDF) congener concentrations are necessary to calculate the toxic equivalent concentration (TEQ) of dioxin. The term dioxin will be used throughout the text to refer to this class of organic compounds. The TEQ was calculated to provide a single value normalized to the toxicity of 2,3,7,8-TCDD that is comparable with benchmark values. Samples were analyzed using United States Environmental Protection Agency (U.S. EPA) test method 8290 (1994). This method requires that ^{13}C labeled analogs of the target analytes be spiked into each sample before extraction. These analogs elute and behave the same as the target analytes, without interfering with the analysis. Since the effects of extraction, cleanup, concentration, and gas chromatography are the same for the analogs and target analytes, recovery correction of the PCDD/PCDF can be performed. Target analytes are quantified relative to the labeled (isotope) analog, and, therefore, their calculated concentration compensates for extraction and cleanup efficiencies (STL, written commun., 2005). The extraction procedure uses a combination of a Dean-Stark water trap and a Soxhlet extractor using toluene. The toluene extracts are cleaned using an acid-base washing treatment and dried. The extract is processed through a solvent exchange, then cleaned up using column chromatography on alumina, silica gel, and activated carbon. The extract is analyzed by injecting 2 µL of solution into a high-resolution gas chromatograph/high-resolution mass spectrometer (HRGC/HRMS). Method 8290 is for samples that contain low concentrations of dioxins/furans (in the part-per-trillion (ppt) to part-per-quadrillion (ppq) range) (U.S. EPA, 1994). Concentrations of the following congeners for PCDD/PCDF were determined: 2,3,7,8-tetrachlorinated dibenzo-p-dioxin (TCDD), 1,2,3,7,8-pentachlorinated dibenzo-p-dioxin (PeCDD), 1,2,3,6,7,8-hexachlorinated dibenzo-p-dioxin (HxCDD), 1,2,3,7,8,9-HxCDD, 1,2,3,4,7,8-HxCDD, 1,2,3,4,6,7,8-heptachlorinated dibenzo-p-dioxins (HpCDD), 1,2,3,4,6,7,8,9-octachlorinated dibenzo-p-dioxins (OCDD), 2,3,7,8-tetrachlorinated dibenzofuran (TCDF), 1,2,3,7,8-pentachlorinated dibenzofuran (PCDF), 2,3,4,7,8-PCDF, 1,2,3,6,7,8-hexachlorinated dibenzofuran (HxCDF), 1,2,3,7,8,9-HxCDF, 1,2,3,4,7,8-HxCDF, 2,3,4,6,7,8-HxCDF, 1,2,3,4,6,7,8-heptachlorinated dibenzofuran (HpCDF), 1,2,3,4,7,8,9-HpCDF, and 1,2,3,4,6,7,8,9-octachlorinated dibenzofuran (OCDF). Results from these analyses are reported in picograms per gram dry weight sediment (pg/g). Each of the above PCDD/PCDF congeners is assigned an international toxicity equivalent factor (I-TEF) (NATO/CCMS, 1988) relating their toxicity to that of 2,3,7,8-TCDD. The individual I-TFE is multiplied by the concentration of the PCDD/PCDF congener, then they are summed together to obtain the TEQ value. STL analyzed one batch-specific Laboratory Control Sample per batch of 20 samples as an ongoing system and standard check for quality control (STL, written commun., 2005).

Statistical Analysis of Element Concentration Results from Standard Reference Materials

Standard reference materials (SRMs) were analyzed along with the samples by both ICP-AES and ICP-MS. The ICP-AES method analyzed three SRMs: NIST-2709, SGR-1,

and SO-2, and the ICP-MS analyzed these three SRMs and MAG-1. These results and the certified values for the SRM are presented in table 4. The accuracy of these methods can be determined by comparing the certified value of the SRM with that obtained from the analysis, whereas the precision of the data can be determined by the standard deviation and relative standard deviation. There is no statistical difference in the data produced by these two analytical methods. Because the detection limits for the ICP-MS are lower, the ICP-MS data were used whenever the concentrations were low for a selected element. The stability of the ICP-AES instrument and the accuracy and precision of the data determined are demonstrated by replicate analyses of these SRMs reported by Fey and others (1999). They analyzed three NIST standard reference materials (SRM-2704, SRM-2709, SRM-2711) more than 50 times over a 3-year period, 1996–98, and found the data to be stable. This report can be accessed at URL http://pubs.usgs.gov/of/1999/ofr-99-0575/.

Results and Discussion

Radioisotope Results

^{137}Cs is a thermonuclear radioisotope resulting from atmospheric testing of nuclear weapons. Most of the early U.S. atmospheric testing was conducted at the Nevada Test Site during the late 1950s. Maxima for ^{137}Cs activity occurred as a result of this atmospheric nuclear testing between 1953 and 1959. Atmospheric testing, measured in terms of the yield of the nuclear weapon, would result in the highest ^{137}Cs activity being released to the atmosphere between 1951–53 (>450 kt) and 1955–58 (>650 kt; http://www.fas.org/nuke/guide/usa/nuclear/usnuctests.hml). Plots showing fallout from atmospheric nuclear testing at the Nevada Test Site (Simon and others, 2004) indicate that ^{137}Cs deposition density from the U.S. nuclear testing should be a factor of 10 less than the density of ^{137}Cs from global fallout resulting from testing in the early 1960s in the Pacific. According to Horowitz and others (1996), the earliest detectable ^{137}Cs activity in sediment occurred in 1953–54. Atmospheric testing in the Pacific peaked from 1962–64 resulting in a second ^{137}Cs activity peak. ^{137}Cs is swept out of the atmosphere by rain and sorbed onto clays in the soil. Surface erosion results in accumulation of ^{137}Cs in sedimentary deposits in lakes and reservoirs. Because the ^{137}Cs peaks represent essentially one-time surficial events, ^{137}Cs accumulates rapidly in lakes and reservoirs and then simply decays in situ with time.

Unlike ^{137}Cs, ^{210}Pb is a part of the ^{238}U radioactive decay series. This series is dynamic; that is, ^{210}Pb is being replenished continuously through time by radioactive decay. During the ^{238}U decay process, ^{226}Ra decays to ^{222}Rn, a gas with a half-life of 3.8 days. A small percentage of ^{222}Rn gas escapes from the rocks at the Earth's surface into the atmosphere where it decays to form ^{210}Pb, which is swept out of the atmosphere by rain. ^{210}Pb is subsequently sorbed to the surface of clays and oxides in the soil and transported to streams, rivers, and ultimately lakes, reservoirs, or the ocean by erosion. In using the ^{210}Pb method to date sediment, one must determine the incident flux of ^{210}Pb in the reservoir. This value, denoted A_o, is measured in the surface sediment layer in the reservoir (Robbins, 1978). ^{7}Be, a cosmogenic nuclide with a half life of 53 days, is used to demonstrate whether this top surface layer was sampled. The determination of the age of the sediment requires that the amount of ^{210}Pb derived from atmospheric sources be determined. In order to obtain that value, the amount of ^{210}Pb supported by radioactive decay by minerals in the sediment must be subtracted from the total ^{210}Pb present. This is done by subtracting the ^{226}Ra activity measured in the sample from the total ^{210}Pb to determine the excess or unsupported ^{210}Pb activity. The equation for the determination of the decay of ^{210}Pb is:

$$A = A_o e^{-\lambda t}$$

where

A is the measured ^{210}Pb activity at some time t,

A_o is the initial ^{210}Pb activity at the sediment-water interface, and

λ is the decay constant for ^{210}Pb (0.03114).

^{210}Pb decay curves for A_o values between 1.0 and 3.5 are shown in figure 9*A*.

Radioisotope geochronology, under ideal conditions, gives the best chronologic results when both the flux rate for the radioisotope over the basin and the sediment-accumulation rate in the reservoir are uniform. ^{137}Cs is sorbed by clay particles in the soil and ^{210}Pb is sorbed by oxides and clay particles in the soil and transported to the reservoir by erosion. Thus, the intensity of the ^{210}Pb or ^{137}Cs activity measured in lake-bed sediment is highly dependent upon the sediment-accumulation rate. Radioisotope flux rates are measured in terms of the activity per unit area per year and are expressed in samples as the number of disintegrations per minute per gram (dpm/g). The radioisotope data measured in samples from the four cores are in tables A5–A8 in the Appendix. Theoretical curves for the deposition and decay of ^{210}Pb and the deposition of ^{137}Cs are shown in figure 9*B*. The 1963 ^{137}Cs peaks are present in all four cores (figs. 10–13) and are always interpreted to represent these dates and to provide anchor points for the interpretation of the ^{210}Pb data.

The 1963 ^{137}Cs peaks occur at nominally similar depths in all four cores: 04SCR110 at a depth of 110 cm, in core 04SCR111 at a depth of 145 cm, in core 04SCR112 at a depth of 180 cm, and in core 04SCR115 at a depth of 190 cm (figs. 10–13). The depths of the 1963 ^{137}Cs activity becomes progressively deeper in the cores as one might expect given the physiographic setting and sediment loads provided by the San Carlos and Gila Rivers (fig. 1). A second ^{137}Cs peak occurs in cores 04SCR112 (210–265 cm) and 04SCR115 (260–295 cm). This second peak is interpreted to be the ^{137}Cs activity resulting from the early atmospheric testing at the Nevada

Table 4. Summary of analytical data from standard reference materials.

[ICP-AES, inductively coupled plasma–atomic emission spectrometry; ICP-MS, inductively coupled plasma–mass spectrometry; *n*, number of samples analyzed; certified values from Potts and others (1992)]

Standard reference material		ICP-AES Na (wt. percent)	ICP-MS Na (ppm)	ICP-AES K (wt. percent)	ICP-MS K (ppm)	ICP-AES Mg (wt. percent)	ICP-MS Mg (ppm)	ICP-AES Ca (wt. percent)	ICP-MS Ca (ppm)	ICP-AES Fe (wt. percent)	ICP-MS Fe (ppm)
MAG-1	Median		28,600		30,100		18,700		9,860		48,600
	Mean		28,480		30,030		18,880		9,939		48,720
	Standard deviation		691		545		396		150		832
	Relative standard deviation (%)		2.4		1.8		2.1		1.5		1.7
	Percent recovery		100		102		104		102		102
	n		5		5		5		5		5
	CERTIFIED VALUE (ICP-MS)		28,400		29,500		18,090		9,790		47,600
SRM-2709	Median	1.2	11,300	2.0	19,700	1.5	15,400	1.9	18,900	3.5	35,000
	Mean	1.2	11,420	2.0	19,900	1.5	15,620	1.9	18,920	3.5	34,940
	Standard deviation	0.0	277	0.0	453	0.0	449	0.1	444	0.0	720
	Relative standard deviation (%)	0.0	2.4	0.0	2.3	0.0	2.9	2.8	2.3	1.4	2.1
	Percent recovery	103	98	99	98	99	103	103	100	101	100
	n	7	5	7	5	7	5	7	5	7	5
	CERTIFIED VALUE (ICP-MS)		11,600		20,300		15,100		18,900		35,000
SGR-1	Median	2.3	21,950	1.4	12,900	2.6	27,500	5.9	58,100	2.0	20,000
	Mean	2.4	22,025	1.4	13,000	2.7	27,450	6.1	58,325	2.1	19,750
	Standard deviation	0.2	741	0.1	510	0.2	1,396	0.5	2,193	0.2	500
	Relative standard deviation (%)	8.1	3.4	7.7	3.9	7.4	5.1	8.4	3.8	7.3	2.5
	Percent recovery	106	99	101	94	101	103	101	97	99	93
	n	7	4	7	4	7	4	7	4	7	4
	CERTIFIED VALUE (ICP-MS)		22,181		13,776		26,779		59,900		21,189
SO-2	Median	1.8	17,800	2.4	23,500	0.5	5,320	1.9	18,800	5.5	54,000
	Mean	1.8	17,580	2.4	23,300	0.5	5,241	1.9	18,670	5.5	53,830
	Standard deviation	0.0	602	0.1	696	0.0	235	0.0	494	0.1	1,340
	Relative standard deviation (%)	2.7	3.4	2.9	3.0	2.1	4.5	2.5	2.6	1.6	2.5
	Percent recovery	96	93	99	95	98	97	98	95	99	97
	n	7	5	7	5	7	5	7	5	7	5
	CERTIFIED VALUE (ICP-MS)		19,000		24,500		5,424		19,600		55,600

Table 4. Summary of analytical data from standard reference materials—*Continued*.

Standard reference material		ICP-AES Al (wt. percent)	ICP-MS Al (ppm)	ICP-AES Ti (wt. percent)	ICP-MS Ti (ppm)	ICP-AES P (wt. percent)	ICP-MS P (ppm)	ICP-AES As (ppm)	ICP-MS As (ppm)	ICP-AES Ba (ppm)	ICP-MS Ba (ppm)
MAG-1	Median		86,200		4,200		720.0		10.4		495.0
	Mean		85,660		4,164		733.3		10.3		493.6
	Standard deviation		2,066		107.1		22.5		0.8		7.2
	Relative standard deviation (%)		2.4		2.6		3.1		7.7		1.5
	Percent recovery		99		92.5		103.1		112		103.0
	n		5		5		5		5		5
	CERTIFIED VALUE (ICP-MS)		86,660		4,500		711.0		9.2		479.0
SRM-2709	Median	7.4	73,600	0.3	3,500	0.1	640.0	<20	18.8	950.0	951.0
	Mean	7.4	74,470	0.3	3,509	0.1	642.9		18.8	935.7	950.3
	Standard deviation	0.2	2,084	0.0	144.6	0.0	18.6		0.8	52.6	12.6
	Relative standard deviation (%)	2.2	2.8	1.1	4.1	0.0	2.9		4.4	5.6	1.3
	Percent recovery	99	99	100	102.6	100	103.7		106	96.7	98.2
	n	7	5	7	5	7	5		5	7	5
	CERTIFIED VALUE (ICP-MS)		75,000		3,420		620.0		17.7		968.0
SGR-1	Median	3.5	33,200	0.1	1,450	0.1	1,300	75.0	65.5	280.0	282.5
	Mean	3.5	33,725	0.1	1,450	0.1	1,275	71.6	65.5	274.3	283.0
	Standard deviation	0.3	1,700	0.0	57.7	0.0	50.0	6.5	2.4	16.2	9.3
	Relative standard deviation (%)	7.7	5.0	5.7	4.0	9.5	3.9	9.0	3.6	5.9	3.3
	Percent recovery	101	98	78	93.0	82	89.1	107	98	94.6	97.6
	n	7	4	7	4	7	4	7	4	7	4
	CERTIFIED VALUE (ICP-MS)		34,516		1,559		1,432		67.0		290.0
SO-2	Median	8.0	78,700	1.0	9,100	0.3	3,300	<20	2.0	1,000	1,020
	Mean	8.0	77,690	0.9	9,136	0.3	3,296		2.1	1,001	1,024
	Standard deviation	0.1	2,669	0.0	263.6	0.0	141.7		1.0	99.2	20.2
	Relative standard deviation (%)	1.0	3.4	3.8	2.9	2.2	4.3		46.2	9.9	2.0
	Percent recovery	99	96	110	106.4	103	109.5			100.1	102.4
	n	7	5	7	5	7	5		5	7	5
	CERTIFIED VALUE (ICP-MS)		80,700		8,584		3,010		1.2		1,000

Table 4. Summary of analytical data from standard reference materials—*Continued*.

Standard reference material		ICP-AES Cd (ppm)	ICP-MS Cd (ppm)	ICP-AES Co (ppm)	ICP-MS Co (ppm)	ICP-AES Cr (ppm)	ICP-MS Cr (ppm)	ICP-AES Cu (ppm)	ICP-MS Cu (ppm)	ICP-AES Mn (ppm)	ICP-MS Mn (ppm)
MAG-1	Median		0.21		21.6		108.0		29.3		756.0
	Mean		0.21		21.6		108.2		29.4		753.5
	Standard deviation		0.01		0.6		2.5		0.8		13.7
	Relative standard deviation (%)		4.02		2.6		2.3		2.7		1.8
	Percent recovery		103		106		112		98		99
	n		5		5		5		5		5
	CERTIFIED VALUE (ICP-MS)		0.20		20.4		97.0		30.0		760.0
SRM-2709	Median	<4	0.37	10.0	12.9	130.0	124.0	31.0	34.3	550.0	546.0
	Mean		0.38	14.3	13.0	125.7	121.6	31.3	34.3	548.6	546.1
	Standard deviation		0.02	5.3	0.3	5.3	5.1	1.1	0.7	22.7	15.4
	Relative standard deviation (%)		5.68	37.4	2.7	4.3	4.2	3.6	2.0	4.1	2.8
	Percent recovery		101	107	97	97	94	90	99	102	102
	n		5	7	5	7	5	7	5	7	5
	CERTIFIED VALUE (ICP-MS)		0.38		13.4		130.0		34.6		538.0
SGR-1	Median	<4	1.10	10.0	11.6	28.0	32.8	63.0	61.7	240.0	236.5
	Mean		1.10	9.9	11.7	28.0	33.1	65.3	62.1	244.3	238.8
	Standard deviation		0.00	0.4	0.4	2.5	1.0	5.2	1.4	22.3	8.3
	Relative standard deviation (%)		0.00	3.8	3.3	9.0	3.1	8.0	2.2	9.1	3.5
	Percent recovery		118	84	99	93	110	99	94	93	91
	n		4	7	4	7	4	7	4	7	4
	CERTIFIED VALUE (ICP-MS)		0.93		11.8		30.0		66.0		263.4
SO-2	Median	<4	0.14	8.0	7.3	<2	10.9	<2	8.2	710.0	699.0
	Mean		0.14	7.7	7.3		10.9		8.3	704.3	695.5
	Standard deviation		0.01	2.4	0.2		0.3		1.2	17.2	16.0
	Relative standard deviation (%)		3.80	31.5	3.1		3.2		14.1	2.4	2.3
	Percent recovery		111	69	66		89		104	98	97
	n		5	7	5		5		5	7	5
	CERTIFIED VALUE (ICP-MS)		0.13		11.1		12.3		8.0		720.0

Table 4. Summary of analytical data from standard reference materials—*Continued.*

Standard reference material		ICP-AES Mo (ppm)	ICP-MS Mo (ppm)	ICP-AES Ni (ppm)	ICP-MS Ni (ppm)	ICP-AES Pb (ppm)	ICP-MS Pb (ppm)	ICP-AES Sr (ppm)	ICP-MS Sr (ppm)	ICP-AES Th (ppm)	ICP-MS Th (ppm)
MAG-1	Median		1.0		51.5		25.4		143.0		12.4
	Mean		1.0		52.2		25.1		142.4		12.4
	Standard deviation		0.1		1.5		1.0		2.6		0.3
	Relative standard deviation (%)		5.4		2.8		4.1		1.8		2.4
	Percent recovery		65		99		105		98		104
	n		5		5		5		5		5
	CERTIFIED VALUE (ICP-MS)		1.6		53.0		24.0		146.0		11.9
SRM-2709	Median	<4	2.1	80.0	82.7	10.0	17.6	230.0	225.0	10.0	11.0
	Mean			79.1	83.6	11.4	17.6	230.0	226.3	9.3	11.1
	Standard deviation		0.1	4.8	3.9	3.8	0.5	0.0	3.6	1.0	0.1
	Relative standard deviation (%)			6.0	4.7	33.1	3.0	0.0	1.6	10.2	1.1
	Percent recovery		0	90	95	60	93	100	98	84	100
	n		5	7	5	7	5	7	5	7	5
	CERTIFIED VALUE (ICP-MS)		2.0		88.0		18.9		231.0		11.0
SGR-1	Median	<4	31.9	28.0	28.0	41.0	41.2	400.0	387.5	<8	4.7
	Mean		31.8	28.1	27.8	40.6	41.2	411.4	386.0		4.7
	Standard deviation		0.4	3.0	1.1	4.2	0.7	28.5	12.8		0.0
	Relative standard deviation (%)		1.1	10.5	3.9	10.3	1.7	6.9	3.3		0.0
	Percent recovery		91	97	96	107	108	98	92		98
	n		4	7	4	7	4	7	4		4
	CERTIFIED VALUE (ICP-MS)		35.1		29.0		38.0		420.0		4.8
SO-2	Median	<4	1.5	<4	3.0	20.0	18.0	340.0	342.0	<8	3.6
	Mean		1.5		3.1	19.1	17.9	341.4	337.7		3.8
	Standard deviation		0.1		0.6	4.2	0.3	12.1	10.2		0.3
	Relative standard deviation (%)		3.6		18.7	21.8	1.6	3.6	3.0		7.8
	Percent recovery		77			96	89	103	102		97
	n		5		5	7	5	7	5		5
	CERTIFIED VALUE (ICP-MS)		2.0				20.0		331.0		3.9

Table 4. Summary of analytical data from standard reference materials—*Continued*.

Standard reference material		ICP-AES U (ppm)	ICP-MS U (ppm)	ICP-AES V (ppm)	ICP-MS V (ppm)	ICP-AES Zn (ppm)	ICP-MS Zn (ppm)
MAG-1	Median		2.70		142.0		135.0
	Mean		2.72		143.2		135.1
	Standard deviation		0.08		2.2		1.9
	Relative standard deviation (%)		2.99		1.5		1.4
	Percent recovery		101		102		104
	n		5		5		5
	CERTIFIED VALUE (ICP-MS)		2.70		140.0		130.0
SRM-2709	Median	<200	2.90	110.0	113.5	100.0	106.0
	Mean		2.93	110.0	113.5	100.0	106.2
	Standard deviation		0.05	0.0	2.1	0.0	1.9
	Relative standard deviation (%)		1.63	0.0	1.8	0.0	1.8
	Percent recovery		98	98	101	94	100
	n		5	7	5	7	5
	CERTIFIED VALUE (ICP-MS)		3.00		112.0		106.0
SGR-1	Median	<200	5.35	120.0	127.0	72.0	74.3
	Mean		5.38	125.7	128.5	73.0	74.2
	Standard deviation		0.10	7.9	3.8	5.9	1.8
	Relative standard deviation (%)		1.78	6.3	2.9	8.1	2.4
	Percent recovery		100	98	100	99	100
	n		4	7	4	7	4
	CERTIFIED VALUE (ICP-MS)		5.40		128.0		74.0
SO-2	Median	<200	0.72	56.0	56.1	120.0	127.0
	Mean		0.73	56.0	55.9	120.0	127.3
	Standard deviation		0.02	1.2	0.8	0.0	3.7
	Relative standard deviation (%)		2.09	2.1	1.5	0.0	2.9
	Percent recovery		76	94	94	98	103
	n		5	7	5	7	5
	CERTIFIED VALUE (ICP-MS)		0.96		59.4		123.0

Test Site. The ^{137}Cs peak from the 1950s atmospheric nuclear testing in core 04SCR115 (fig. 13) shows a smoothed version of the ^{137}Cs peak (fig. 9*B*) that would result from erosion. This same peak in core 04SCR112, however, is sharper and occurs over a shorter core interval. We interpret this phenomenon to be the result of the fact that the reservoir bed was dry at this site during much of the 1950s (fig. 2). The total ^{137}Cs activity for the two lower curves in cores 04SCR112 and 04SCR115 is comparable (about 12.0 and 11.4 dpm/g, respectively). These data indicate a lower sediment-accumulation rate at site 04SCR112 than at site 04SCR115, which is located in the Gila River channel in the reservoir. This observation is confirmed by the presence of Cu peaks found in at deeper levels in core 04SCR115 as discussed below. There is no ^{137}Cs activity in core 04SCR115 below 350 cm, indicating that material below this level in the core predates 1953.

According to Robbins (1978), interpretation of the ^{210}Pb geochronological data is straightforward when the sediment-accumulation rate is relatively uniform. Unfortunately, this is not generally the case for the cores collected from irrigation reservoirs such as the San Carlos Reservoir (Horowitz and others, 1996). The four cores have a range of values for A_o, and only core 04SCR110 has a detectable ^{7}Be anomaly. The ^{7}Be anomaly at the surface layer in the core collected from the San Carlos River arm (table A5) indicates that the material from this site was undisturbed by erosion prior to sampling. The ^{210}Pb activity at the surface of core 04SCR110 was higher than that observed at the surface in either of the two reservoir cores (04SCR112 or 04SCR115), resulting in a higher calculated A_o in core 04SCR110 than that calculated for sediment in the two reservoir cores (figs. 12 and 13, tables A7 and A8). Furthermore, the shapes of the excess ^{210}Pb curves from cores from the arms (04SCR110 and 04SCR111) have near-zero excess ^{210}Pb values below about 50 cm and do not fit an exponential decay curve. This is likely the result of lower clay and oxide content in the cores resulting from sediment accumulation in a more deltaic setting. Due to this discontinuous sedimentation history for the two sites sampled on the San

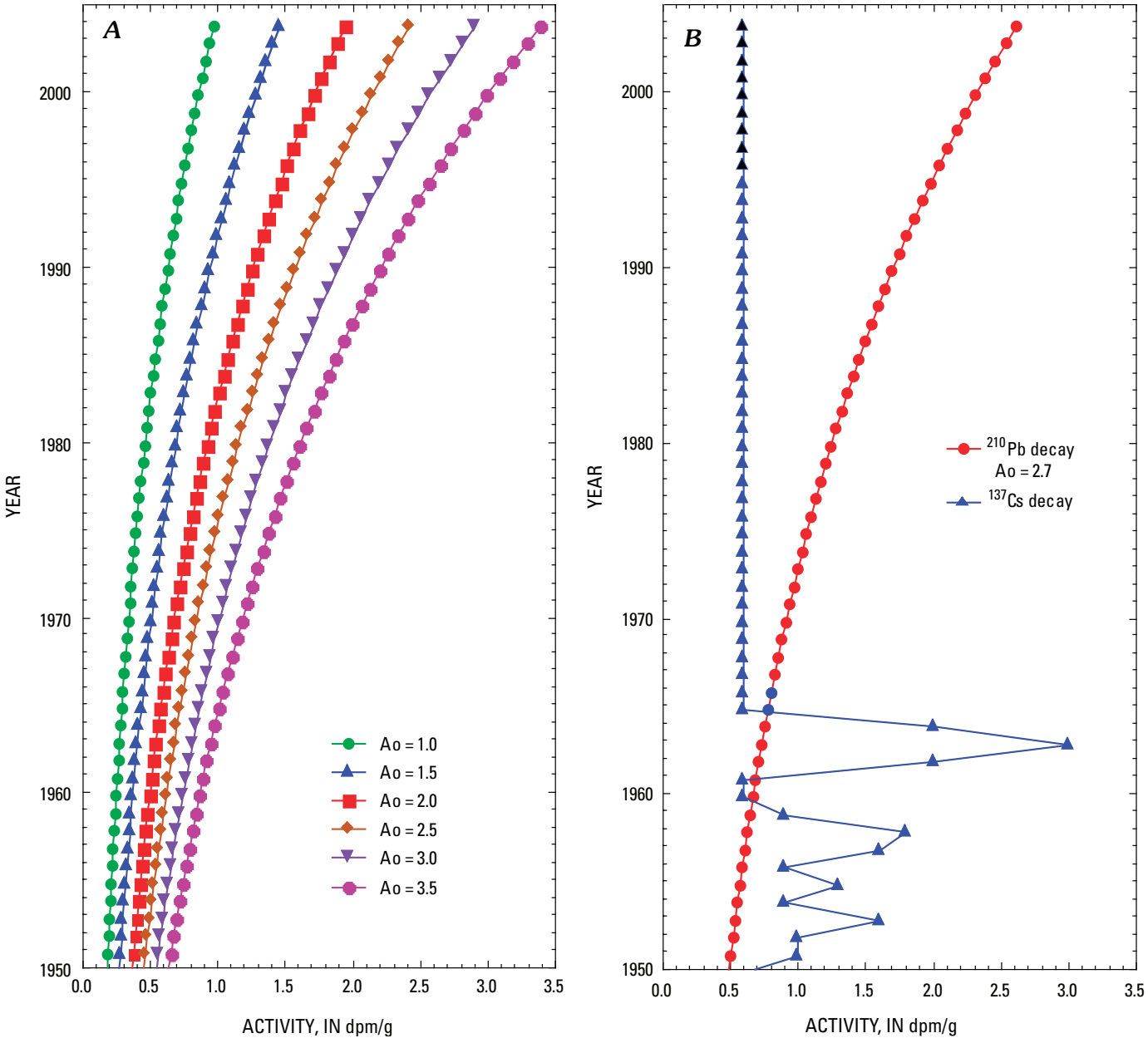

Figure 9. *A*, plot of decay curves for ^{210}Pb at different A_o values. *B*, theoretical ^{210}Pb and ^{137}Cs observed activity curves versus time. ^{137}Cs activity scaled in proportion to bomb yields. ^{137}Cs activity in sediment was too low prior to 1953 to detect today. Activity units (dpm/g) are disintegrations per minute per gram.

Carlos and Gila River arms of the reservoir, only the ^{137}Cs peak (1963) will be used to provide geochronological information from those cores. The ^{137}Cs data will be used to correlate the radioisotope data with the Cu anomalies discussed below. Secondly, the depth of penetration of these two cores was not as deep as those from the reservoir and there is no indication of the 1953–59 ^{137}Cs peak. Thus, the oldest sediment collected from these two cores would date from about 1960.

Penetration into the reservoir sediment by cores 04SCR112 and 04SCR115 resulted in recovery of much older material. However, the low values of A_o and the irregular nature of the excess ^{210}Pb data (figs. 12 and 13) make it difficult to provide a precise ^{210}Pb chronology. The fluctuation of water levels in the reservoir (fig. 2), which resulted in a dry lake bed, particularly in the 1950s, is a good indication that the uniform-sediment-accumulation model assumed by the ^{210}Pb dating method has not been met. Because there are many similarities between the geochemistry and the ^{210}Pb activity of these two cores (figs. 12 and 13), and because the two cores were taken only about 100 ft apart in the reservoir, the interpretation of the ^{210}Pb geochronology will be developed only for core 04SCR112.

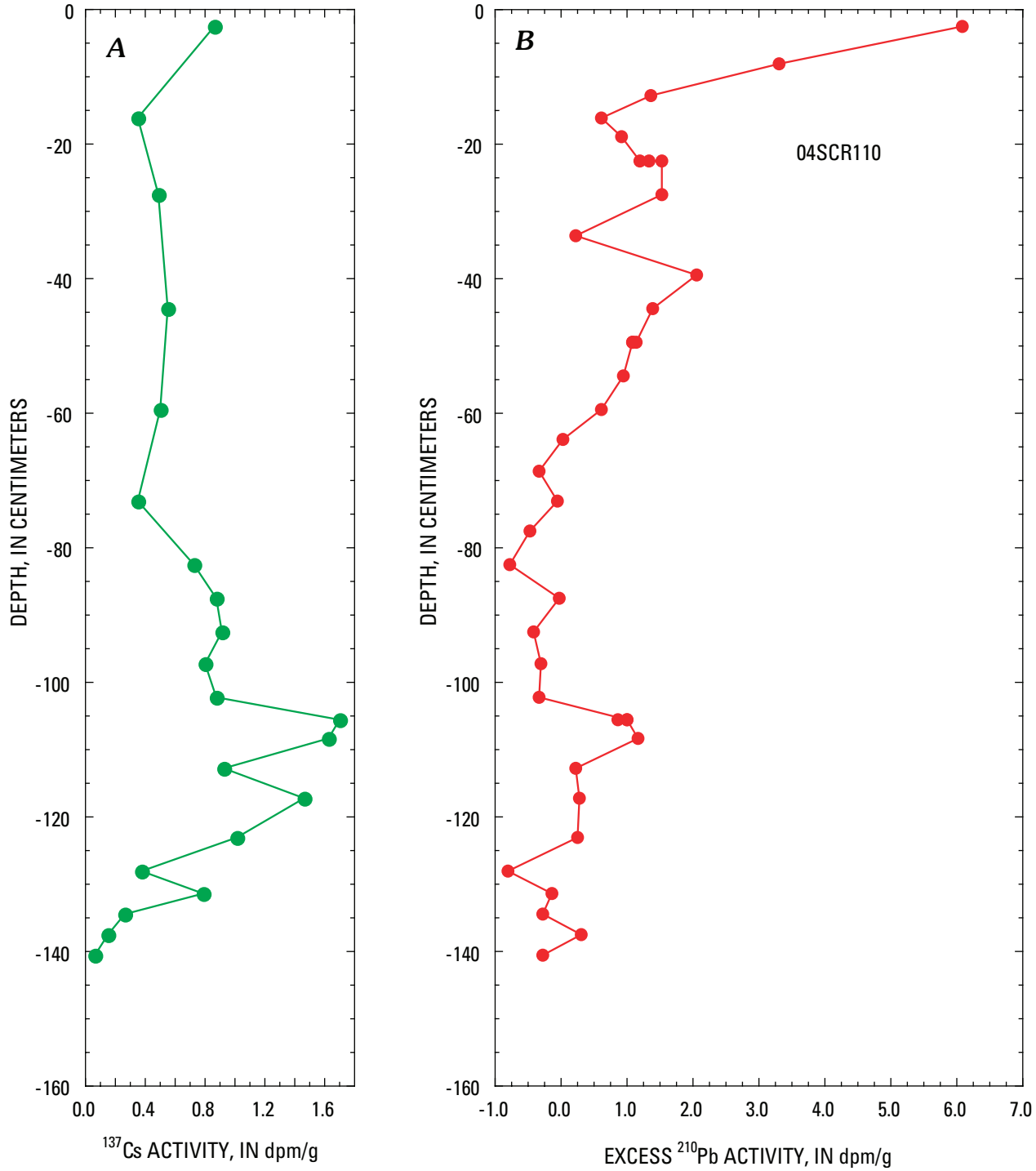

Figure 10. Plot of *A*, ^{137}Cs and *B*, ^{210}Pb data from core 04SCR110. Activity units (dpm/g) are disintegrations per minute per gram.

Geochronological data from core 04SCR112 show a number of ^{210}Pb activity peaks in the depth profile (fig. 12). These ^{210}Pb peaks occur at mean depths of 57.5 cm, 117.5 cm, 162.5 cm, and 197.5 cm and can be correlated with ^{210}Pb peaks in the 04SCR115 core (fig. 13) at similar or slightly deeper depths. ^{137}Cs activities peak at depths of 217.5–262.5 cm (1953–59 peak) and 162.5–197.5 cm (1963 peak). Two of the ^{210}Pb peaks occur within the 1962–64 ^{137}Cs peak. The large ^{210}Pb spike at 197.5 cm (core 04SCR112, fig. 12) correlates with the smaller peak at 250 cm in core 04SCR115 (fig. 13) and indicates a higher rate of sediment accumulation at site 04SCR115 during the late 1950s. Furthermore, there is a great deal of variation in the ^{210}Pb data, which is outside the statistical counting errors (table A7). These fluctuations

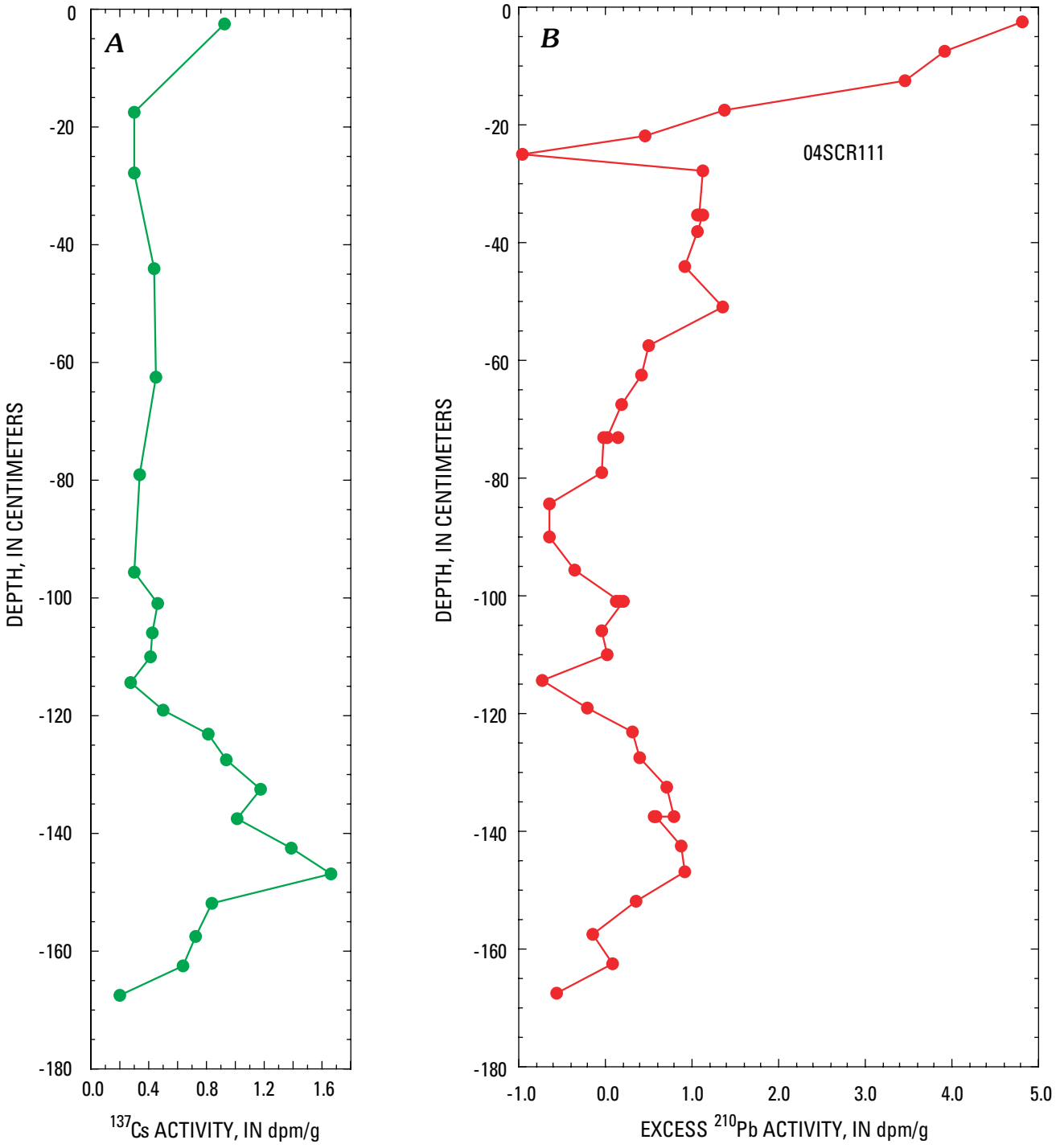

Figure 11. Plot of *A*, ^{137}Cs and *B*, ^{210}Pb data from core 04SCR111. Activity units (dpm/g) are disintegrations per minute per gram.

are caused by variations in the sedimentological history that reflect reservoir-wide conditions. In figure 14*B*, we plot the minimum and maximum water levels of the reservoir for each year based upon the gauge height measured at Coolidge Dam (gauge 09469000) and the depth of sample from core 04SCR112 versus time. Stratigraphic ages are approximated using the 1962–64 ^{137}Cs peak and the top of the core. No ^{210}Pb chronology has been developed prior to 1960. Several important observations that affect the thickness of sediment deposited in the reservoir versus time can be made from these data. First, between 1938 to 1940 and 1945 to 1962, the reservoir at the core sites was dry at least some time during the year except for 1958. And, in the years 1938, 1947, 1948, 1951, and probably 1953, the reservoir bed at the sampling

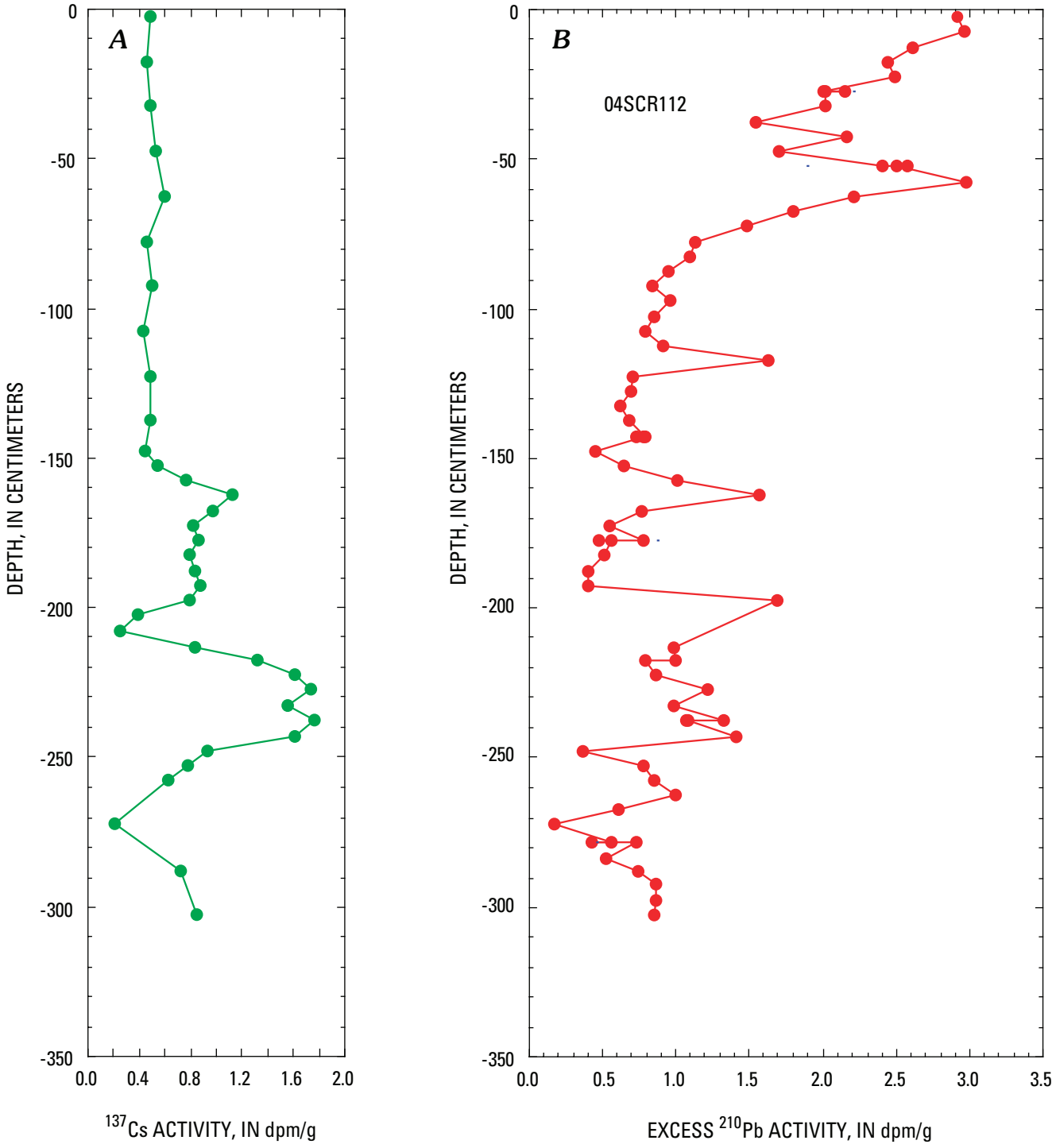

Figure 12. Plot of *A*, ^{137}Cs and *B*, ^{210}Pb data from core 04SCR112. Activity units (dpm/g) are disintegrations per minute per gram.

point was dry all year. ^{210}Pb data from the cores taken in the dry reservoir bed in both the San Carlos (04SCR110, fig. 10 and table A5) and the Gila River arms (04SCR111, fig. 11 and table A6) indicate that the ^{210}Pb activity is higher at the dry reservoir bed surface because the sediment-accumulation rate was low and the ^{210}Pb activity was not diluted by barren sediment containing silicate mineral or rock fragments. High ^{210}Pb activity in core 04SCR112 below depths of 250 cm is interpreted to reflect the capture of ^{210}Pb on clays exposed on the dry reservoir bed (fig. 12 and table A7). Thus, the deepest penetration of core 04SCR112 would be during the dry period in the early 1950s. Because there is still some ^{137}Cs activity at the base of core 04SCR112, the oldest sediment must have been deposited after 1953. However the oldest sediment recov-

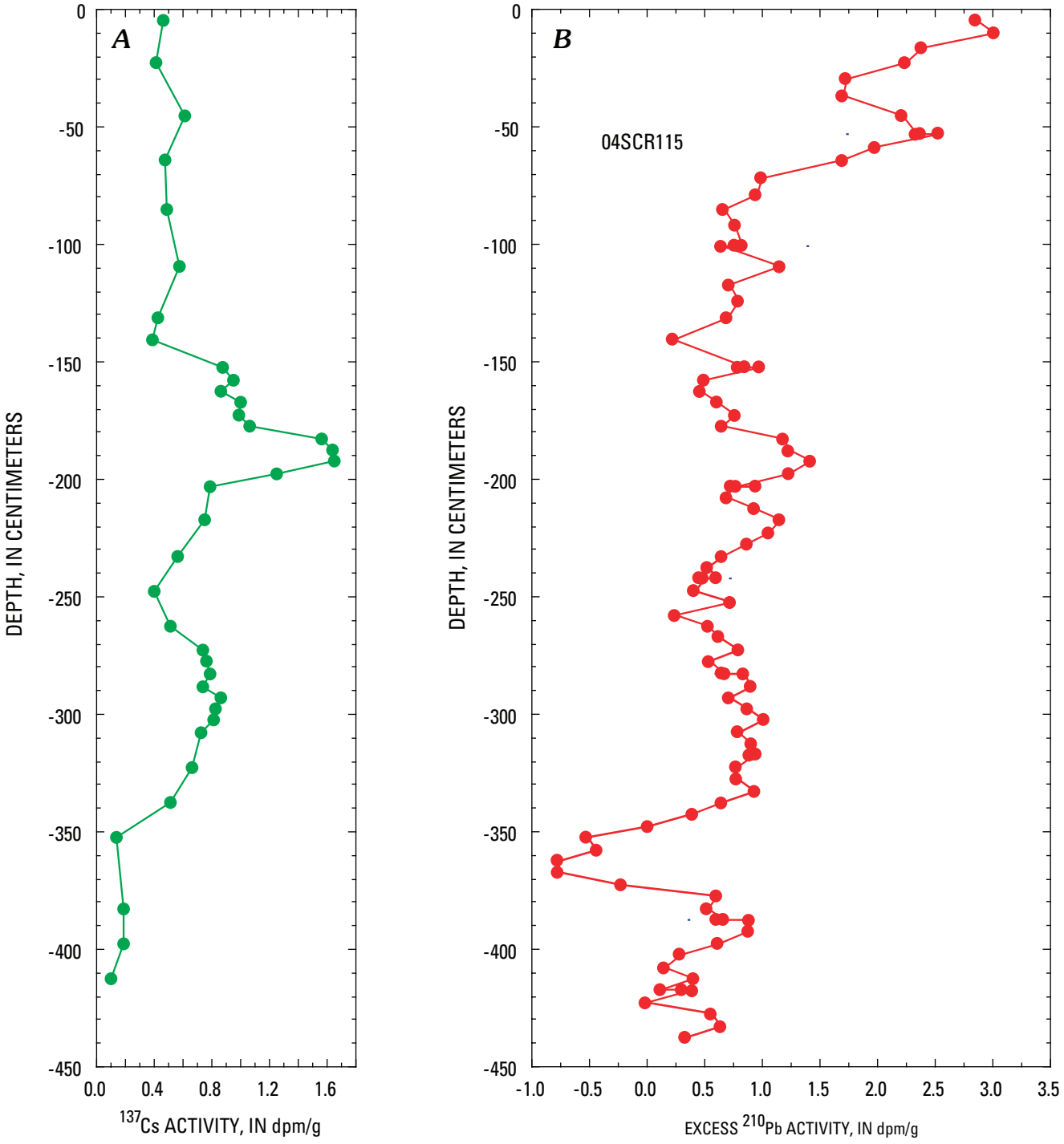

Figure 13. Plot of *A*, ^{137}Cs and *B*, ^{210}Pb data from core 04SCR115. Activity units (dpm/g) are disintegrations per minute per gram.

ered in core 04SCR115 is possibly from the early 1940s or late 1930s because there is no ^{137}Cs activity below a depth of 350 cm (fig. 13*A*). Because of the many probable gaps in the sedimentary record, we have not attempted to fit a ^{210}Pb decay curve to segments of core 04SCR112 below 200 cm depth in the core, or about 1960 (fig. 12).

Sediment at site 04SCR112, beginning about 1960 (figs. 12 and 15), appears to have accumulated at a relatively uniform rate. The bulk of the ^{210}Pb data plot very near the A_o = 2.0 ^{210}Pb decay curve (fig. 15, A_o = 1.5 plotted so as not to obscure ^{210}Pb data). The high ^{210}Pb activity peak at 197.5 cm is interpreted to be the 1961 surface when the reservoir

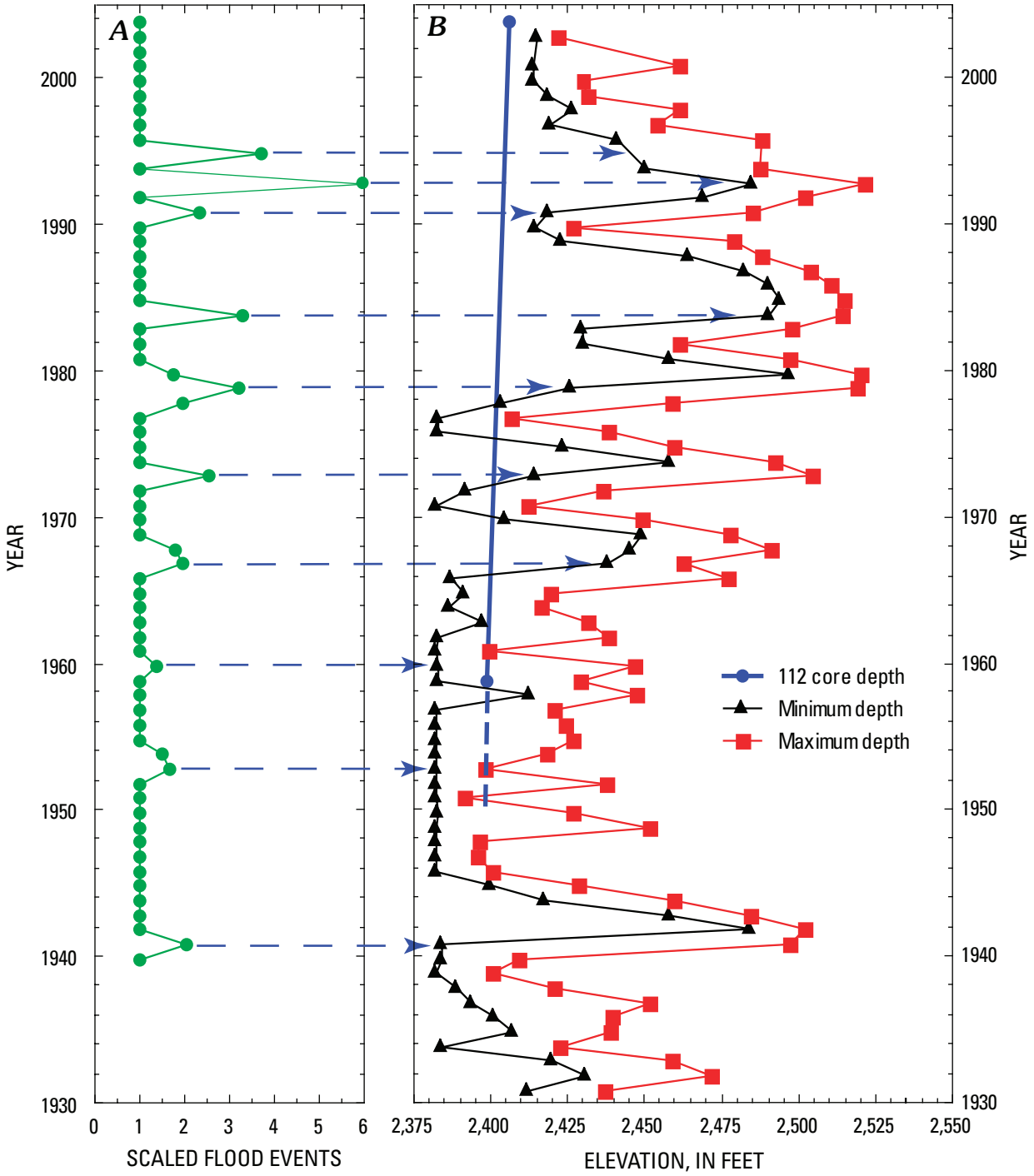

Figure 14. *A*, Plot of scaled flood events and *B*, reservoir minimum and maximum depths versus time. Depth of penetration for core 04SCR112 is also plotted on *B*.

bed at the site of the core was exposed for the entire year. This depth is at the beginning of the elevated ^{137}Cs activity, which we interpreted to be the 1962–64 peak formed by atmospheric nuclear testing in the Pacific. During 1958, the core site would have been under water all year, and the ^{210}Pb activity at a depth of 248 cm falls on the ^{210}Pb decay curve where it should occur had sediment accumulation been continuous—this is in good agreement with the ^{137}Cs data (fig. 12).

Flood events also impact the sediment-accumulation rate in the reservoir. The thickness of the sediment lens and the type of sediment deposited at the core site during any given event is dependent on two conditions: the depth of the

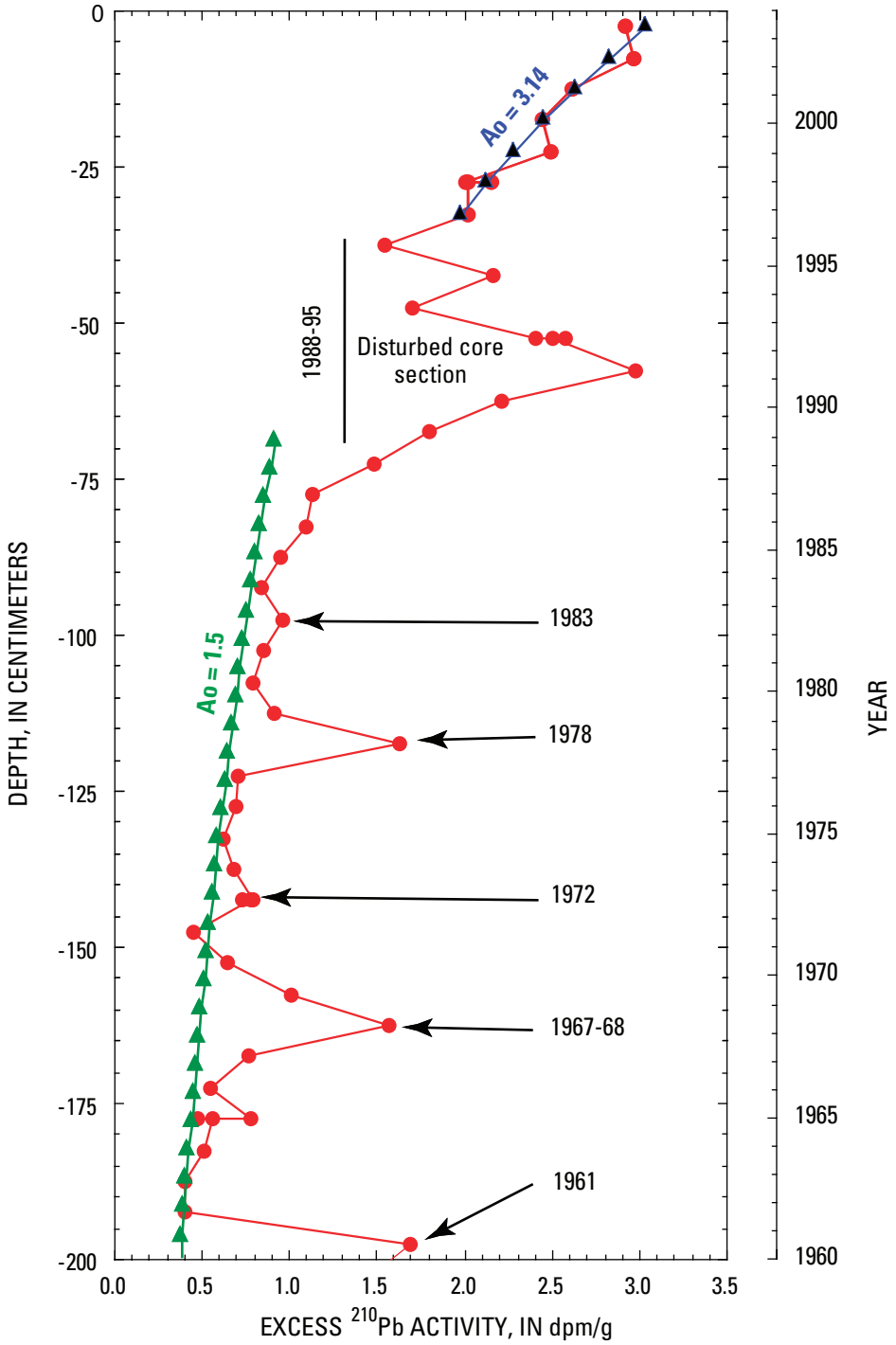

Figure 15. Model ages derived from ^{210}Pb and ^{137}Cs data from core 04SCR112. ^{210}Pb decay approximates A_o = 2.0, A_o of 1.5 shown for period from 1960–1988 so it would not obscure the data. A_o of 3.14 fits data from the upper part of the core. Model ages are also constrained by flood data from the San Carlos and Gila River gauging stations; arrows indicate major flood events (fig. 14). Activity units (dpm/g) are disintegrations per minute per gram.

water at the time of the flood event and the magnitude of the flood event. Using the records from the two gauge stations located on the San Carlos River at Peridot (09468500) and the Gila River at Calva (09466500), large discharge events have been plotted, scaled to the maximum discharge event in winter 1991–92 (fig. 14*A*). Two different classes of floods can be identified (fig. 14*B*): those that occurred when the water level at the core site was shallow, and those that

occurred when it was deep (> 50 ft). The floods of 1983–84, 1993–94, and 1995–96 occurred when the core site was in fairly deep water, whereas the flood events in 1951–52, 1960–61, 1965–67, 1972, 1978–79, and 1991–92 occurred when the core site was in relatively shallow water (fig. 14*B*). Floods that occurred when the water at the core site was deep have relatively minor effects on the sediment-accumulation rate because most of the sediment would have been deposited upstream from the core site in deltas. There would be an expected increase in the ^{210}Pb activity in core 04SCR112 when the water was deep because the clays, which are the residence site of the ^{210}Pb, would be moved into the deeper part of the reservoir as suspended sediment. The suspended sediment would settle out from the water column, following Stoke's law, after the flood event, forming a ^{210}Pb-enriched layer at the top of the sediment sequence resulting from the flood. These flood events correlate with spikes of high ^{210}Pb activity (that is, low sediment-accumulation rates) in the 04SCR112 core (fig. 12). Four such peaks occur in the core: a large peak at 50–60 cm depth associated with the 1991–95 events, one at 110–120 cm depth associated with the 1983–84 flood event, one at 145–170 cm associated with the 1978–79 flood, and one at 195 to 210 cm depth associated with the 1960–61 flood event.

According to Robbins (1978, p. 356–358) removal of these flood sequences from the core should result in an undisturbed and dateable stratigraphy. The family of ^{210}Pb decay curves is shown in fig. 9*A*. The shapes of the curves are similar, and the level of activity is dependent upon the initial starting activity, A_o. The upper part of the ^{210}Pb activity curve from core 04SCR112 (fig. 15), when the reservoir was relatively deep, is best matched by a ^{210}Pb decay curve with $A_o = 3.14$, whereas the lower part of the curve is best matched by a ^{210}Pb decay curve with an A_o of 2.0. This sediment-accumulation model gives dates for the ^{210}Pb activity shown in figure 15, and peak ^{210}Pb activities match the flood events recorded at the San Carlos and Gila River gauges (fig. 14*A*). The interval between 35 and 75 cm depth (1988–95) has been disturbed, presumably by the 1991–95 flood events, and cannot be dated directly (fig. 15).

Geochemical Results from Modern Stream-Bed-Sediment Samples

Data from samples of stream-bed sediment are in table 5 (table A13). Trace-element data from samples collected in 1990 (Baker and King, 1994) are in table 6. We reoccupied many of the same sites, although we did collect samples along the Gila River with higher frequency to give more spatial resolution in the data. Profile plots for both data sets are in figures 16*A*–16*D*. No analytical methods were given in Baker and King (1994), and no SRM data were reported to allow assessment of accuracy or precision of the 1990 stream-bed-sediment data. The concentrations of Cu between samples from the two data sets are in good agreement and the downstream trends in the data match very well (fig. 16*A*). The same is true for the Pb (fig.16*B*) and Zn data (fig. 16*C*), although there is a negative bias in the 1990 Pb and Zn data, which suggests that a partial digestion was used. However, the downstream trends between both data sets match very well. There is one exception; the sample from the Ft. Thomas site (fig. 1; table 5) contains high concentrations of Fe, Cr, V, and Zn, but not Cd or Cu. This pattern suggests anthropogenic contamination of the sediment sample from this site, possibly by discarded metal or galvanized pipe in the river upstream. The reported Cd data (table 6, Baker and King, 1994) are very high—we believe they are in error by about an order of magnitude based on our Cd data (table 5). The crustal abundance value for Cd is 0.16 ppm (Fortescue, 1992). Thus, the 1990 Cd data have not been plotted (fig. 16*D*). Concentrations of these four metals (Cu, Cd, Pb, and Zn) are elevated, as expected, in sediment from the San Francisco River near Clifton, Ariz. Upstream from the confluence of the Gila River with the San Francisco River, sediment from the Gila River has low concentrations of all four metals, near that of crustal abundance (Fortescue, 1992), indicating that the porphyry Cu mineralization in the Morenci district is responsible for the elevated concentrations of these four metals in Gila River sediment downstream from the confluence. The lower two stream-bed-sediment samples from the San Carlos River also contain elevated concentrations of Zn. This result is unexpected and may result from reworking of reservoir-bed material in the lowest reach of the San Carlos River. Both samples 04SCR101 and 04SCR102 contain high concentrations of Fe and V and reflect the accumulation of magnetite in the samples by normal sedimentation processes observed in the field. Metal concentrations from further upstream on the San Carlos River (04SCR103) are not elevated and agree well with those in the lower Gila River.

A sample of suspended sediment was collected from the site at Calva (table 5). The concentration of the suspended sediment was 60 mg/L of river water. Metal concentrations for Cu, Pb, Zn, and As (table 5; figs. 16*A*–16*C*) are substantially elevated above that in the stream-bed sediment at the Calva site. These four metals are sorbed on clays, as indicated by the elevated Al in suspended sediment (table 5), when the pH of the water (table 3) is at or above neutral (Smith, 1999). These data suggest that the mechanism of transport of elevated metal concentrations to the reservoir sediment is via suspended sediment.

Geochemical Results from Terrace-Sediment Samples

Terrace-sediment samples were collected at two sites on the lower Gila River and one on the San Carlos River to determine the variation of geochemistry in sediment with time. The geochemical variation of the samples analyzed at each site was minimal; therefore, geochemical data from each terrace section are presented as a statistical summary giving the median, mean, standard deviation, relative standard deviation,

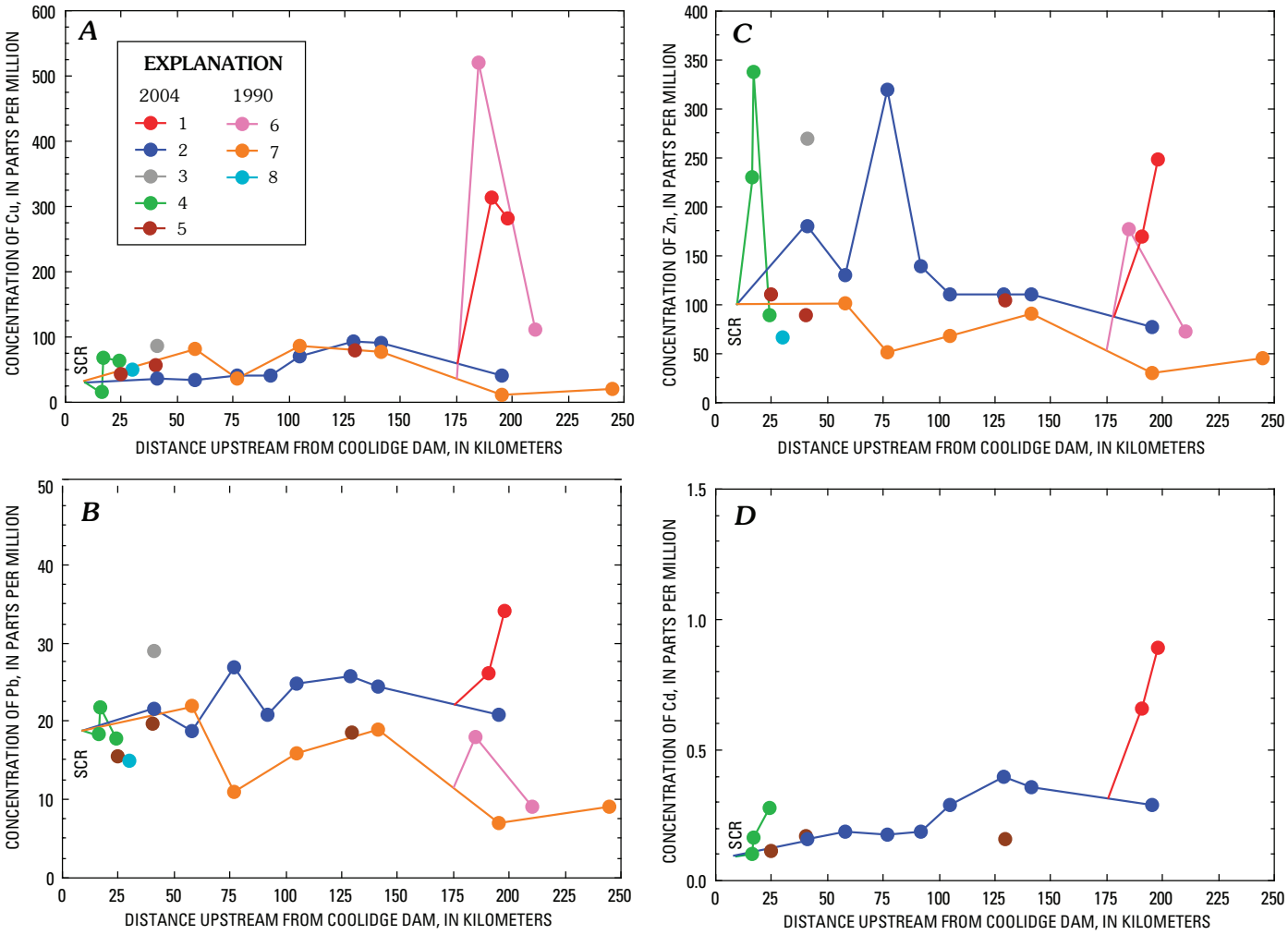

Figure 16. Plot of the variation of concentration of *A*, Cu; *B*, Pb; *C*, Zn; and *D*, Cd in stream-bed-sediment and terrace-sediment samples as a function of distance upstream from the gauge at Coolidge Dam. Crustal abundance for Cu is 68 ppm; Pb, 13 ppm; Zn, 76 ppm; and Cd, 0.16 ppm (Fortescue, 1992). Data from this study: 1, stream-bed sediment from San Francisco River; 2, stream-bed sediment from Gila River; 3, suspended sediment from Gila River at Calva; 4, stream-bed sediment from San Carlos River; 5, terrace sediment (table 5)—data from Baker and King (1994); 6, stream-bed sediment from San Francisco River; 7, stream-bed sediment from Gila River; 8, stream-bed sediment from San Carlos River (table 6). End points of river tie lines are connected at the confluence and are shown ending schematically in San Carlos Reservoir (SCR).

and the number of samples analyzed (table 7; analytical data are in table A14). In comparing the terrace-sediment data with data from modern sediment from the sites, there are generally only minor changes in concentration for many of the elements. Median values for the three terrace sediment localities are plotted on figure 16. Differences in the concentration of Cu, Pb, and Zn are present in the data. In figure 17, the terrace-sediment data are shown in a box plot for each site with the data from the stream-bed sediment from the same locality. The data clearly show that Cu and Zn have been added to the surface drainages by anthropogenic activity, some of which may be the result of mining activity.

Geochemical Results from Reservoir-Sediment Samples

Geochemical data for many of the elements determined in the cores showed little variation with depth or time. These data are summarized in tables 8–11; complete geochemical data are in tables A9–A12 (on CD-ROM). Concentrations of Cu, Pb, Zn, Cd, As, and Hg determined in sediment from the reservoir (cores 04SCR110, 04SCR111, 04SCR112, and 04SCR115) are in tables 12–15 and figures 18–21, respectively.

Two prominent sets of Cu peaks and one minor Cu peak are identified. The Cu peak highest in the stratigraphic

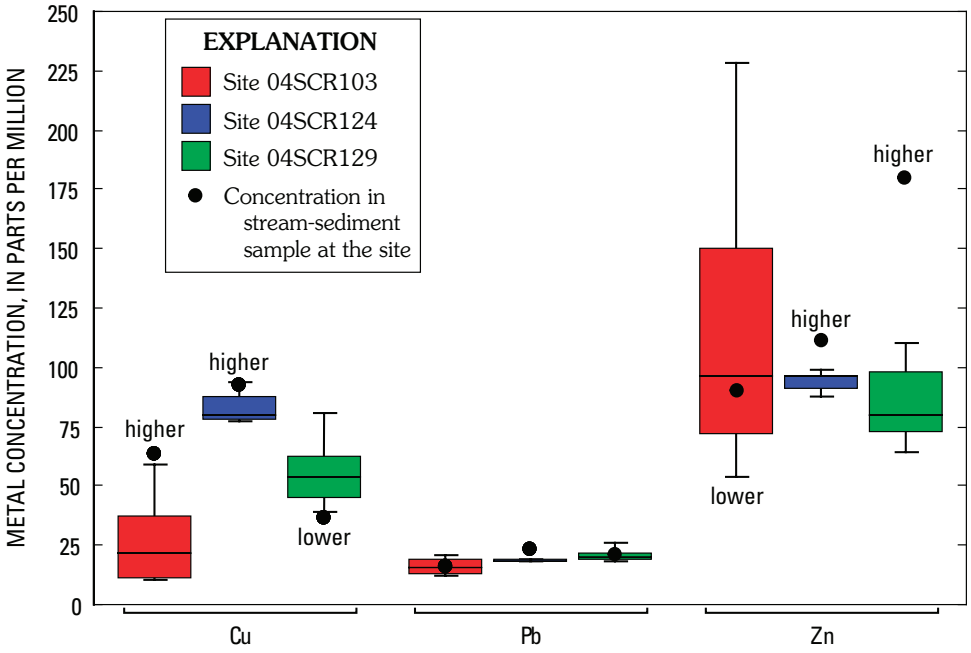

Figure 17. Box plot of the data from Cu, Pb, and Zn for each of the three terrace-sediment sites (table 7). Values shown on the box plot are the 10th, 25th, 50th or median, 75th, and 90th percentiles of the data (table A14). Concentrations of these metals in the stream-bed-sediment data (table 5) are plotted on the figure as black dots.

section is present in all four cores (figs. 18–21), and the peak Cu concentration would have been deposited in about 1985–86 based on the ^{210}Pb chronology for core 04SCR112 assuming a uniform sediment-accumulation rate (fig. 15). The concentration of Cu is much higher in the core from the Gila River arm (fig. 19, depth of 65 cm; Cu concentration of about 700 ppm) than in the San Carlos River arm, (fig. 18, depth of 45 cm; Cu concentration of about 160 ppm). This same Cu peak occurs in the reservoir at depths of about 85 cm in both reservoir cores (figs. 20 and 21) and has peak Cu concentrations of about 600 ppm. The peak is broad, covering tens of centimeters in depth in the cores, and represents a large, prolonged event spanning several years. Thus, this deposit does not represent deposition resulting from a single flood event. There are also small Pb, Zn, and Cd anomalies associated with this event in the cores. We interpret these data to indicate that the source of the metal anomaly was upstream on the Gila River. Discharge data for the San Francisco River measured at Clifton gauge (09444500) are shown in figure 22. The data indicate that the highest discharge recorded at Clifton occurred in July 1983 (52,200 cfs, fig. 22*C*). A very large 3-day storm having a total discharge of about 60,000 cfs occurred in December 1978 (fig. 22*C*). The stratigraphic intervals in the cores containing the high Cu concentrations (table 16) are dominated by deposition of silt (tables A1–A4) that would have been deposited in deep water (figs. 2*C* and 14). We interpret this broad Cu peak to be the result of material released from the Morenci site. The initial rise in Cu concentration occurs at a depth of 120–125 cm and correlates well with the peak in ^{210}Pb activity (fig. 15) dated at 1978. The amount of metal released steadily increased over this period before it was abruptly stopped in about 1983. The sediment-accumulation rate over his interval was higher than normal as indicated by the later date (1985–86) for the Cu peak from the ^{210}Pb model (fig. 16). Assuming an average concentration of 200 ppm over a 55-cm interval and using an area of 4,000 acres for the San Carlos Reservoir at an elevation of 2,430 ft, the total mass of Cu deposited during this event in an elliptical basin would contain a minimum of 600 metric tons of Cu. The maximum concentration of Cu in reservoir sediment exceeded the toxic concentration for sediment quality guidelines of 149 ppm (MacDonald and others, 2000) from 1978 to 1983. It is highly likely that Cu concentrations in river sediment would also have exceeded these sediment-quality guidelines over this same period.

Schmittt and Brumbaugh (1990) report data collected during the National Contaminant Biomonitoring Program (NCBP; http://www.cerc.usgs.gov/data/ncbp/ncbp.html) for

Table 5. Geochemical data from stream-bed-sediment samples, San Carlos, Gila, and San Francisco Rivers, Arizona.

[ICP-AES, inductively coupled plasma–atomic emission spectrometry; ICP-MS, inductively coupled plasma–mass spectrometry; Hg CVAA, mercury cold-vapor atomic absorption]

Field no.	Locality	River	ICP-AES Na (wt. %)	ICP-AES K (wt. %)	ICP-AES Mg (wt. %)	ICP-AES Ca (wt. %)	ICP-AES Fe (wt. %)	ICP-AES Al (wt. %)	ICP-AES Ti (wt. %)	ICP-AES P (wt. %)	ICP-MS As (ppm)	ICP-AES Ba (ppm)	ICP-MS Cd (ppm)	ICP-MS Co (ppm)
04SCR101S	In delta in San Carlos Res.	San Carlos River	0.69	0.71	2.1	3.8	20	2.8	7.5	0.14	11	436	0.10	57.2
04SCR102S*	At mouth of river	San Carlos River	0.62	0.84	2.2	4.1	21.5	3.4	8.2	0.13	12	269	0.17	61.3
04SCR103S	Upstream fr San Carlos Res.	San Carlos River	1.0	1.7	1.6	6.6	4.9	5.8	0.97	0.09	12	514	0.28	19.9
04SCR120S	Upstream from Clifton	San Francisco R.	1.3	2.3	1.3	4.1	4.7	7.4	0.43	0.15	9.5	649	0.89	15.9
04SCR121S	Clifton	San Francisco R.	1.5	2.3	1.2	5.4	4.3	7.2	0.58	0.13	12	1,010	0.66	15.6
04SCR122S	Guthrie	Gila River	1.8	2.4	1.1	3.7	3.2	7.2	0.42	0.097	5.3	789	0.29	13.0
04SCR123S	San Jose	Gila River	1.5	2.3	1.4	3.9	4.0	7.4	0.53	0.11	6.0	722	0.36	15.4
04SCR124S	Soloman	Gila River	1.2	2.3	1.5	4.0	3.8	7.5	0.45	0.10	6.4	682	0.40	14.5
04SCR125S	Pima	Gila River	1.2	2.5	1.6	3.0	3.8	7.7	0.43	0.10	6.0	604	0.29	16.0
04SCR126S	Eden	Gila River	1.6	1.9	1.6	4.2	8.8	6.0	1.4	0.12	5.1	591	0.19	26.0
04SCR127S	Ft. Thomas	Gila River	1.1	1.3	1.2	2.8	20.1	4.2	2.7	0.087	5.8	618	0.18	50.3
04SCR128S	Bylas	Gila River	1.5	1.8	1.5	3.9	9.0	6.0	1.3	0.079	4.8	564	0.19	26.4
04SCR129S	Calva	Gila River	1.4	1.8	1.3	4.1	11	5.5	1.5	0.087	5.1	620	0.16	27.8
04SCR129SS#	Calva	Gila River	0.62	1.9	1.9	12	3.6	7.0	0.30	0.10	10	420	--	2.0

* ICP-MS data only.

ICP-AES data; 60 mg of suspended sediment recovered from 1L of water collected from this site.

Table 5. Geochemical data from stream-bed-sediment samples, San Carlos, Gila, and San Francisco Rivers, Arizona—*Continued.*

Field no.	Locality	River	ICP-MS Cr (ppm)	ICP-AES Cu (ppm)	Hg CVAA Hg (ppm)	ICP-AES Mn (ppm)	ICP-MS Mo (ppm)	ICP-AES Ni (ppm)	ICP-MS Pb (ppm)	ICP-AES Sr (ppm)	ICP-AES V (ppm)	ICP-AES Zn (ppm)
04SCR101S	In delta in San Carlos Reservoir	San Carlos River	457	16	<0.02	3,540	1.9	75	18.3	140	878	231
04SCR102S*	At mouth of river	San Carlos River	447	69	<0.02	3,940	2.1	89	21.9	168	1,040	338
04SCR103S	Upstream from San Carlos Res.	San Carlos River	101	64	<0.02	921	1.5	56	17.8	322	150	89
04SCR120S	Upstream from Clifton	San Francisco R.	47.2	281	0.07	1,000	4.0	33	34.1	414	77	249
04SCR121S	Clifton	San Francisco R.	79	314	0.07	715	3.5	41	26.1	846	110	170
04SCR122S	Guthrie	Gila River	53.6	41	<0.02	744	0.9	26	20.8	457	83	77
04SCR123S	San Jose	Gila River	81.8	92	0.02	663	1.6	35	24.4	430	100	110
04SCR124S	Soloman	Gila River	57	93	0.04	628	1.7	34	25.9	398	88	110
04SCR125S	Pima	Gila River	51.8	71	0.04	828	1.0	36	24.9	333	84	110
04SCR126S	Eden	Gila River	186	41	<0.02	1,400	1.4	45	20.8	334	256	140
04SCR127S	Ft. Thomas	Gila River	359	40	<0.02	2,640	2.3	65	26.9	249	604	320
04SCR128S	Bylas	Gila River	165	35	<0.02	1,370	0.9	41	18.8	305	305	130
04SCR129S	Calva	Gila River	214	36	<0.02	1,480	1.2	47	21.6	374	338	180
04SCR129SS#	Calva	Gila River	31	86	--	890	--	40	29.0	540	75	270

Table 6. Geochemical data for trace-element concentrations from stream-bed sediment collected in 1990.

[Sediment data reported by Baker and King (1994)]

Sample site	Locality	River	As (ppm)	Ba (ppm)	Cd (ppm)	Cr (ppm)	Cu (ppm)	Pb (ppm)	Mn (ppm)	Hg (ppm)	Ni (ppm)	Sr (ppm)	V (ppm)	Zn (ppm)
1	upstream from Clifton	San Francisco River	3.8	161	5.7	21	112	9	678	0.11	49	184	45	73
2	Clifton	San Francisco River	9.4	277	9.9	31	521	18	578	0.06	65	557	86	177
3	Virdin, N. Mex.	Gila River	3.8	244	4.4	16	20	9	492	< 0.04	18	169	31	46
4	Guthrie	Gila River	1.9	106	2.4	9	12	7	197	< 0.03	11	88	5	31
5	San Jose	Gila River	6.7	228	6.6	21	77	19	898	< 0.07	34	289	43	91
6	Pima	Gila River	4.6	199	5.1	17	86	16	580	< 0.05	31	280	36	68
7	Ft. Thomas	Gila River	5	127	< 0.4	12	37	11	708	< 0.04	18	189	27	51
8	Bylas	Gila River	10.4	214	8.6	31	82	22	1,072	< 0.05	33	219	72	102
9	San Carlos Reservoir	San Carlos Reservoir	8.7	186	6.9	20	135	21	885	0.09	33	206	58	87
10	Talkalai Lake	San Carlos River	14.6	279	8.3	41	51	15	772	< 0.06	57	100	62	66

Table 7. Statistical summary of geochemical data from terrace-sediment samples by site.

[STD, standard deviation; RSD, relative standard deviation, in percent. ICP-AES, inductively coupled plasma–atomic emission spectrometry; ICP-MS, inductively coupled plasma–mass spectrometry; Hg CVAA, mercury cold-vapor atomic absorption; *n*, number of samples analyzed]

Field no.	Depth (cm)		ICP-AES Na (wt. %)	ICP-AES K (wt. %)	ICP-AES Mg (wt. %)	ICP-AES Ca (wt. %)	ICP-AES Fe (wt. %)	ICP-AES Al (wt. %)	ICP-AES Ti (wt. %)	ICP-AES P (wt. %)	ICP-MS As (ppm)	ICP-AES Ba (ppm)	ICP-MS Cd (ppm)	ICP-MS Co (ppm)
04SCR103	5–200	Median	1.4	1.9	1.6	4.6	6.0	6.0	1.6	0.09	7.8	544	0.12	24.9
		Mean	1.4	1.8	1.4	4.2	9.1	5.5	2.6	0.09	7.7	549	0.13	29.0
		STD	0.42	0.58	0.36	1.00	7.34	1.30	2.59	0.03	2.3	46	0.06	14.9
		RSD	30	33	25	24	80	23	101	30	30	8.4	50	51
		n	12	12	12	12	12	12	12	12	12	12	12	12
04SCR124	0–122	Median	2.0	2.3	1.3	3.2	5.3	7.4	0.7	0.10	4.2	826	0.16	19.0
		Mean	2.0	2.3	1.3	3.2	5.1	7.3	0.7	0.09	4.1	821	0.16	18.6
		STD	0.05	0.04	0.04	0.05	0.29	0.09	0.05	0.00	0.6	16.9	0.01	1.0
		RSD	2.7	1.9	3.4	1.7	5.6	1.2	7.5	2.9	14	2.1	7.0	5.2
		n	5	5	5	5	5	5	5	5	5	5	5	5
04SCR129	5–265	Median	2.1	2.4	1.1	3.1	4.1	7.5	0.6	0.10	4.8	819	0.17	15.1
		Mean	2.1	2.5	1.1	3.0	4.1	7.5	0.6	0.10	4.8	844	0.19	14.9
		STD	0.16	0.13	0.12	0.28	0.76	0.16	0.14	0.01	0.8	63	0.06	2.2
		RSD	8.0	5.1	11	9.4	18	2.1	23	8.1	16	7.4	31	15
		n	15	15	15	15	15	15	15	15	15	15	15	15

Field no.	Depth (cm)		ICP-MS Cr (ppm)	ICP-AES Cu (ppm)	Hg CVAA Hg (ppm)	ICP-AES Mn (ppm)	ICP-MS Mo (ppm)	ICP-AES Ni (ppm)	ICP-MS Pb (ppm)	ICP-AES Sr (ppm)	ICP-MS Th (ppm)	ICP-MS U (ppm)	ICP-AES V (ppm)	ICP-AES Zn (ppm)
04SCR103	5–200	Median	105	21.5	0.03	1,050	0.8	46.5	15.5	260	8.8	1.6	202	97
		Mean	177	27.0	0.06	1,485	0.9	46.7	16.0	251	16.6	1.8	363	123
		STD	168	18.0	0.06	1,060	0.6	16.2	3.3	52	28	1.2	385	80
		RSD	95	67	101	71	65	35	20.6	21	171	69	106	65
		n	12	12	12	12	12	12	12	12	12	12	12	12
04SCR124	0–122	Median	137	80.0	0.02	771	1.1	43.0	18.5	545	9.4	1.8	160	96
		Mean	132	82.8	0.02	755	1.1	42.2	18.5	541	9.6	1.8	160	94
		STD	13.8	7.0	0.00	35.3	0.1	2.6	0.5	16	0.9	0.1	12.2	4.3
		RSD	10	8.4	0.00	5	9.0	6.1	2.6	3.0	9.5	4.9	7.7	4.5
		n	5	5	5	5	5	5	5	5	5	5	5	5
04SCR129	5–265	Median	80.9	54.0	0.03	676	0.9	33.0	19.7	503	11.0	2.2	120	80
		Mean	86.0	55.9	0.03	683	0.9	32.3	20.8	499	11.1	2.2	115	85
		STD	26.6	16.4	0.01	128	0.2	4.3	2.7	57	1.4	0.2	24.2	16.9
		RSD	31	29	32	19	17	13	13.2	11	13	7.7	21	20
		n	15	15	15	15	15	15	15	15	15	15	15	15

Table 8. Statistical summary of geochemical data for major and selected trace elements, core 04SCR110, San Carlos River arm, San Carlos Reservoir.

[STD, standard deviation; RSD, relative standard deviation, in percent. ICP-AES, inductively coupled plasma–atomic emission spectrometry; ICP-MS, inductively coupled plasma–mass spectrometry]

	ICP-AES Na (wt. %)	ICP-AES K (wt. %)	ICP-AES Mg (wt. %)	ICP-AES Ca (wt. %)	ICP-AES Fe (wt. %)	ICP-AES Al (wt. %)	ICP-AES Ti (wt. %)	ICP-AES P (wt. %)	ICP-AES Ba (ppm)
Median	1.04	1.9	1.8	4.4	4.7	7.5	0.52	0.12	508
Mean	1.04	2.0	1.8	4.5	4.7	7.5	0.54	0.13	510
STD	0.23	0.2	0.2	0.9	0.5	0.7	0.16	0.02	61
RSD	22.3	9.2	12.0	20.0	10.7	9.6	28.7	14.2	12.0

	ICP-MS Co (ppm)	ICP-MS Cr (ppm)	ICP-AES Mn (ppm)	ICP-MS Mo (ppm)	ICP-AES Ni (ppm)	ICP-AES Sr (ppm)	ICP-MS Th (ppm)	ICP-MS U (ppm)	ICP-AES V (ppm)
Median	26.8	68.7	901	1.08	52	278	11.9	2.6	94
Mean	26.6	69.4	881	1.15	52	284	12.4	2.6	98
STD	2.2	14.4	138	0.24	5	30	2.3	0.4	18
RSD	8.3	20.7	15.7	20.9	10.6	10.4	18.7	14.0	18.2

Table 9. Statistical summary of geochemical data for major and selected trace elements, core 04SCR111, Gila River arm, San Carlos Reservoir.

[STD, standard deviation; RSD, relative standard deviation, in percent. ICP-AES, inductively coupled plasma–atomic emission spectrometry; ICP-MS, inductively coupled plasma–mass spectrometry]

	ICP-AES Na (wt. %)	ICP-AES K (wt. %)	ICP-AES Mg (wt. %)	ICP-AES Ca (wt. %)	ICP-AES Fe (wt. %)	ICP-AES Al (wt. %)	ICP-AES Ti (wt. %)	ICP-AES P (wt. %)	ICP-AES Ba (ppm)
Median	1.51	2.6	1.8	4.0	4.4	8.6	0.52	0.13	766
Mean	1.47	2.7	1.9	4.0	4.3	8.6	0.52	0.13	775
STD	0.35	0.3	0.4	0.8	0.6	0.9	0.06	0.02	151
RSD	24.0	10.2	18.8	19.6	13.0	10.2	12.2	13.6	19.5

	ICP-MS Co (ppm)	ICP-MS Cr (ppm)	ICP-AES Mn (ppm)	ICP-MS Mo (ppm)	ICP-AES Ni (ppm)	ICP-AES Sr (ppm)	ICP-MS Th (ppm)	ICP-MS U (ppm)	ICP-AES V (ppm)
Median	19.3	51.6	900	1.08	41	436	14.6	3.0	100
Mean	18.9	53.1	917	1.09	41	433	14.1	3.0	100
STD	2.5	4.2	189	0.16	6	73	1.8	0.4	11
RSD	13.1	8.0	20.6	14.7	15.3	16.9	12.9	14.4	10.5

Table 10. Statistical summary of geochemical data for major and selected trace elements, core 04SCR112, San Carlos Reservoir.

[STD, standard deviation; RSD, relative standard deviation, in percent. ICP-AES, inductively coupled plasma–atomic emission spectrometry; ICP-MS, inductively coupled plasma–mass spectrometry]

	ICP-AES Na (wt. %)	ICP-AES K (wt. %)	ICP-AES Mg (wt. %)	ICP-AES Ca (wt. %)	ICP-AES Fe (wt. %)	ICP-AES Al (wt. %)	ICP-AES Ti (wt. %)	ICP-AES P (wt. %)	ICP-AES Ba (ppm)
Median	0.94	2.5	2.0	3.3	4.6	9.0	0.48	0.13	532
Mean	0.99	2.5	2.0	3.6	4.6	8.8	0.50	0.13	545
STD	0.20	0.2	0.3	0.9	0.4	0.8	0.08	0.02	70
RSD	20.4	8.0	13.3	25.9	8.5	9.0	16.9	14.5	12.8

	ICP-MS Co (ppm)	ICP-MS Cr (ppm)	ICP-AES Mn (ppm)	ICP-MS Mo (ppm)	ICP-AES Ni (ppm)	ICP-AES Sr (ppm)	ICP-MS Th (ppm)	ICP-MS U (ppm)	ICP-AES V (ppm)
Median	22.9	57.4	1,057	1.2	54	319	17.2	3.4	99
Mean	23.1	56.3	1,147	1.3	54	315	16.9	3.5	99
STD	3.16	6.43	706	0.44	7	37	2.0	0.5	9
RSD	13.7	11.4	61.5	33.8	13.4	11.7	11.8	13.1	9.2

Table 11. Statistical summary of geochemical data for major and selected trace elements, core 04SCR115, San Carlos Reservoir.

[STD, standard deviation; RSD, relative standard deviation, in percent. ICP-AES, inductively coupled plasma–atomic emission spectrometry; ICP-MS, inductively coupled plasma–mass spectrometry]

	ICP-AES Na (wt. %)	ICP-AES K (wt. %)	ICP-AES Mg (wt. %)	ICP-AES Ca (wt. %)	ICP-AES Fe (wt. %)	ICP-AES Al (wt. %)	ICP-AES Ti (wt. %)	ICP-AES P (wt. %)	ICP-AES Ba (ppm)
Median	0.95	2.4	2.0	3.3	4.6	9.0	0.48	0.13	658
Mean	1.00	2.4	1.9	3.4	4.6	8.9	0.48	0.13	660
STD	0.20	0.1	0.3	0.6	0.5	0.5	0.03	0.01	60
RSD	19.8	5.3	13.3	17.1	9.9	6.1	6.2	10.2	9.1

	ICP-MS Co (ppm)	ICP-MS Cr (ppm)	ICP-AES Mn (ppm)	ICP-MS Mo (ppm)	ICP-AES Ni (ppm)	ICP-AES Sr (ppm)	ICP-MS Th (ppm)	ICP-MS U (ppm)	ICP-AES V (ppm)
Median	22.1	56.7	1,007	1.07	50	322	17.4	3.3	97
Mean	22.1	56.5	1,021	1.12	50	323	17.3	3.3	96
STD	2.5	3.1	212	0.25	5	43	1.8	0.4	7
RSD	11.5	5.4	20.7	22.0	10.6	13.2	10.6	10.5	7.7

Table 12. Geochemical data for Cu, Pb, Zn, Cd, As, and Hg from core 04SCR110, San Carlos River arm, San Carlos Reservoir.

[ICP-AES, inductively coupled plasma–atomic emission spectrometry; ICP-MS, inductively coupled plasma–mass spectrometry; Hg CVAA, mercury cold-vapor atomic absorption]

Field no.	Depth (cm)	Loss on ignition (percent)	ICP-AES Cu (ppm)	ICP-MS Pb (ppm)	ICP-AES Zn (ppm)	ICP-MS Cd (ppm)	ICP-MS As (ppm)	Hg CVAA Hg (ppm)
04SCR110La	0–5	10.98	135	37.9	146	0.48	15.7	0.08
04SCR110Lb	5–11	10.40	112	38.5	134	0.51	15.6	0.07
04SCR110Lc	11–14.5	7.20	108	30.0	119	0.40	10.8	0.06
04SCR110Ld	14.5 -17.5	7.78	104	33.6	119	0.41	9.5	0.08
04SCR110Le	17.5–20	6.80	101	30.8	106	0.39	8.6	0.06
04SCR110Lf	20–25	8.10	120	32.0	131	0.39	12.0	0.07
04SCR110Lg	25–30	7.97	109	29.0	109	0.37	10.9	0.04
04SCR110Lh	30–37	4.79	66	22.5	98	0.27	11.6	0.04
04SCR110Li	37–42	7.39	130	32.4	108	0.51	15.1	0.08
04SCR110Lj	42–47	7.37	184	32.1	140	0.46	15.1	0.06
04SCR110Lk	47–52	6.57	107	28.9	107	0.42	15.0	0.04
04SCR110Ll	52–57	6.77	101	28.7	107	0.39	16.1	0.06
04SCR110Lm	57–62	7.58	108	29.5	119	0.38	15.1	0.06
04SCR110Ln	62–66	5.59	94	27.1	96	0.33	11.7	0.06
04SCR110Lo	66–71	4.19	55	20.8	91	0.22	11.5	0.02
04SCR110Lp	71–75	4.79	63	20.5	105	0.21	10.5	0.05
04SCR110Lq	75–80	3.78	55	18.6	101	0.19	11.4	0.07
04SCR110Lr	80–85	3.37	64	22.1	85	0.27	9.2	0.04
04SCR110Ls	85–90	4.80	72	22.5	93	0.26	10.5	0.03
04SCR110Lt	90–95	4.39	74	24.9	89	0.31	12.6	0.04
04SCR110Lu	95–99.5	3.38	60	22.9	91	0.27	10.3	0.03
04SCR110Lv	99.5–104	4.78	60	24.5	92	0.25	10.1	0.03
04SCR110Lw	104–107	7.08	104	32.1	118	0.44	14.0	0.05
04SCR110Lx	107–109.5	7.17	101	33.4	118	0.46	18.3	0.06
04SCR110Ly	109.5–114.5	6.00	79	27.0	103	0.31	12.8	0.04
04SCR110Lz	114.5–120	4.39	78	27.1	115	0.33	13.6	0.05
04SCR110Laa	120–126	5.18	86	28.7	104	0.38	14.8	0.05
04SCR110Lab	126–130	2.98	43	19.1	96	0.16	12.4	<0.02
04SCR110Lac	130–133	6.57	67	24.3	95	0.31	13.9	0.03
04SCR110Lad	133–136	4.39	76	26.1	100	0.30	15.7	0.03
04SCR110Lae	136–139	4.39	72	25.7	100	0.28	15.7	0.05
04SCR110Laf (mean)	139–142	4.39	85	25.3	113	0.31	11.9	0.05

the San Carlos Reservoir (site 94). Samples of carp and large mouth bass were collected from the reservoir periodically from 1970–86. Cu concentrations (reported as µg/g wet weight from composites of five whole fish) in carp, which are bottom foragers, range from 0.83 to 1.92 µg/g wet weight over the period when Cu concentrations were elevated in reservoir sediment. Samples of carp had lower Cu concentrations in samples collected in 1986 (0.7–0.74 µg/g wet weight). Largemouth bass also had low Cu concentrations (0.3 to 0.88 µg/g wet weight) during the 1978–84 period. In comparison, carp from other nearby reservoirs (Elephant Butte in New Mexico, site 63; and two sites on the Colorado River, sites 92 and 93) over this same period had values that range much closer to ~ 1 µg/g wet weight. Largemouth bass had concentrations similar to those from the San Carlos Reservoir, ~ 0.5 µg/g wet weight. We interpret these data to mean that the carp ingested Cu-rich sediment, causing the elevated Cu concentrations in whole fish during the 1978–84 period. Thus, the data are consistent with our interpretation that the elevated Cu concentrations in San Carlos Reservoir sediment were entering the food chain.

Following completion of this report, we were provided with a copy of the Chase Creek Consent Decree, U.S. Department of Justice and Phelps Dodge Corporation, Aug. 25, 1986, filed with the U.S. District Court in Arizona. According to that decree, Phelps Dodge Corp. agreed to several engineering remedies to capture storm water from both Gold Gulch and Chase Creek. Storm runoff from Chase Creek had been formerly polluting the San Francisco River. Phelps Dodge alleged in the decree that no runoff had occurred from the Morenci site since early 1984. Thus, Phelps Dodge Corp. took engineering measures to cut off the source of metals to the San Carlos River, and that effort is what resulted in the abrupt

Table 13. Geochemical data for Cu, Pb, Zn, Cd, As, and Hg from core 04SCR111, Gila River arm, San Carlos Reservoir.

[ICP-AES, inductively coupled plasma–atomic emission spectrometry; ICP-MS, inductively coupled plasma–mass spectrometry; Hg CVAA, mercury cold-vapor atomic absorption]

Field no.	Depth (cm)	Loss on ignition (percent)	ICP-AES Cu (ppm)	ICP-MS Pb (ppm)	ICP-AES Zn (ppm)	ICP-MS Cd (ppm)	ICP-MS As (ppm)	Hg CVAA Hg (ppm)
04SCR111La	0–5	10.98	99	29.9	124	0.49	9.4	0.03
04SCR111Lb	5–10	9.38	104	28.7	132	0.43	8.4	0.04
04SCR111Lc	10–15	10.98	92	26.6	112	0.45	8.0	0.03
04SCR111Ld	15–20	7.98	107	26.8	130	0.38	6.8	0.03
04SCR111Le	20–24	6.79	107	24.2	102	0.38	7.2	0.03
04SCR111Lf	24–26	2.60	59	18.5	73	0.17	4.9	<0.02
04SCR111Lg	26–29.5	7.37	94	23.4	98	0.35	6.7	0.03
04SCR111Lh	29.5–35	7.58	130	30.3	151	0.44	7.2	0.04
04SCR111Li	35–41	7.75	141	30.0	152	0.43	7.9	0.04
04SCR111Lj (mean)	41–47	8.93	143	30.1	143	0.42	8.3	0.04
04SCR111Lk	47–55	8.91	143	30.4	121	0.46	9.6	0.04
04SCR111Ll	55–60	7.16	215	28.3	129	0.47	8.1	0.05
04SCR111Lm	60–65	8.12	666	27.9	152	0.48	7.1	0.04
04SCR111Ln	65–70	6.52	339	29.6	139	0.40	7.1	0.05
04SCR111Lo	70–76	6.88	204	27.6	118	0.41	6.9	0.05
04SCR111Lp	76–82	5.59	106	25.2	97	0.36	6.0	0.03
04SCR111Lq	82–87	4.00	69	46.8	76	0.24	5.2	0.03
04SCR111Lr	87–93	4.20	82	20.1	95	0.25	5.8	0.02
04SCR111Ls	93–98	5.59	106	25.0	117	0.35	6.4	0.04
04SCR111Lt	98–104	7.45	130	29.0	130	0.43	7.0	0.04
04SCR111Lu	104–108	6.99	140	28.0	118	0.45	6.5	0.06
04SCR111Lv	108–112	7.77	119	25.2	100	0.34	6.7	0.07
04SCR111Lw	112–117	3.59	63	19.6	76	0.23	5.5	0.02
04SCR111Lx	117–121	5.20	101	26.1	105	0.38	6.9	0.03
04SCR111Ly	121–125	8.37	107	26.8	109	0.44	7.9	0.04
04SCR111Lz	125–130	8.96	121	26.5	121	0.46	8.5	0.04
04SCR111Laa	130–135	9.80	133	29.0	144	0.44	8.1	0.04
04SCR111Lab	135–140	9.97	94	26.1	144	0.41	9.3	0.04
04SCR111Lac	140–145	10.76	84	26.9	112	0.38	6.4	0.03
04SCR111Lad	145–149	10.40	85	31.1	134	0.42	6.7	0.06
04SCR111Lae	149–155	9.80	155	29.9	122	0.43	7.3	0.04
04SCR111Laf (mean)	155–160	6.77	134	28.7	123	0.46	7.4	0.03
04SCR111Lag	160–165	8.00	109	31.5	120	0.55	7.2	0.04
04SCR111Lah	165–170	6.19	117	26.2	128	0.38	5.2	0.03

cutoff of the upper part of this large metal anomaly preserved in the reservoir cores. The timing of these engineering changes and the date we derived from our ^{210}Pb chronology are in good agreement.

The second set of prominent Cu peaks is present in the two reservoir cores (figs. 20 and 21) and is coincident with the lower ^{137}Cs peak that we have identified as the result of atmospheric nuclear testing in 1953–59. In core 04SCR112, this Cu peak (600 ppm) occurs at a depth of 250 cm (fig. 20), whereas the depth of the Cu peak in core 04SCR115 (1,000 ppm) is at 303 cm (fig. 21). A large Zn anomaly of about 600 ppm is also present in core 04SCR115 at this depth. Relying on discharge data measured at the gauge sites to interpret this event is enigmatic. With the exception of 1958, the reservoir was dry every year during part of the year in the 1950s (fig. 2*B*). Because the large Cu peak occurs well within the ^{137}Cs peak, we interpret the event to have been in the late 1950s. Discharge data from the Clifton gauge for this period (fig. 22*C*) show only small rainfall events in 1957 and 1959. The discrete nature of this Cu peak and the presence of a Zn anomaly accompanying this event suggest that this was a release of low-pH metal-contaminated water rather than a release of tailings materials. The event would have occurred in about 1957, based on the location of the Cu peak (303 cm, table 16) in the 1953–59 ^{137}Cs peak in core 04SCR115 (fig. 13) and the low incidence of rainfall in the Clifton, Ariz., area during this period (fig. 22*B*). The total mass of Cu released in this event, using the same parameters described above would be about 200

Table 14. Geochemical data for Cu, Pb, Zn, Cd, As, and Hg from core 04SCR112, San Carlos Reservoir.

[ICP-AES, inductively coupled plasma–atomic emission spectrometry; ICP-MS, inductively coupled plasma–mass spectrometry; Hg CVAA, mercury cold-vapor atomic absorption]

Field no.	Depth (cm)	Loss on ignition (percent)	ICP-AES Cu (ppm)	ICP-MS Pb (ppm)	ICP-AES Zn (ppm)	ICP-MS Cd (ppm)	ICP-MS As (ppm)	Hg CVAA Hg (ppm)
04SCR112La	0–5	11.13	135	29.7	135	0.47	12.4	0.05
04SCR112Lb	5–10	10.36	134	30.3	134	0.44	11.2	0.04
04SCR112Lc	10–15	10.38	134	30.1	134	0.42	10.7	0.04
04SCR112Ld	15–20	10.78	123	31.0	134	0.45	10.8	0.03
04SCR112Le	20–25	10.18	122	31.0	134	0.43	11.1	0.04
04SCR112Lf	25–30	9.81	133	32.9	133	0.45	12.2	0.04
04SCR112Lg	30–35	10.58	145	32.3	134	0.45	10.2	0.04
04SCR112Lh	35–40	9.58	144	34.9	144	0.44	10.0	0.06
04SCR112Li	40–45	9.94	133	33.6	133	0.46	12.2	0.06
04SCR112Lj	45–50	10.78	134	35.0	146	0.44	12.3	0.04
04SCR112Lk	50–55	11.12	146	34.0	135	0.45	13.5	0.05
04SCR112Ll	55–60	11.11	146	36.9	146	0.51	12.4	0.06
04SCR112Lm	60–65	11.18	180	33.3	135	0.47	13.5	0.06
04SCR112Ln	65–70	10.18	178	33.8	122	0.45	13.4	0.04
04SCR112Lo	70–75	9.98	178	32.5	133	0.49	11.1	0.07
04SCR112Lp	75–80	10.80	344	34.2	135	0.61	10.3	0.09
04SCR112Lq	80–85	10.58	613	31.6	179	0.75	9.5	0.10
04SCR112Lr	85–90	10.56	534	33.3	168	0.74	7.8	0.10
04SCR112Ls	90–95	11.18	433	31.3	158	0.65	7.4	0.10
04SCR112Lt	95–100	9.54	334	31.3	144	0.55	6.7	0.08
04SCR112Lu	100–105	8.95	280	31.1	132	0.51	8.6	0.07
04SCR112Lv	105–110	9.78	255	30.6	133	0.49	7.5	0.06
04SCR112Lw	110–115	8.95	209	29.9	121	0.47	9.4	0.05
04SCR112Lx	115–120	10.12	178	33.5	134	0.49	14.5	0.06
04SCR112Ly	120–125	9.96	178	32.0	144	0.49	7.9	0.08
04SCR112Lz	125–130	8.75	153	34.5	132	0.45	8.0	0.08
04SCR112Laa (mean)	130–135	9.98	156	34.3	139	0.46	8.2	0.08
04SCR112Lab	135–140	10.10	156	33.6	133	0.47	9.8	0.10
04SCR112Lac	140–145	8.92	154	32.9	132	0.47	8.3	0.10
04SCR112Lad	145–150	8.58	153	31.7	120	0.42	7.7	0.11
04SCR112Lae	150–155	10.91	146	31.0	135	0.47	10.7	0.07
04SCR112Laf	155–160	9.60	188	33.2	133	0.46	11.0	0.09
04SCR112Lag	160–165	9.78	133	44.7	144	0.52	12.2	0.04
04SCR112Lah	165–170	7.97	141	31.6	130	0.49	8.0	0.04
04SCR112Lai	170–175	8.37	120	30.6	109	0.46	8.9	0.04
04SCR112Laj	175–180	8.38	109	32.4	109	0.49	9.3	0.04
04SCR112Lak	180–185	8.60	100	30.6	98	0.47	8.8	0.03
04SCR112Lal	185–190	7.78	130	34.3	130	0.49	9.4	0.03
04SCR112Lam (mean)	190–195	7.55	103	32.6	114	0.47	8.1	0.04
04SCR112Lan	195–200	11.20	73	29.3	96	0.36	9.8	0.03
04SCR112Lao	200–205	3.78	43	22.3	73	0.23	6.9	<0.02
04SCR112Lap	205–211	2.60	49	22.0	86	0.27	8.4	0.03
04SCR112Laq	211–215	10.56	111	33.0	110	0.49	13.4	0.04
04SCR112Lar	215–220	10.18	156	34.0	122	0.49	13.4	0.06
04SCR112Las	220–225	9.40	103	33.3	132	0.46	10.4	0.08
04SCR112Lat	225–230	11.00	80	32.4	124	0.47	10.0	0.06
04SCR112Lbj	230–230.2	10.50	72	25.1	112	0.42	9.3	0.02
04SCR112Lau	230.2–235	10.00	82	32.7	133	0.58	8.2	0.04
04SCR112Lav	235–240	10.85	146	34.5	135	0.50	11.1	0.06
04SCR112Law	240–246	11.75	125	43.7	159	0.54	11.3	0.06
04SCR112Lax	246–250	7.80	574	32.4	141	0.51	11.9	0.04
04SCR112Lay	250–255	10.20	108	30.8	111	0.42	8.1	0.04

Table 14. Geochemical data for Cu, Pb, Zn, Cd, As, and Hg from core 04SCR112, San Carlos Reservoir—*Continued.*

Field no.	Depth (cm)	Loss on ignition (percent)	ICP-AES Cu (ppm)	ICP-MS Pb (ppm)	ICP-AES Zn (ppm)	ICP-MS Cd (ppm)	ICP-MS As (ppm)	Hg CVAA Hg (ppm)
04SCR112Laz	255–260	9.94	133	32.8	122	0.47	9.3	0.06
04SCR112Lba	260 -265	10.00	178	31.1	122	0.47	10.7	0.04
04SCR112Lbb	265–270	8.80	66	29.4	110	0.34	7.8	0.03
04SCR112Lbc	270–275	9.36	63	29.1	132	0.34	7.2	0.02
04SCR112Lbd	275–281	8.38	57	29.3	131	0.35	7.6	0.02
04SCR112Lbe	281–286	6.56	58	28.8	118	0.35	7.4	0.04
04SCR112Lbf	286–290	9.36	84	32.5	121	0.43	10.2	0.04
04SCR112Lbg	290–295	9.96	90	31.4	133	0.42	8.3	0.04
04SCR112Lbh	295–300	9.92	85	30.4	133	0.46	8.0	0.04
04SCR112Lbi	300–305	10.40	90	31.9	112	0.42	10.7	0.06

metric tons of Cu, much smaller that the 1978–83 event, even though the maximum Cu concentration exceeds 1,000 ppm in the core interval analyzed in 04SCR115 (300–305 cm depth). The concentration of Cu in reservoir sediment at the time of this event greatly exceeded the recommended toxic concentration for sediment quality guidelines of 149 ppm. The concentration of Zn in reservoir sediment at the time of this event also exceeded the recommended toxic concentration for sediment quality guidelines of 459 ppm (MacDonald and others, 2000) for a short period.

There is a small Pb peak at 155 cm depth in core 04SCR112 (fig. 20) and at 165 cm depth in core 04SCR115 (fig. 21) that may be the result of sediment deposited in the 1965 flood event. There is also a small Pb, Zn, Cd, and As anomaly present at the base of core 04SCR115 at a depth of 375–400 cm. This segment of the core has not been dated, but it is older than sediment at the base of core 04SCR112. This suite of anomalies may represent the stripping phase (1937–42) during the development of the open pit at Morenci (Moolick and Durek, 1966).

Measured concentrations of Pb, Cd, As, and Hg in reservoir-sediment samples have never exceeded the recommended toxic concentration for sediment quality guidelines for sensitive aquatic species (MacDonald and others, 2000).

One of the checks for dates assigned to events by use of the ^{210}Pb method is the calculation of sediment-accumulation rates using both the assigned ages and their intervals (Horowitz and others, 1996). These calculations are presented in table 16. Sediment-accumulation rates calculated for various events in cores 04SCR112 and 04SCR115 show that the sediment-accumulation rate decreased somewhat with time. Only the segment containing sediment from the 1967 flood event in cores 04SCR112 and 04SCR115 contained abnormally high sediment-accumulation rates. Given the fact that the reservoir is filling with sediment over time, the rates of sediment accumulation over the measured intervals appear to be in relatively good agreement with those discussed by Kipple (1977).

Leachable Metal and Pb Isotope Results

Lead isotope and geochemical data for Mn, Cu, Pb, and Zn from leachates of 14 stream-bed-sediment, 7 terrace-sediment, and 24 reservoir-sediment samples are shown in table 17. Samples were selected from the cores on the basis of their Cu contents (tables 12–15). Samples containing median, low, and high concentrations of Cu were selected. Concurrent analyses of the NIST Pb isotope SRM-981 (n = 7) gave very high precision and accuracy with measured Pb isotope ratios accurate to within 1 part in 10,000 (table 17) of the certified values. Lead isotope analyses of the other three SRM standard samples gave Pb isotope results that are in good agreement with long-term analyses of these standards using the leachate digestion method (Unruh and others, 2000). Analysis of the geochemical data shows a good correlation between leachable and total Cu (fig. 23*A*) and Pb (fig. 23*B*), but not Zn (fig. 23*C*). There are two populations of minerals containing Zn, one of which is not leachable, indicating that some of the Zn resides in a nonleachable silicate mineral. Likewise, these two populations are evident in the plot of total Cu versus total Zn (fig. 23*F*). There is good correlation between total Mn and leachable Pb concentrations, indicating that the Mn oxide minerals are one residence site for leachable Pb (fig. 23*D*) but a poor correlation with leachable Zn (fig. 23E). Manganese concentrations are only slightly elevated in sediment from the area drained by the San Francisco River (Morenci area), but Zn concentrations exceed four times crustal abundance (76 ppm, Fortescue, 1992) in the sediment from the San Francisco River (table 5). Finally, the plot of leachable Cu and leachable Pb concentrations indicates that there are two populations of Cu-bearing material in sediment analyzed from the San Carlos Reservoir cores (fig. 24*B*). The population of interest is the one showing elevated concentrations of leachable Cu, which are also the samples containing the elevated Cu concentrations in the reservoir-sediment cores. The second population is the geochemical background suite of reservoir-sediment samples.

Table 15. Geochemical data for Cu, Pb, Zn, Cd, As, and Hg from core 04SCR115, San Carlos Reservoir.

[ICP-AES, inductively coupled plasma–atomic emission spectrometry; ICP-MS, inductively coupled plasma–mass spectrometry; Hg CVAA, mercury cold-vapor atomic absorption]

Field no.	Depth (cm)	Loss on ignition (percent)	ICP-AES Cu (ppm)	ICP-MS Pb (ppm)	ICP-AES Zn (ppm)	ICP-MS Cd (ppm)	ICP-MS As (ppm)	Hg CVAA Hg (ppm)
04SCR115La	2–7.5	10.69	123	28.7	134	0.41	10.2	0.07
04SCR115Lb	7.5–13	10.40	123	29.7	134	0.42	11.0	0.04
04SCR115Lc	13–20	10.76	123	30.0	134	0.41	11.2	0.06
04SCR115Ld	20–26	10.38	123	30.8	134	0.41	12.3	0.06
04SCR115Le	26–33	9.76	144	31.8	133	0.41	9.5	0.06
04SCR115Lf	33–41	10.12	145	32.9	145	0.46	11.0	0.07
04SCR115Lg	41–49.5	11.11	158	32.6	146	0.45	11.3	0.05
04SCR115Lh	49.5–56	10.88	157	33.9	146	0.47	11.2	0.07
04SCR115Li	56–61	10.71	190	32.1	134	0.46	12.3	0.06
04SCR115Lj	61–67.5	10.52	201	32.3	134	0.47	12.3	0.06
04SCR115Lk	67.5–75.7	8.98	379	31.4	143	0.57	10.0	0.10
04SCR115Ll	75.5–82	10.30	540	32.2	178	0.71	8.0	0.09
04SCR115Lm	82–89	11.07	405	30.9	157	0.58	7.4	0.09
04SCR115Ln	89–96	9.74	299	30.0	144	0.52	7.3	0.07
04SCR115Lo	96–105.5	9.06	239	28.9	132	0.48	6.8	0.07
04SCR115Lp	105.5–113	10.34	201	32.0	134	0.47	11.2	0.08
04SCR115Lq	113–121	9.80	166	31.9	144	0.42	7.8	0.08
04SCR115Lr	121–127	10.00	167	32.9	144	0.44	9.3	0.08
04SCR115Ls	127–135.5	11.00	169	33.0	135	0.48	7.4	0.09
04SCR115Lt	135.5– 150	8.57	142	29.7	131	0.39	7.4	0.11
04SCR115Lu	150–155	9.83	133	32.8	133	0.42	10.5	0.06
04SCR115Lv	155–160	8.38	131	31.7	131	0.45	8.1	0.04
04SCR115Lw	160–165	8.20	131	30.7	120	0.42	8.2	0.04
04SCR115Lx	165–170	9.15	143	36.1	143	0.46	8.5	0.04
04SCR115Ly	170- 175	8.37	131	32.7	131	0.46	8.7	0.03
04SCR115Lz	175–180	8.37	142	33.6	142	0.45	8.7	0.04
04SCR115Laa	180–185	10.71	123	33.2	146	0.50	9.4	0.04
04SCR115Lab (mean)	185–190	11.46	177	32.9	152	0.47	9.8	0.06
04SCR115Lac	190–195	10.91	135	37.7	168	0.49	10.0	0.06
04SCR115Lad	195–200	10.61	157	37.9	157	0.50	10.7	0.06
04SCR115Lae	200–206	10.30	312	32.0	145	0.46	9.6	0.03
04SCR115Laf	206–210	10.16	156	31.6	134	0.47	8.2	0.04
04SCR115Lag	210–215	10.08	200	32.9	156	0.48	8.1	0.06
04SCR115Lah	215–220	9.82	226	31.6	144	0.44	9.8	0.06
04SCR115Lai	220–225	9.76	188	30.4	144	0.43	10.2	0.03
04SCR115Laj	225–230	9.22	132	30.4	132	0.40	8.8	0.03
04SCR115Lak	230–235	9.72	122	31.5	155	0.39	8.9	0.04
04SCR115Lal	235–240	8.98	93	30.3	143	0.37	9.0	0.03
04SCR115Lam	240–245	9.25	90	31.0	143	0.37	9.8	0.03
04SCR115Lan	245–250	9.18	79	30.8	132	0.39	7.9	0.03
04SCR115Lao	250–255	8.78	100	32.0	143	0.38	10.1	0.04
04SCR115Lap	255–260	7.75	90	31.0	130	0.40	9.6	0.03
04SCR115Laq	260–265	9.13	91	31.5	132	0.42	9.7	0.03
04SCR115Lar (mean)	265–270	7.55	80	31.3	124	0.41	8.5	0.04
04SCR115Las	270–275	8.15	84	32.0	131	0.39	9.0	0.04
04SCR115Lat	275–280	8.76	142	36.7	164	0.50	11.0	0.04
04SCR115Lau	280–285	8.63	97	31.1	142	0.39	8.2	0.04
04SCR115Lav	285–291.5	8.73	90	32.0	142	0.48	8.0	0.04
04SCR115Law	291.5–295	9.15	106	33.1	154	0.44	10.5	0.04
04SCR115Lax	295–300	9.31	332	32.9	241	0.43	10.8	0.06
04SCR115Lay	300–305	8.73	1054	35.0	593	0.39	8.3	0.04
04SCR115Laz	305–310	9.36	93	33.5	154	0.43	9.9	0.04

Table 15. Geochemical data for Cu, Pb, Zn, Cd, As, and Hg from core 04SCR115, San Carlos Reservoir—*Continued.*

Field no.	Depth (cm)	Loss on ignition (percent)	ICP-AES Cu (ppm)	ICP-MS Pb (ppm)	ICP-AES Zn (ppm)	ICP-MS Cd (ppm)	ICP-MS As (ppm)	Hg CVAA Hg (ppm)
04SCR115Lba	310–315	10.20	94	35.0	156	0.42	9.1	0.06
04SCR115Lbb	315–320	10.23	89	33.4	134	0.45	8.9	0.03
04SCR115Lbc	320–325	9.98	103	31.8	144	0.43	8.6	0.04
04SCR115Lbd	325–330	8.98	103	32.3	132	0.40	9.1	0.04
04SCR115Lbe	330–335	9.78	133	36.9	144	0.48	11.0	0.04
04SCR115Lbf	335–340	9.98	100	31.8	133	0.44	11.1	0.03
04SCR115Lbg	340–345	8.98	91	30.7	132	0.37	9.8	0.04
04SCR115Lbh	345–350	7.19	83	28.2	108	0.37	7.5	0.04
04SCR115Lbi	350 -355	5.57	79	25.7	98	0.30	6.5	0.03
04SCR115Lbj	355–360	8.17	77	25.6	87	0.35	6.9	0.04
04SCR115Lbk (mean)	360–365	4.97	66	22.8	80	0.25	6.4	0.02
04SCR115Lbl	365–370	5.38	59	21.8	79	0.26	5.3	0.02
04SCR115Lbm	370–375	7.39	76	32.7	140	0.39	8.0	0.03
04SCR115Lbn	375–380	9.98	81	42.4	156	0.51	9.1	0.04
04SCR115Lbo	380–385	9.18	83	32.2	132	0.41	8.5	0.04
04SCR115Lbp	385–390	9.08	78	36.3	121	0.44	10.6	0.05
04SCR115Lbq	390–395	9.78	79	41.7	133	0.51	9.2	0.08
04SCR115Lbr	395–400	9.56	75	37.5	122	0.46	8.5	0.06
04SCR115Lbs	400–405	7.75	70	29.3	106	0.35	8.2	0.04
04SCR115Lbt	405–410	7.19	66	27.6	101	0.32	6.6	0.04
04SCR115Lbu	410–415	9.36	95	31.9	121	0.35	9.5	0.04
04SCR115Lbv	415–420	7.76	83	31.7	119	0.37	8.5	0.04
04SCR115Lbw	420–425	7.16	71	30.1	97	0.34	8.2	0.04
04SCR115Lbx	425–430	9.74	111	31.0	133	0.39	9.5	0.06
04SCR115Lby	430–435	8.78	79	33.0	143	0.36	9.2	0.03
04SCR115Lbz	435–440	8.00	92	28.3	130	0.33	8.9	0.02

Lead isotope data from stream-bed-sediment samples are shown in figure 24*A*. Because the Pb isotope ratios covary, $^{206}Pb/^{204}Pb$ values will be used throughout the discussion of these data. The $^{206}Pb/^{204}Pb$ data from sediment from the San Francisco River drainage have low $^{206}Pb/^{204}Pb$ values, but those $^{206}Pb/^{204}Pb$ values are substantially higher than the data published for ore Pb from the Morenci porphyry Cu deposit. Bouse and others (1999) report $^{206}Pb/^{204}Pb$ data from three Cu sulfide samples (chalcopyrite) from Morenci deposit with $^{206}Pb/^{204}Pb$ values that range from 17.403 to 17.503 and a single analysis of Pb in chalcopyrite from the unmined Dos Pobres porphyry Cu deposit with a $^{206}Pb/^{204}Pb$ value of 17.550. These data are in good agreement with the $^{206}Pb/^{204}Pb$ data from the Dos Pobres pluton (17.540 to 17.557) and with the Lone Star pluton in the Safford area (fig. 1), which has $^{206}Pb/^{204}Pb$ values between 17.40 and 17.678. Lead isotope signatures in the alteration halos surrounding porphyry deposits often have Pb isotope values that are higher than the ore because of the complex nature of the hydrothermal circulation pattern established during deposit formation (for example, Gulson and others, 1992). Unfortunately, the uniformity of the $^{206}Pb/^{204}Pb$ data requires that we rely heavily on both geochemical and spatial data to pinpoint the source of the contaminated sediment in the San Carlos Reservoir.

The Pb isotope composition of sediment from the upper Gila River, upstream from the confluence with the San Francisco River (fig. 24*A*), has a $^{206}Pb/^{204}Pb$ value of 18.608. In contrast, the Pb isotope composition in sediment from the San Francisco River near the Morenci mine is 18.20 and 18.41 (table 17 and fig. 24*A*) and reflects the composition of Pb in the Morenci deposit and the surrounding mineralized rock. Lead in sediment in the Gila River downstream from the confluence but upstream from the Safford Valley has lower $^{206}Pb/^{204}Pb$ values that are depressed (18.47 to 18.48) by the addition of sediment from the San Francisco River. The modern sediment load being supplied by the Safford Valley reach of the Gila River raises the $^{206}Pb/^{204}Pb$ values in the Safford Valley reach to > 18.65 (fig. 24*A*), values that exceed that of two of the three $^{206}Pb/^{204}Pb$ values measured in terrace-sediment samples from the Calva site. Pulses of Cu-rich sediment from the Morenci mine area preserve the lower $^{206}Pb/^{204}Pb$ signature (fig. 24*B*) in sediment upstream from the Safford Valley but not the ore-Pb signature in sediment in either the lower Gila River or the San Carlos Reservoir. The

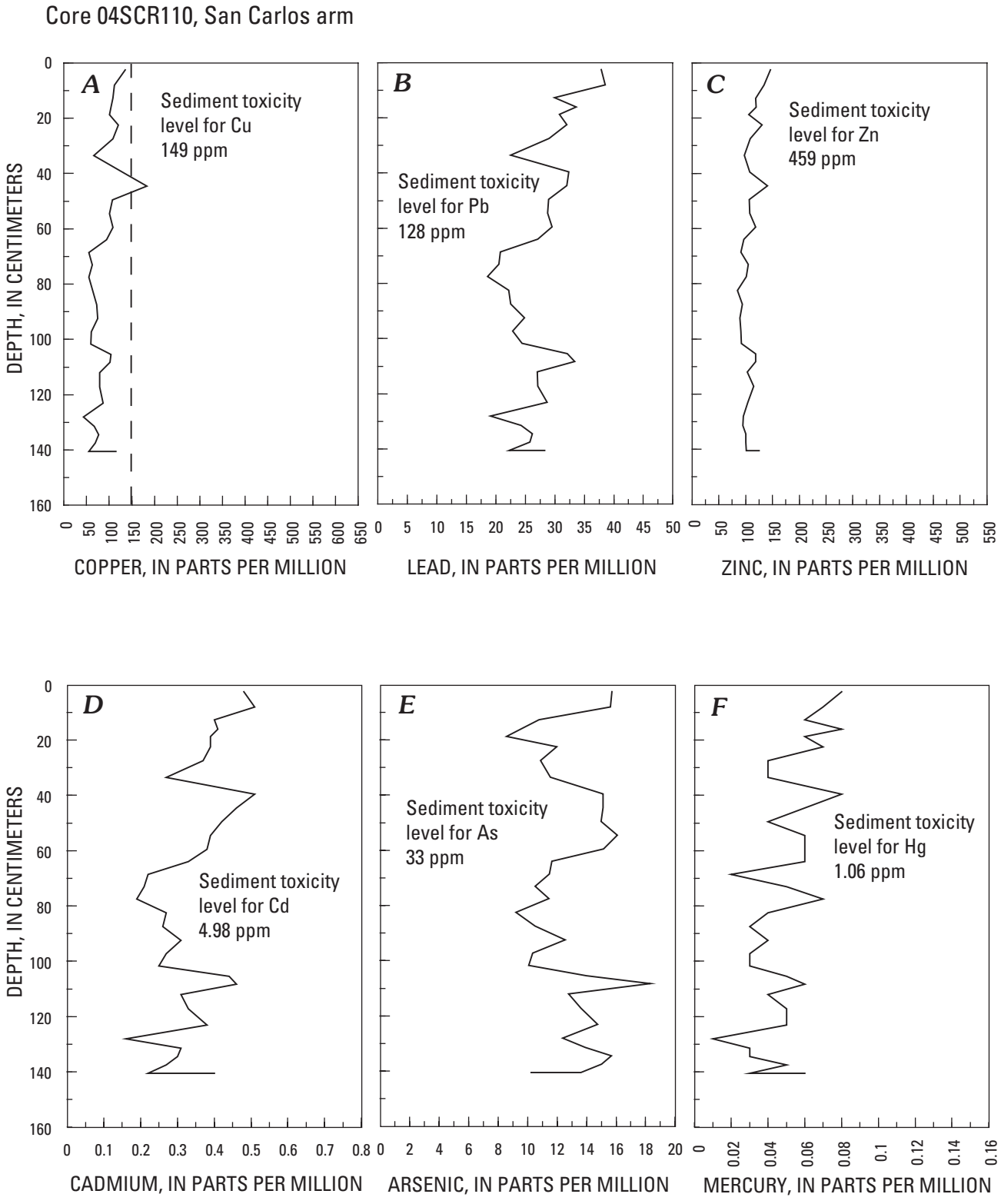

Figure 18. Plot of the variation of concentration of *A*, Cu; *B*, Pb; *C*, Zn; *D*, Cd; *E*, As; and *F*, Hg as a function of depth in core 04SCR110, San Carlos River arm, San Carlos Reservoir.

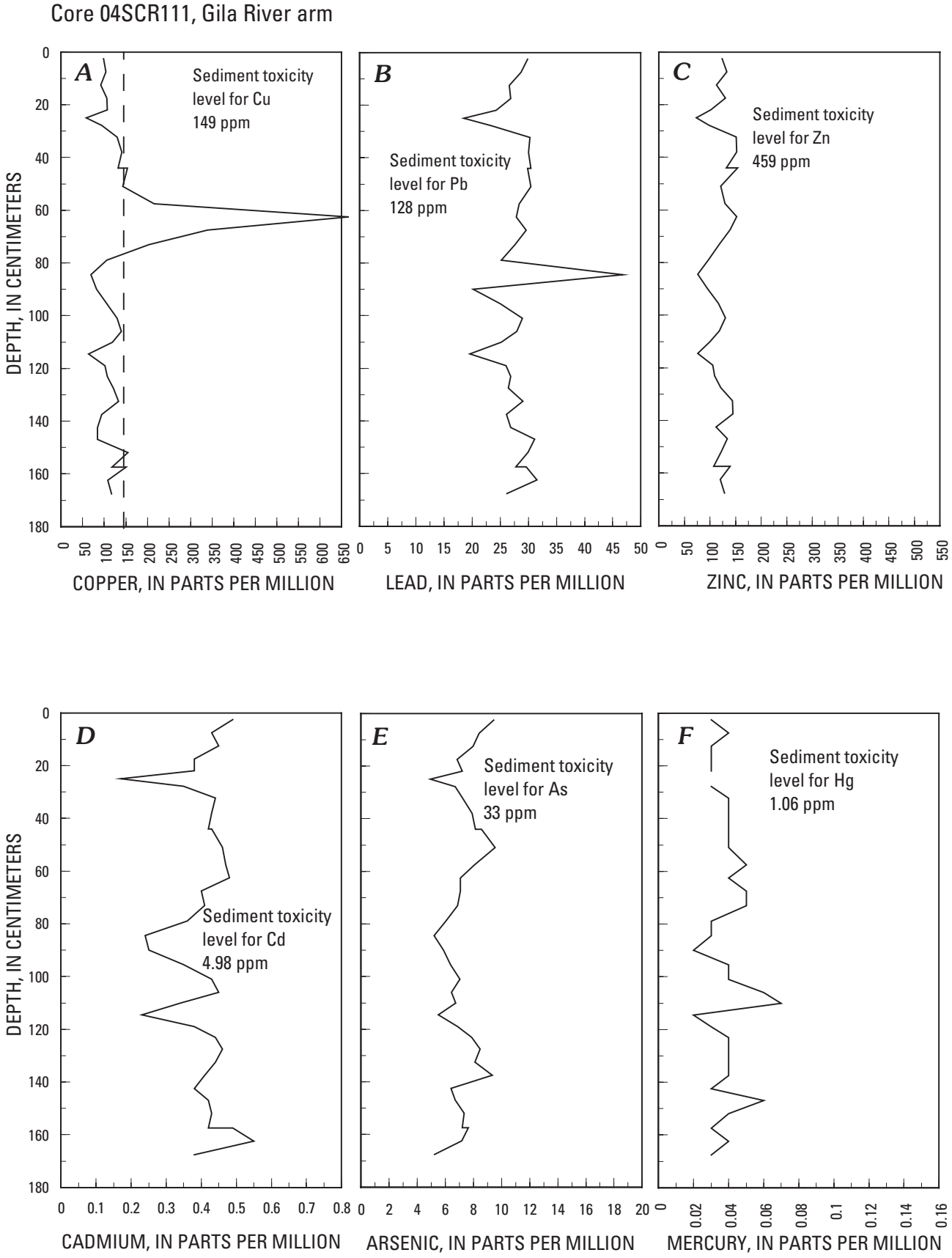

Figure 19. Plot of the variation of concentration of *A*, Cu; *B*, Pb; *C*, Zn; *D*, Cd; *E*, As; and *F*, Hg as a function of depth in core 04SCR111, Gila River arm, San Carlos Reservoir.

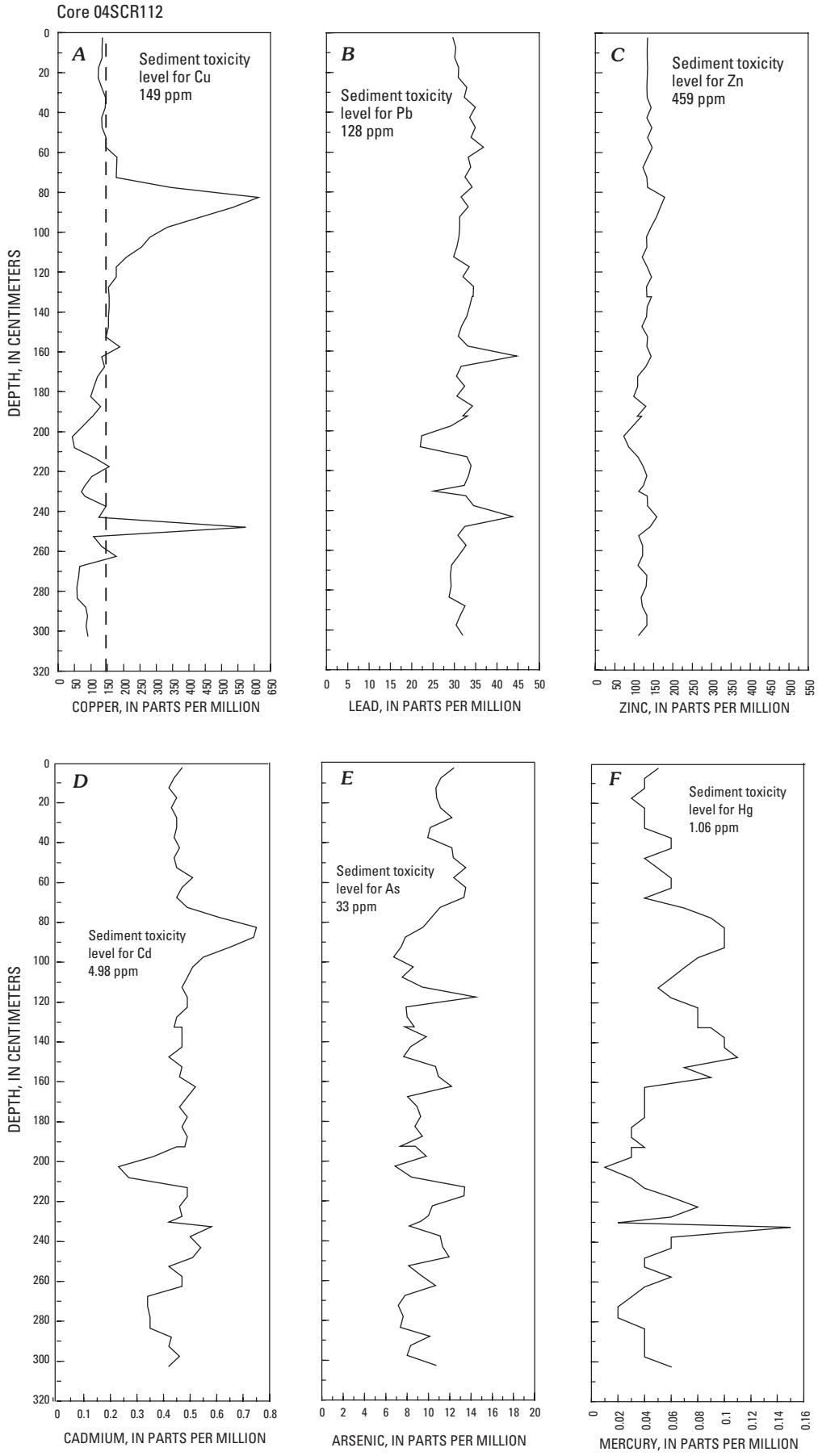

Figure 20. Plot of the variation of concentration of *A*, Cu; *B*, Pb; *C*, Zn; *D*, Cd; *E*, As; and *F*, Hg as a function of depth in core 04SCR112, San Carlos Reservoir.

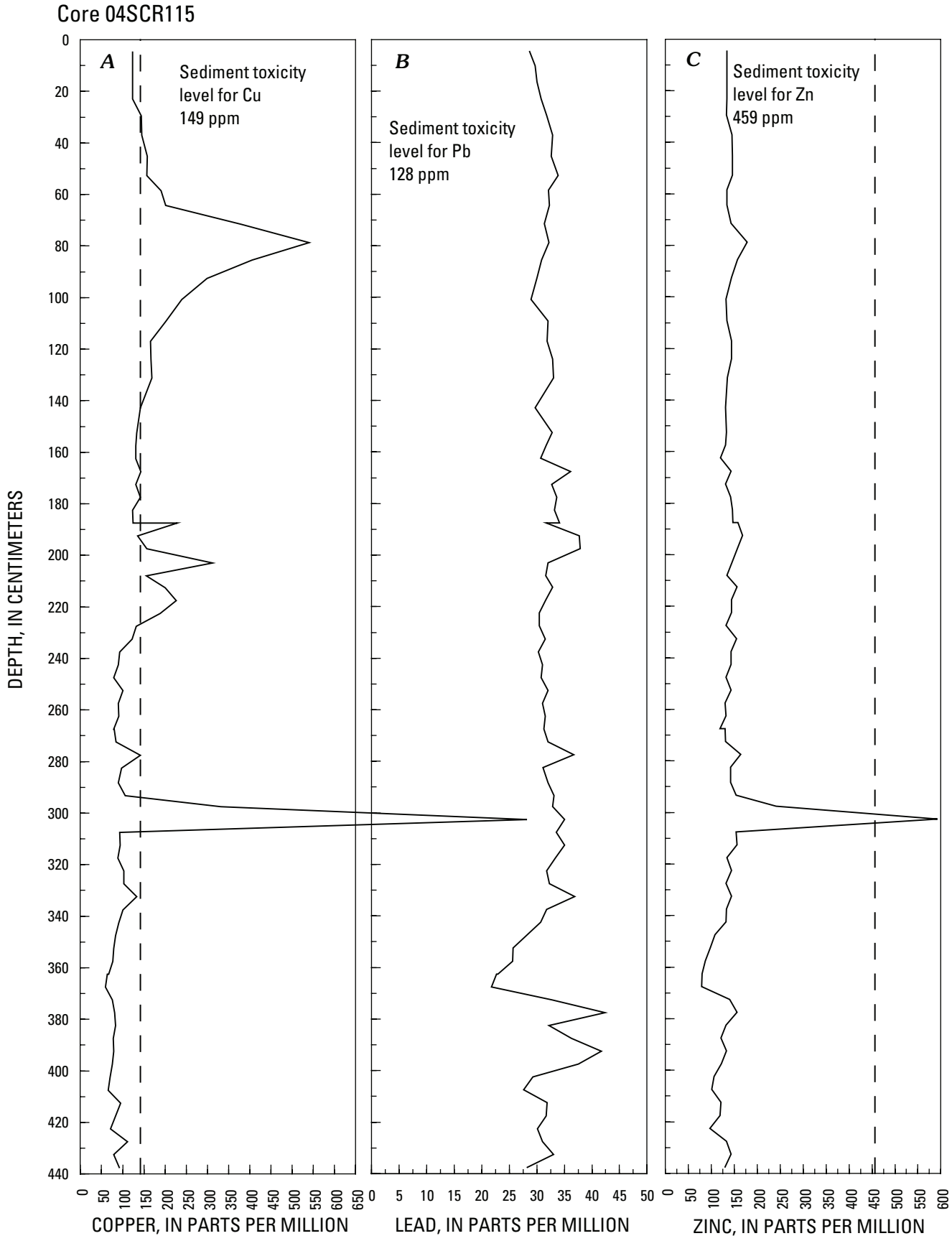

Figure 21. Plot of the variation of concentration of *A*, Cu; *B*, Pb; *C*, Zn; *D*, Cd; *E*, As; and *F*, Hg as a function of depth in core 04SCR115, San Carlos Reservoir.

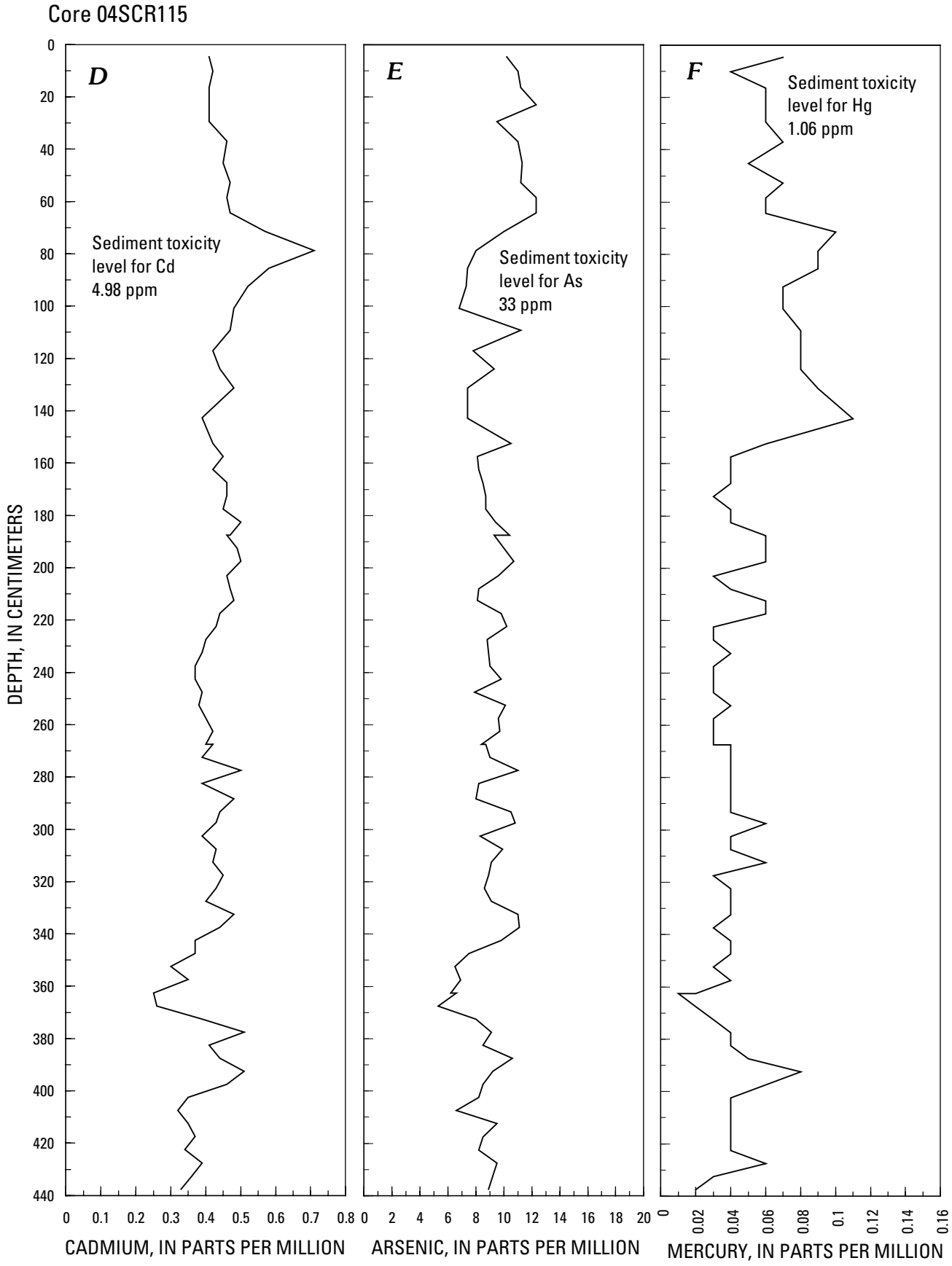
Core 04SCR115
D
Sediment toxicity level for Cd 4.98 ppm
E
Sediment toxicity level for As 33 ppm
F
Sediment toxicity level for Hg 1.06 ppm
DEPTH, IN CENTIMETERS
0
20
40
60
80
100
120
140
160
180
200
220
240
260
280
300
320
340
360
380
400
420
440
0 0.1 0.2 0.3 0.4 0.5 0.6 0.7 0.8
CADMIUM, IN PARTS PER MILLION
0 2 4 6 8 10 12 14 16 18 20
ARSENIC, IN PARTS PER MILLION
0 0.02 0.04 0.06 0.08 0.1 0.12 0.14 0.16
MERCURY, IN PARTS PER MILLION

Table 16. Calculated sediment-accumulation rates using radiometric and geochemical markers identified in San Carlos Reservoir cores.

	Depth to 1963 ^{137}Cs peak (cm)	Sedimentation rate (cm/yr)	Depth to Cu peak or interval (cm)	Assigned date	Sedimentation rate (cm/yr)	Sedimentation rate over dated interval (cm/yr)
04SCR110	108	2.6	48	1978–83	1.8	
04SCR111	150	3.7	33–73	1978–83	2.8	
04SCR112	180	4.4	63–123	1978–83	4.7	
			158	1967	4.3	3.2
			248	1957?	5.3	9.0
04SCR115	190	4.6	70–135	1978–83	5.2	
			203	1967	5.5	6.2
			303	1957?	6.4	10.0
			375–405	1937?	6.0	5.1

ore-Pb isotope signature in core intervals from the San Carlos Reservoir are diluted by the higher ^{206}Pb/^{204}Pb composition of Pb in the surrounding sediment in the 5-cm intervals analyzed. The lower ^{206}Pb/^{204}Pb values measured in the terrace sediment from Calva (fig. 24) suggest that sediment in the lower Gila River reach today contains a larger component of material introduced by the agricultural practices in the Safford Valley than in the past. Prior to mining, erosion of the porphyry Cu deposit exposed in the Morenci area had a larger affect on the sediment preserved in the terrace deposits, as indicted by the lower ^{206}Pb/^{204}Pb values in the terrace sediment. Whereas the ^{206}Pb/^{204}Pb signature and the reservoir-sediment chemistry of Cu peaks in the reservoir sediment (table 17) indicate a source upstream on the San Francisco River, Cu concentration data from the terrace deposits in the Safford Valley (table 7 and fig. 17) are not sufficiently high to implicate these terrace deposits as possible erosional sources of the elevated Cu concentrations in the San Carlos Reservoir. The ^{206}Pb/^{204}Pb data, elevated Pb and Cu concentrations, and the geochronological data from the San Carlos Reservoir sediment implicate the Morenci porphyry Cu deposit as the source of these Cu anomalies.

Results from Dioxins/Furans Analysis

Concentrations for 17 dioxin and furan congeners were determined in the 30-cm intervals from core 04SCR112. The toxic equivalent concentrations (TEQ) were calculated assuming that the concentration of congeners reported as nondetected have a concentration of one-half the detection limit; these data are reported in table 18. The total HpCDD concentration was used instead of the 1,2,3,4,6,7,8-HpCDD concentration in the TEQ calculation because it was measured. The TEQ concentration verses depth is plotted in figure 25. The United States does not have sediment quality guidelines for dioxin, but the benchmark TEQ values most often cited include the U.S. Army Corps of Engineers (1,000 pg/g), the U.S. EPA, Region 10 dredge spoils disposal guideline (4 pg/g), U.S. EPA Fish and Wildlife (bird and mammal) guidelines developed specifically for Lake Ontario (2.5–210 pg/g), and the dioxin benchmark of 10 pg/g proposed by the Science Advisory Board of the International Joint Commission for Great Lakes sediments (Wenning and others, 2004). The TEQ values for core 04SCR112 are less than any of these benchmark TEQ values, and, thus, dioxin in reservoir sediment does not pose a threat to benthic or aquatic biota on the basis of these criteria.

Conclusions

Detailed geochemical studies of stream-bed sediment, terrace sediment, and sediment cored from the San Carlos Reservoir in October 2004 document the effect of development of the Safford Valley and the Morenci mine on the geochemical landscape upstream from Coolidge Dam. Geochemical and radioisotope data from four cores collected from the San Carlos Reservoir define the spatial and chronological variation of six potentially toxic metals—Cu, Pb, Zn, Cd, As, and Hg. Water levels in the San Carlos Reservoir were at a 20-year low in the fall of 2004, at an elevation of 2,409 ft, which allowed coring of the reservoir at sites with recovery of as much as 4 m of sediment from the San Carlos Reservoir. Four cores were taken from the reservoir: one from the San Carlos River arm, one from the Gila River arm, and two from the upper part of the San Carlos Reservoir. ^{7}Be, ^{137}Cs, and ^{210}Pb activities were determined, and a chronology for sediment deposition was developed on the basis of measured radioisotope activities in conjunction with discharge records and water levels. A good chronological model from the data can be derived back to 1959. The chronology prior to 1953 is speculative and based

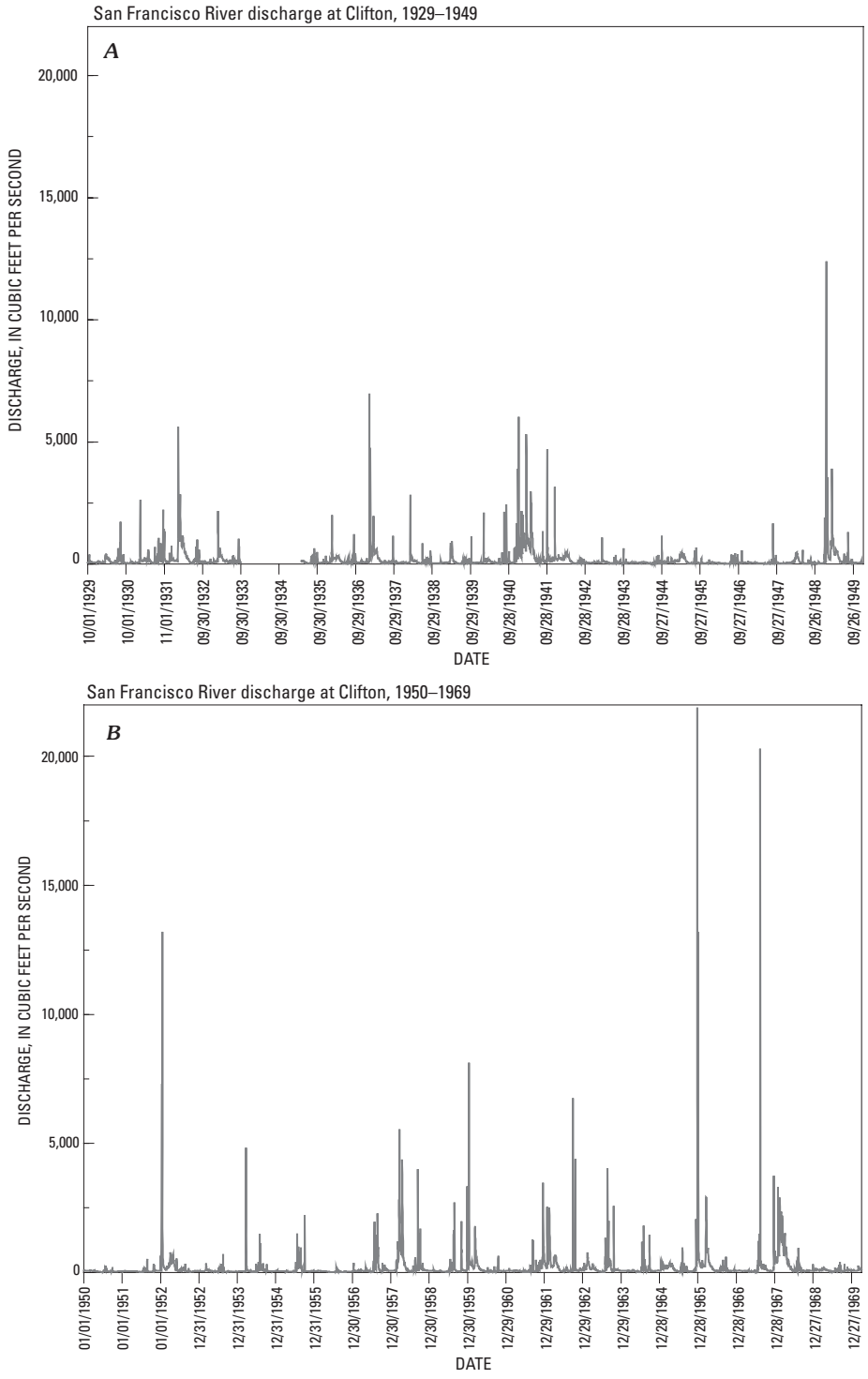

Figure 22 (above and facing page). Annual discharge records for San Francisco River at Clifton (1929–2004; USGS gauging station 09444500). Dates on *x*-axis expressed as month, day, year for maximum discharge.

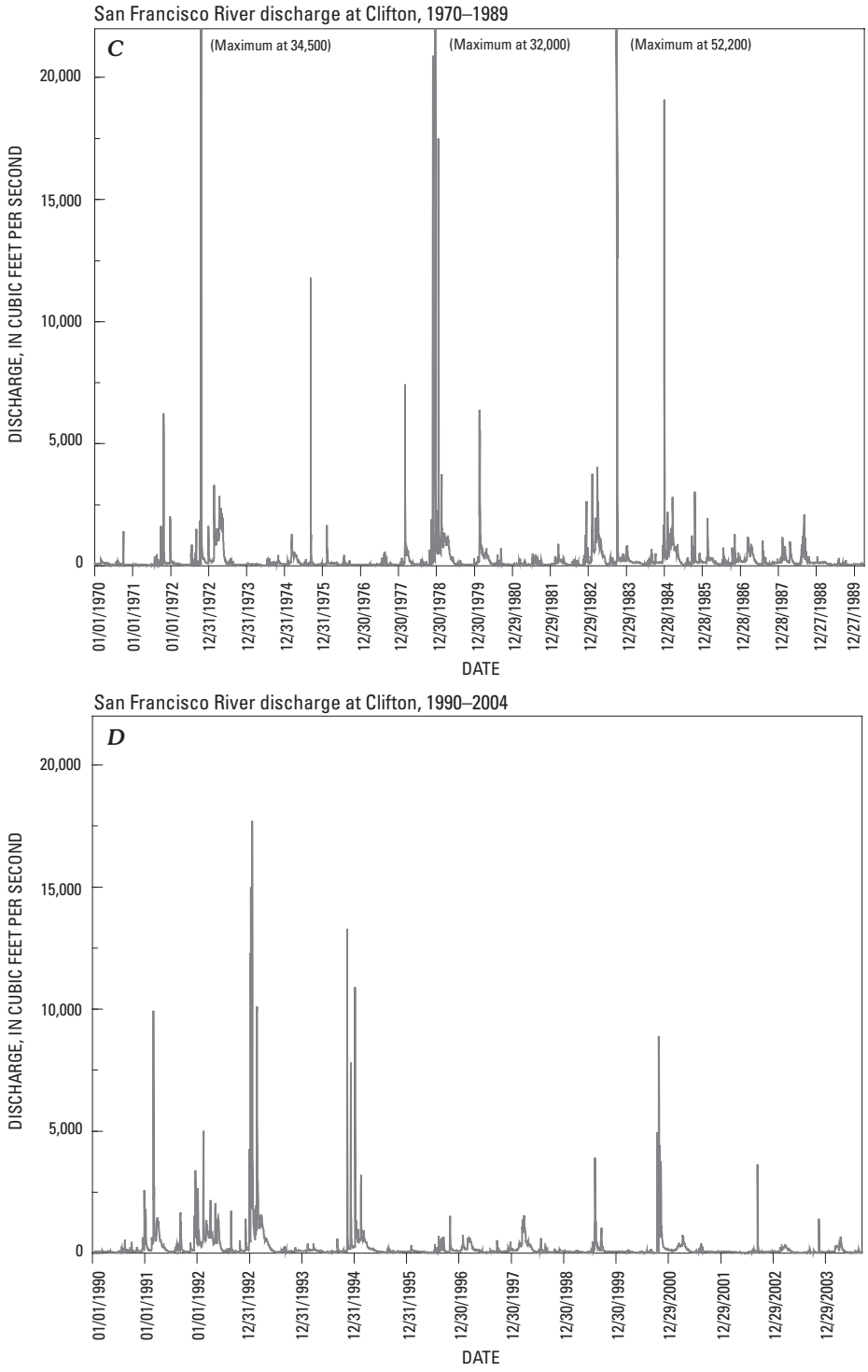
San Francisco River discharge at Clifton, 1970–1989
C
(Maximum at 34,500)
(Maximum at 32,000)
(Maximum at 52,200)
DISCHARGE, IN CUBIC FEET PER SECOND
20,000
15,000
10,000
5,000
0
01/01/1970
01/01/1971
01/01/1972
12/31/1972
12/31/1973
12/31/1974
12/31/1975
12/30/1976
12/30/1977
12/30/1978
12/30/1979
12/29/1980
12/29/1981
12/29/1982
12/29/1983
12/28/1984
12/28/1985
12/28/1986
12/28/1987
12/27/1988
12/27/1989
DATE
San Francisco River discharge at Clifton, 1990–2004
D
DISCHARGE, IN CUBIC FEET PER SECOND
20,000
15,000
10,000
5,000
0
01/01/1990
01/01/1991
01/01/1992
12/31/1992
12/31/1993
12/31/1994
12/31/1995
12/30/1996
12/30/1997
12/30/1998
12/30/1999
12/29/2000
12/29/2001
12/29/2002
12/29/2003
DATE

Table 17. Lead isotope data and concentrations of Mn, Cu, Pb, and Zn determined from 2M HCl–1 percent H_2O_2 leaches of selected sediment samples.

[ICP-AES, inductively coupled plasma–atomic emission spectrometry; ICP-MS, inductively coupled plasma–mass spectrometry]

Sample no.	$^{206}Pb/^{204}Pb$	$^{206}Pb/^{204}Pb$ ±1 σ	$^{207}Pb/^{204}Pb$	$^{207}Pb/^{204}Pb$ ±1 σ	$^{208}Pb/^{204}Pb$	$^{208}Pb/^{204}Pb$ ±1 σ	ICP-Leach Mn (ppm)	ICP-AES Mn (ppm)	ICP-Leach Cu (ppm)	ICP-AES Cu (ppm)	ICP-Leach Pb (ppm)	ICP-MS Pb (ppm)	ICP-Leach Zn (ppm)	ICP-AES Zn (ppm)	ICP-MS Cd (ppm)
Stream-bed-sediment samples															
04SCR101S	18.907	0.001	15.633	0.001	38.876	0.002	200	3,540	10	16	8	18.3	14	231	0.10
04SCR102S	18.847	0.002	15.630	0.001	38.800	0.003	270	3,940	16	69	10	22	17	338	0.17
04SCR103S	18.658	0.001	15.605	0.001	38.559	0.002	520	921	37	64	9	17.8	13	89	0.28
04SCR120S	18.198	0.001	15.548	0.001	38.322	0.002	680	1,000	200	281	17	34.1	70	249	0.89
04SCR121S	18.414	0.001	15.575	0.001	38.338	0.002	410	715	200	314	12	26.1	46	170	0.66
04SCR122S	18.608	0.001	15.589	0.001	38.593	0.002	450	744	22	41	7	20.8	10	77	0.29
04SCR123S	18.485	0.001	15.576	0.001	38.468	0.002	310	663	61	92	10	24.4	19	110	0.36
04SCR124S	18.475	0.001	15.580	0.001	38.489	0.002	350	628	59	93	14	26	23	110	0.40
04SCR125s	18.960	0.001	15.622	0.001	38.850	0.003	540	828	44	71	14	24.9	22	110	0.29
04SCR126S	18.726	0.002	15.605	0.001	38.812	0.004	290	1,400	26	41	10	20.8	13	140	0.19
04SCR127S	18.647	0.002	15.601	0.003	38.585	0.005	280	2,640	18	40	8	27	11	320	0.18
04SCR128S	18.878	0.001	15.621	0.001	38.846	0.003	260	1,370	20	35	8	18.8	13	130	0.19
04SCR129S	18.638	0.002	15.596	0.001	38.649	0.003	240	1,480	18	36	9	21.6	12	180	0.16
04SCR129SS	18.784	0.000	15.598	0.000	38.754	0.003		890		86		29		270	
Terrace-sediment samples															
04SCR103Td	18.807	0.001	15.621	0.001	38.796	0.002	210	1,560	10	23	4	15.3	11	130	0.11
04SCR103Th	18.815	0.001	15.632	0.001	38.745	0.002	490	2,500	30	42	10	21.3	14	180	0.19
04SCR124TD	18.288	0.001	15.552	0.001	38.291	0.003	240	791	59	85	7	18.5	14	99	0.17
04SCR129Tb	18.504	0.001	15.570	0.001	38.502	0.002	160	509	23	39	6	17.4	6	64	0.12
04SCR129Th	18.518	0.002	15.575	0.001	38.500	0.004	350	723	52	81	9	21.3	14	100	0.22
04SCR129Tk	18.749	0.001	15.602	0.001	38.825	0.002	390	949	19	40	12	25.7	13	120	0.27
04SCR129Tm	18.586	0.001	15.585	0.001	38.579	0.003	250	637	39	62	7	19.5	13	80	0.15
San Carlos River arm, San Carlos Reservoir															
04SCR110Lb	18.539	0.001	15.593	0.001	38.553	0.003	770	833	82	100	23	34.5	45	120	0.46
04SCR110Lj	18.734	0.001	15.614	0.001	38.706	0.002	770	990	130	170	20	29.7	42	130	0.43
04SCR110Lr	18.839	0.001	15.623	0.001	38.782	0.003	370	595	53	62	13	21.4	30	82	0.26
04SCR110Lx	18.838	0.001	15.624	0.001	38.780	0.002	560	719	80	94	23	31	43	110	0.43
Gila River arm, San Carlos Reservoir															
04SCR111Ld	18.715	0.001	15.606	0.001	38.686	0.002	620	1,010	52	98	12	24.7	21	120	0.35
04SCR111Lf	18.600	0.001	15.584	0.001	38.572	0.003	310	611	37	57	7	18	11	71	0.17
04SCR111Lq	18.643	0.001	15.597	0.001	38.622	0.003	350	558	49	66	9	44.9	15	73	0.23
04SCR111Lw	18.609	0.001	15.591	0.001	38.595	0.002	290	497	48	61	9	18.9	16	73	0.22

Table 17. Lead isotope data and concentrations of Mn, Cu, Pb, and Zn determined from 2M HCl–1 percent H_2O_2 leaches of selected sediment samples—*Continued*.

Sample no.	$^{206}Pb/^{204}Pb$	$^{206}Pb/^{204}Pb$ ±1 σ	$^{207}Pb/^{204}Pb$	$^{207}Pb/^{204}Pb$ ±1 σ	$^{208}Pb/^{204}Pb$	$^{208}Pb/^{204}Pb$ ±1 σ	ICP-Leach Mn (ppm)	ICP-AES Mn (ppm)	ICP-Leach Cu (ppm)	ICP-AES Cu (ppm)	ICP-Leach Pb (ppm)	ICP-MS Pb (ppm)	ICP-Leach Zn (ppm)	ICP-AES Zn (ppm)	ICP-MS Cd (ppm)
San Carlos Reservoir															
04SCR112Lb	18.626	0.002	15.599	0.001	38.611	0.004	670	875	86	120	17	27.2	37	120	0.39
04SCR112Lq	18.534	0.001	15.586	0.001	38.533	0.003	840	1,100	480	548	21	28.3	67	160	0.67
04SCR112Lx	18.633	0.001	15.597	0.001	38.592	0.003	1,000	1,290	130	160	20	30.1	38	120	0.44
04SCR112Laf	18.576	0.001	15.594	0.001	38.561	0.003	600	844	130	170	19	30	42	120	0.42
04SCR112Lag	18.726	0.002	15.610	0.001	38.678	0.003	820	1,010	87	120	25	40.3	46	130	0.47
04SCR112Lao	18.760	0.001	15.610	0.001	38.697	0.002	450	733	34	41	11	21.5	18	70	0.22
04SCR112Lax	18.596	0.001	15.596	0.001	38.603	0.003	620	856	460	529	19	29.9	48	130	0.47
04SCR112Lbd	19.068	0.001	15.643	0.001	39.002	0.003	820	1,070	29	52	17	26.8	25	120	0.32
04SCR115Lc	18.636	0.002	15.604	0.001	38.645	0.003	700	888	81	110	21	26.8	40	120	0.37
04SCR115Ll	18.539	0.001	15.588	0.001	38.542	0.002	820	1,070	420	484	20	28.9	61	160	0.64
04SCR115Lad	18.897	0.002	15.621	0.001	38.779	0.003	760	970	110	140	24	33.9	46	140	0.45
04SCR115Lae	18.648	0.001	15.598	0.001	38.608	0.002	620	851	250	280	20	28.7	42	130	0.41
04SCR115Lay	18.732	0.002	15.605	0.001	38.725	0.003	680	825	270	962	21	31.9	190	541	0.36
04SCR115Lbe	18.775	0.002	15.611	0.002	38.774	0.004	800	989	120	120	28	33.3	52	130	0.43
04SCR115Lbq	18.432	0.001	15.582	0.001	38.524	0.003	750	907	60	71	28	37.6	42	120	0.46
04SCR115Lbx	18.782	0.002	15.617	0.001	38.796	0.003	520	702	59	100	18	28	28	120	0.35
Standard Reference Materials (NIST)															
SRM-2704	18.856	0.002	15.657	0.002	38.507	0.004	400		78		130		310		
SRM-2709	19.078	0.002	15.664	0.002	38.912	0.004	410		20		7		41		
SRM-2711	17.140	0.002	15.461	0.002	37.006	0.004	450		82		970		210		
SRM 981 certified value	16.933	0.0004	15.485	0.0004	36.680	0.0008									
Average (*n*=7)	16.935	0.0004	15.487	0.0004	36.684	0.0009									
Obs. mean / certified value	1.00011		1.00010		1.00013										

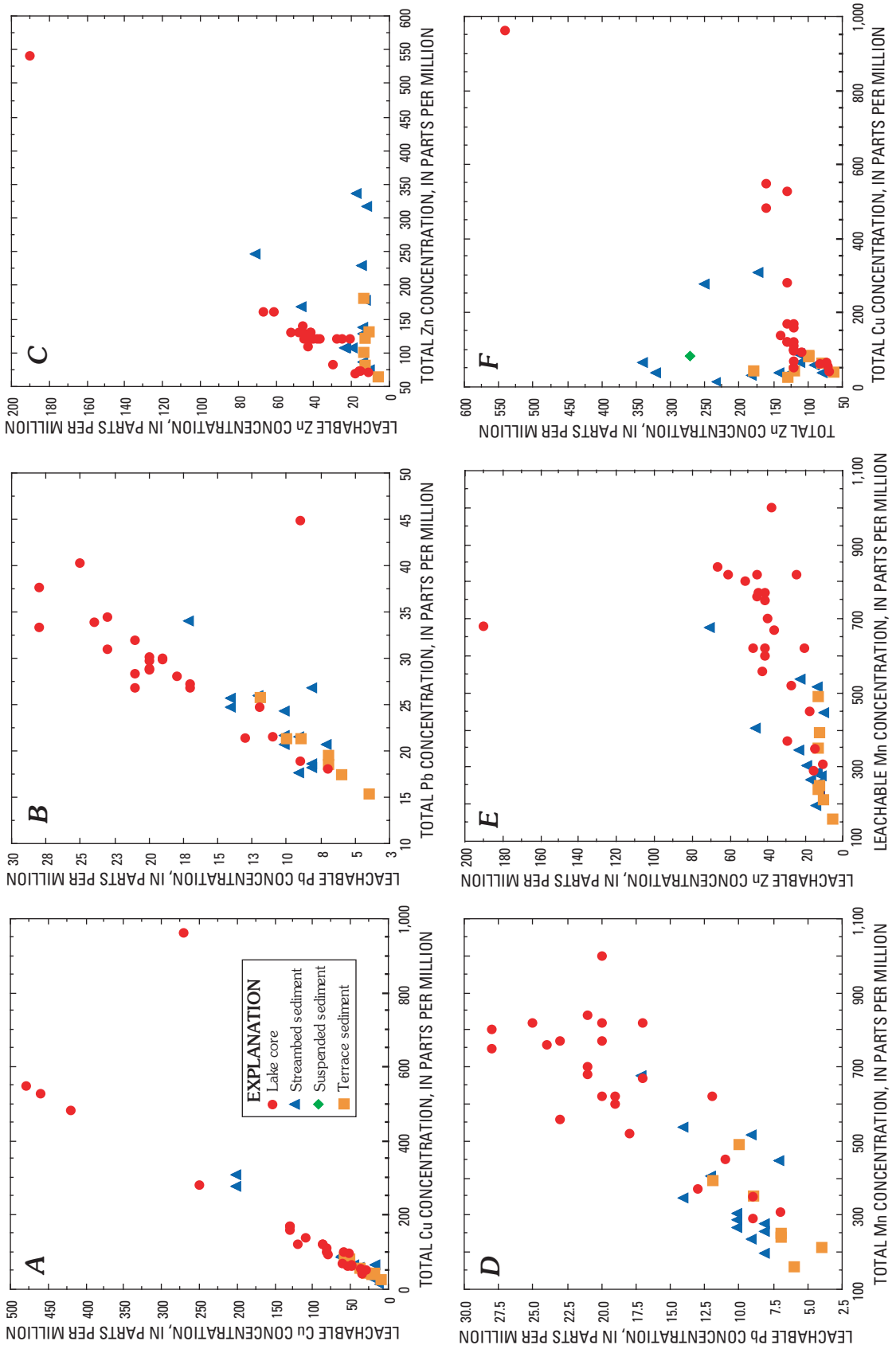

Figure 23. Plots of leachable and total metal concentrations (table 17) showing variance between *A*, Cu; *B*, Pb; *C*, Zn; *D*, Mn and Pb; *E*, Mn and Zn; and *F*, Cu and Zn.

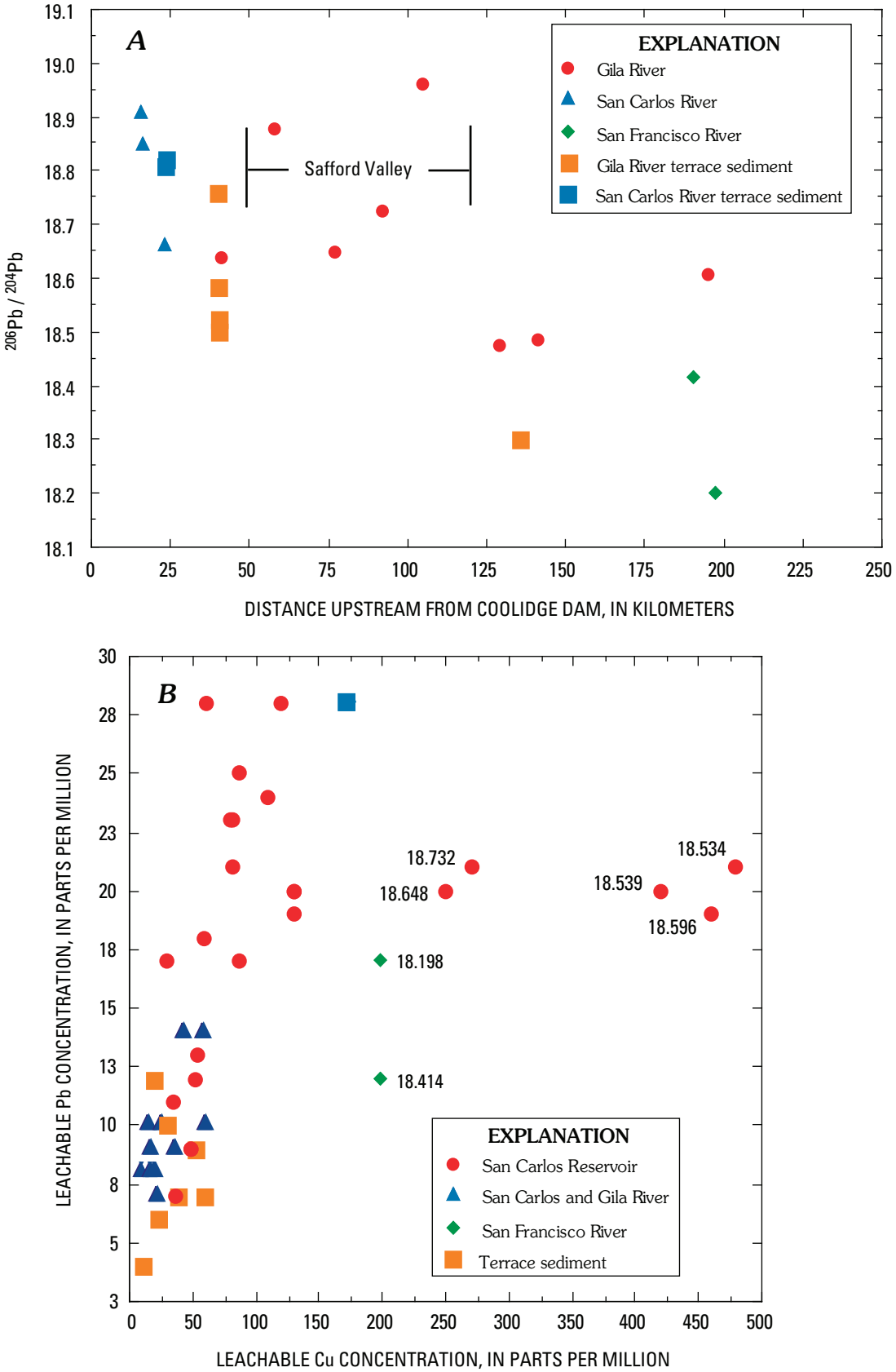

Figure 24. *A*, Plot of the $^{206}Pb/^{204}Pb$ values in stream-bed sediment as a function of distance upstream from the Coolidge Dam. *B*, plot of the concentration of leachable Cu versus leachable Pb showing $^{206}Pb/^{204}Pb$ values associated with Cu anomalies in San Carlos Reservoir sediment.

Table 18. Dioxin concentrations, expressed as Toxic Equivalents (TEQ), in core 04SCR112, San Carlos Reservoir (October 2004).

Blind sample ID	Depth interval (cm)	Mid depth (cm)	TEQ (pg/g dry weight)
10	0–30	1.5	0.83
5	30–60	45	1.37
7	60–90	75	1.19
6	90–120	105	0.86
9	120–150	135	0.77
2	150–180	165	0.70
1	180–211	195.5	0.85
3	211–240	225.5	0.70
8	240–270	255	0.75
4	270–305	287.5	0.68

upon correlation of geochemical and historical data. Radioisotope chronology prior to 1953 was not possible because the reservoir was dry during a substantial portion of the record and sediment-accumulation rates were not uniform. We recovered sediment at the base of a 4-m-long core (04SCR115) that may date back to the late 1930s or early 1940s. The sedimentological record contains two discrete events, one between 1978 and 1983 and one during the late 1950s (1957?), where the Cu concentration in reservoir sediment exceeded recommended sediment-quality guidelines and should have had an effect on sensitive aquatic and benthic organisms. Concentrations of Zn determined in sediment deposited during the 1957(?) event recorded in core 04SCR115 in the reservoir also exceeded recommended sediment-quality guidelines. Concentration data for Cu from the four cores clearly indicate that the source of this material was upstream on the Gila River. The 1957(?) event was a single pulse, probably of metal-contaminated water that may or may not correspond with a flood event recorded at the gauge on the San Francisco River. This event represents a discrete pulse that would have had only a short-term effect on benthic and aquatic life in the reservoir. The second event is interpreted to be the result of mining practices at the Morenci open pit. As mining proceeded, the mine encroached on—and eventually completely removed—Chase Creek. As a result, several tens of centimeters of reservoir sediment were contaminated during this time period, and benthic and aquatic life in both the Gila River and San Carlos Reservoir were exposed to elevated concentrations of Cu that greatly exceeded recommended sediment-toxicity guidelines. The metals released during these events show no evidence that they have been recycled by burrowing organisms in the reservoir, as indicated by the sharp boundaries at the top of the sediment interval representing these events.

Lead isotope data, coupled with the geochemical data from a 2M HCl–1 percent H_2O_2 leach of selected reservoir-sediment samples, show two discrete populations of data. One represents the abundant sediment derived from the Safford Valley, and a second reflects sediment derived from the San Francisco River. The Cu spikes in contaminated intervals from the reservoir cores have chemical and Pb isotope signatures that indicate that open-pit mining at Morenci is the likely source of the Cu-rich sediment layers in the cores from the San Carlos Reservoir. Copper concentrations and Pb isotope data in the premining terrace-sediment deposits indicate that the Cu peaks could not have resulted from erosion of premining sediment. The chemical and Pb isotope data also indicate that agricultural practices in the Safford Valley have resulted in an increased sediment load to the Gila River since large-scale farming began, prior to the time when the San Carlos Reservoir was built.

Analysis of dioxin, which is an impurity in one of the herbicides used in the late 1960s and early 1970s to attempt to eradicate tamarisk, were completed in sediment from core 04SCR112 from the reservoir to determine whether any of these pesticide residues have accumulated in reservoir sediment. These data were determined using the very low concentration EPA method 8290 (U.S. EPA, 1994). Dioxin concentration is expressed in terms of its toxicity (TEQ). Concentrations in the sediment ranged from 0.68 to 1.37 pg/g and are less than any of the benchmark concentrations recommended as threshold values for dioxin in sediment (2.5–10 pg/g).

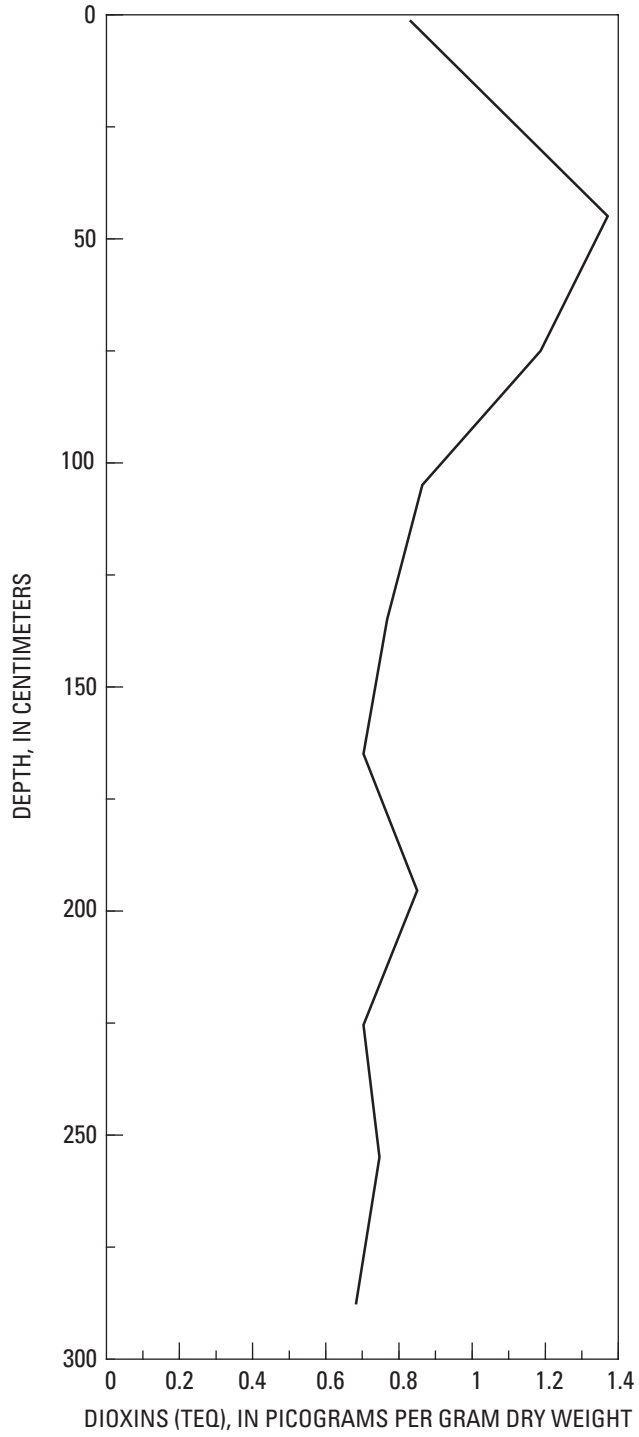

Figure 25. Plot of dioxin concentrations, expressed in TEQ units, versus depth in core 04SCR112. Recommended benchmark values of TEQs are: U.S Army Corps of Engineers, 1,000 pg/g; U.S. EPA, Region 10, 4 pg/g; U.S. EPA Fish and Wildlife guidelines, 2.5–210 pg/g; Science Advisory Board of the International Joint Commission on Great Lakes sediment, 10 pg/g.

References Cited

Baker, D.L., and King, K.A., 1994, Environmental contaminant investigation of water quality, sediment and biota of the upper Gila River, Arizona: U.S. Fish and Wildlife Report, 27 p., available at URL http://arizonaes.fws.gov/Documents/InvestigationReports/UpperGilaRiver1994.pdf.

Bouse, R.M., Ruiz, Joaquin, Titley, S.R., Tosdal, R.M., and Wooden, J.L., 1999, Lead isotope compositions of Late Cretaceous and early Tertiary igneous rocks and sulfide minerals in Arizona—Implications for the sources of plutons and metals in porphyry copper deposits: Economic Geology, v. 94, p. 211–244.

Burkham, D.E., 1970, Precipitation, streamflow, and major floods at selected sites in the Gila River drainage basin above Coolidge Dam, Arizona—Gila River Phreatophyte Project, Graham County, Arizona: U.S. Geological Survey Professional Paper 655-B, 33 p.

Burkham, D.E., 1972, Channel changes of the Gila River in Safford Valley, Arizona 1846–1970—Gila River Phreatophyte Project, Graham County, Arizona: U.S. Geological Survey Professional Paper 655-G, 24 p.

Briggs, P.H., 2002, The determination of forty elements in geological and botanical samples by inductively coupled plasma–atomic emission spectrometry: U.S. Geological Survey Open-File Report 02-223-G, 20 p.

Briggs, P.H., and Meier, A.L., 2002, The determination of forty-two elements in geological materials by inductively coupled plasma–mass spectrometry: U.S. Geological Survey Open-File Report 02-223-I, 16 p.

Brown, Z.A., O'Leary, R.M., Hageman, P.L., and Crock, J.G., 2002, Mercury in water, geologic, and plant materials by continuous-flow cold-vapor atomic absorption spectrometry: U.S. Geological Survey Open-File Report 02-223-M, 11 p.

Church, S.E., Kimball, B.A., Fey, D.L., Ferderer, D.A., Yager, T.J., and Vaughn, R.B., 1997, Source, transport and partitioning of metals between water, colloids, and bed sediments of the Animas River, Colorado: U.S. Geological Survey Open-File Report 97-151, 135 p.

Cox, D.P., 1986, Descriptive model of porphyry Cu, *in* Cox, D.P., and Singer, D.E., eds., Mineral deposit models: U.S. Geological Survey Bulletin 1693, p. 76.

Culler, R.C., Leppanen, O.E., Matalas, N.C., Davidson, E.S., Weist, W.G., Jr., Collins, M.R., Burkham, D.E., Myrick, R.M., Turner, R.M., Laney, R.L., Miller, R.F., and McQueen, I.S., 1970, Objectives, methods, and environment—Gila River Phreatophyte Project, Graham County, Arizona: U.S. Geological Survey Professional Paper 655-A, 25 p.

Culler, R.C., Hanson, R.L., Myrick, R.M., Turner, R.M., and Kipple, F.P., 1982, Evaporatranspiration before and after clearing phreatophytes, Gila River flood plain, Graham County, Arizona: U.S. Geological Survey Professional Paper 655-P, 67 p.

Cutshall, N.H., Larsen, I.L., and Olsen, C.R., 1983, Direct analysis of ^{210}Pb in sediment samples: Self-adsorption corrections: Nuclear Instrumental Methods Physics Research, v. 26, p. 309–312.

Enders, M.S., 2000, The evolution of supergene enrichment in the Morenci porphyry copper deposit, Greenlee County, Arizona: University of Arizona, Tucson, Ph.D. dissertation, 517 p.

Fey, D.L., Unruh, D.M., and Church, S.E., 1999, Chemical data and lead isotopic compositions in stream-sediment samples from the Boulder River watershed, Jefferson County, Montana: U.S. Geological Survey Open-File Report 99-575, 147 p., available at URL http://pubs.usgs.gov/of/1999/ofr-99-0575/.

Fortescue, J.A.S., 1992, Landscape geochemistry—Retrospect and prospect—1990: Journal of Applied Geochemistry, v. 7, p. 1–54.

Flynn, W.W., 1968, The determination of polonium-210 in environmental materials: Analytica Chimica Acta, v. 43, p. 121–131.

Gulson, B.L., Church, S.E., Mizon, K.G., and Meier, A.L., 1992, Lead isotopes in iron and manganese oxide coatings and their use as a guide for concealed mineralization: Applied Geochemistry, v. 7, p. 495–511.

Horowitz, A.J., Robbins, J.A., Elrick, K.A., and Cook, R.B., 1996, Bed sediment–trace element geochemistry of Terrace Reservoir, near Summitville, southwestern Colorado: U.S. Geological Survey Open-File Report 96-344, 41 p.

Houser, B.B., Richter, D.H., and Shafiquallah, M., 1985, Geologic map of the Safford quadrangle, Graham County, Arizona: U.S. Geological Survey Miscellaneous Investigations Map I-1617, scale 1:48,000.

Kamilli, R.J., and Richard, S.M., eds., 1998, Geologic highway map of Arizona: Tucson: Arizona Geological Society and Arizona Geological Survey, scale 1:1,000,000.

Keith, S.B., Gest, D.E., DeWitt, Ed, Toll, N.W., and Everson, B.A., 1983, Metallic mineral districts and production in Arizona: Arizona Bureau of Geology and Mineral Technology Bulletin 194, 58 p.

Kipple, F.P., 1977, The hydrologic history of the San Carlos Reservoir, Arizona, 1929–71, with particular reference to evapotranspiration and sedimentation: U.S. Geological Survey Professional Paper 655-N, 11 p.

Lindgren, Waldemar, 1905, The copper deposits of the Clifton-Morenci district, Arizona: U.S. Geological Survey Professional Paper 43, 375 p.

MacDonald, D.D., Ingersoll, C.G., and Berger, T.A., 2000, Development and evaluation of consensus-based sediment quality guidelines for freshwater ecosystems: Archives of Environmental Contamination and Toxicology, v. 39, p. 20–31.

Moolick, R.T., and Durek, J.J., 1966, The Morenci district, *in* Titley, S.R., and Hicks, C.L., eds., Geology of the porphyry copper deposits—Southwestern North America: Tucson, University of Arizona Press, p. 221–231.

NATO/CCMS, 1988, International toxicity equivalence factor (I-TEF) method of risk assessment for complex mixtures of dioxins and related compounds: NATO, Committee on Challenges of Modern Society, Report 176, August 1988.

Potts, P.J., Tindle, A.G., and Webb, P.C., 1992, Geochemical reference material compositions: rocks, minerals, sediments, soils, carbonates, refractories and ores used in research and industry: Boca Raton, CRC Press, 313 p.

Richard, S.M., Reynolds, S.J., Spencer, J.E., and Pearthree, P.A., compilers, 2000, Geologic map of Arizona: Arizona Geologic Survey Map 35, scale: 1,000,000.

Robbins, J.A., 1978, Geochemical and geophysical applications of radioactive lead, *in* Nriagu, J.O., ed., Biogeochemistry of lead in the environment, Part A.: Amsterdam, Netherlands, Elsevier Scientific Publishers, v. 1A, p. 285–393.

Robbins, J.A., Reddy, K.R., Holmes, C.W., Morehead, N.R., Marot, M.E., and Rood, R.W., 1999, Sediment core dating: West Palm Beach, Fla., Report of South Florida Water Management District, C-5324, 56 p.

Robbins, J.A., Holmes, C.W., Halley, R.B., Bothner, M.A., Shinn, E.A., Graney, J., Keeler, G., TenBrink, M., Orlandini, K.A., and Rudnick, D.E., 2000, Time-averaged flux of lead and fallout radionuclides to sediment in Florida Bay: Journal of Geophysical Research, v. 105, p. 28,805–28,821.

Schmitt, C.J., and Brumbaugh, W.G., 1990, National contaminant biomonitoring program—Concentrations of arsenic, cadmium, copper, lead, mercury, selenium, and zinc in U.S. freshwater fish, 1976–1984: Archives of Environmental Contamination and Toxicology, v. 19, p. 731–747.

Sellers, W.D., ed., 1960, Arizona climate: Tucson, University of Arizona Press, 60 p.

Simon, S.L., Bouville, André, and Beck, H.L., 2004, The geographic distribution of radionuclide deposition across the continental U.S. from atmospheric nuclear testing: Journal of Environmental Radioactivity, v. 74, p. 91–105.

Smith, K.S., 1999, Metal sorption on mineral surfaces—An overview with examples relating to mineral deposits, *in* Plumlee, G.S., and Logsdon, M.J., eds., The environmental geochemistry of mineral deposits—Part A, Processes, techniques, and health issues: Society of Economic Geologists, Reviews in Economic Geology, v. 6, p. 161–182.

Turner, R.M., 1974, Quantitative and historical evidence of vegetation changes along the upper Gila River, Arizona—Gila River Phreatophyte Project, Graham County, Arizona: U.S. Geological Survey Professional Paper 655-H, 20 p.

Unruh, D.M., Fey, D.L., and Church, S.E., 2000, Chemical data and lead isotopic compositions of geochemical baseline samples from streambed sediments and smelter slag, lead isotopic compositions in fluvial tailings, and dendrochronology results from the Boulder River watershed, Jefferson County, Montana: U.S. Geological Survey Open-File Report 00-38, 75 p.

U.S. Department of Energy, 2000, United States nuclear tests, July 1945 through Sept., 1992 (15th ed.), 162 p., available at URL http://www.fas.org/nuke/guide/usa/nuclear/usnuctests.htm.

U.S. Geological Survey, 1974, State of Arizona, scale 1:1,000,000, 1 sheet.

U.S. Geological Survey, station number 09469000, San Carlos Reservoir at Coolidge Dam, AZ, State 04, county latitude: 331032, longitude: 1103138, NAD 27 DATUM 25 39.54 NGV D29, date processed: 2004-09 17:13 by sdfran, Observation at 2400, Gage height reservoir ELEV COMP DD3.

U.S. Geological Survey, Water-Supply Papers: Surface Water Supply of the United States, Part 9 Colorado River Basin, U.S. Department of the Interior, [see table 1 for listing of individual reports].

U.S. Geological Survey in cooperation with the State of Arizona and other agencies, Water Resources Data for Arizona: U.S. Geological Survey Water-Data Reports, [see table 1 for listing of individual reports].

U.S. Geological Survey—Water Resources Division, Surface water Records for Arizona: U.S. Department of the Interior, 1961–1964.

U.S. Geological Survey—Water Resources Division, Water-resources data for Arizona, Part 1: Surface-Water Records: U.S. Department of the Interior, 1965–1974.

U.S. Environmental Protection Agency test methods SW 846 online, 1994: U.S. Environmental Protection Agency, available at URL http://www.epa.gov/epaoswer/hazwaste/test/pdfs/8290.pdf.

Wenning, R., Von Burg, A., Martello, L., Pekala, J., Maier, M., and Luksemburg, W., 2004, Levels of polychlorinated dibenzo-p-dioxins (PCDDS), dibenzofurans (PCDFS), and polychlorinated biphenyls (PCBS) in the Hackensack River and Newark Bay, New Jersey, USA: Organohalogen compounds, v. 66, p. 1,509–1,515.

Published in the Central Region, Denver, Colorado
Manuscript approved for publication April 26, 2005
Editing, page layout, photocomposition—Richard W. Scott, Jr.
Graphics—Stanley E. Church and Barbara J. Ramsey